Relaxation and Dynamic Processes

Arthur G. Palmer, III
Department of Biochemistry and Molecular Biophysics
Columbia University

Contents

Although multiple pulse and multi-dimensional NMR techniques permit generation of off-diagonal density matrix elements and observation of complex coherence transfer processes, eventually the density operator returns to an equilibrium state in which all coherences (off-diagonal elements of the density operator) have decayed to zero and the populations of the energy levels of the system (diagonal elements of the density operator) have been restored to the Boltzmann distribution. Analogously with similar phenomena in other areas of spectroscopy, the process by which an arbitrary density operator returns to the equilibrium operator is called nuclear magnetic, or spin, relaxation. The following sections will describe the general features of spin relaxation and important consequences of spin relaxation processes for multi-dimensional NMR experiments. In addition, other dynamic processes, such as chemical reactions and conformational exchanges, that transfer nuclei between magnetic environments can affect the NMR experiment; these processes also are discussed.

As relaxation is one of the fundamental aspects of magnetic resonance, an extensive literature on theoretical and experimental aspects of relaxation has developed since the earliest days of NMR spectroscopy (see (*1*) and references therein). At one level, relaxation has important consequences for the NMR experiment: the relaxation rates of single quantum transverse operators determine the linewidths of the resonances detected during the acquisition period of an NMR experiment; the relaxation rates of the longitudinal magnetization and off-diagonal coherences generated by the pulse sequence determine the length of the recycle delay needed between acquisitions; and the relaxation rates of

operators of interest during multi-dimensional experiments determine the linewidths of resonances in the indirectly detected dimensions and affect the overall sensitivity of the experiments. At a second level, relaxation affects quantitative measurement and interpretation of NMR experimental parameters, including chemical shifts and scalar coupling constants and At a third level, relaxation provides experimental information on the physical processes governing relaxation, including molecular motions and intramolecular distances. In particular, cross-relaxation gives rise to the nuclear Overhauser effect (NOE) and makes possible the determination of three-dimensional molecular structures by NMR spectroscopy. Additionally, a variety of chemical kinetic processes can be studied through effects manifested in the NMR spectrum; in many cases, such phenomena can be studied while the molecular system remains in chemical equilibrium.

Because the theoretical formalism describing relaxation is more complicated mathematically than the product operator formalism, the present treatment will emphasize application of semi-classical relaxation theory to cases of practical interest, rather than fundamental derivations. Semi-quantitative or approximate results are utilized when substantial simplification of the mathematical formalism thereby is obtained. More detailed descriptions of the derivation of the relaxation equations are presented elsewhere (*2, 1, 3*).

1 Introduction and survey of theoretical approaches

Introductory theoretical treatments of optical spectroscopy emphasize the role of spontaneous and stimulated emission in relaxation

from excited states back to the ground state of a molecule. The probability per unit time, W, for transition from the upper to lower energy state of an isolated magnetic dipole by spontaneous emission of a photon of energy $\Delta E = h\omega$ is given by (*2*),

$$W = \frac{2\hbar\gamma^2\omega^3}{3c^3} \qquad [1]$$

in which c is the speed of light. For a proton with a Larmor frequency of 500 MHz, $W \approx 10^{-21}$ s^{-1}; thus, spontaneous emission is a completely ineffective relaxation mechanism for nuclear magnetic resonance. Calculation of stimulated emission transition probabilities is complicated by consideration of the coil in the probe; nonetheless, stimulated emission also can be shown to have a negligible influence on nuclear spin relaxation. Spontaneous and stimulated emission are important in optical spectroscopy because the relevant photon frequencies are orders of magnitude larger.

Instead, nuclear spin relaxation is a consequence of coupling of the spin system to the *surroundings*. The surroundings have historically been termed the *lattice* following the early studies of NMR relaxation in solids where the surroundings were genuinely a solid lattice. The lattice includes other degrees of freedom of the molecule containing the spins (such as rotational degrees of freedom) as well as other molecules comprising the system. The energy levels of the lattice are assumed to be quasi-continuous with populations that are described by a Boltzmann distribution. Furthermore, the lattice is assumed to have an infinite heat capacity and consequently to be in thermal equilibrium at all times. The lattice modifies the local magnetic fields at the locations of the nuclei and thereby (weakly) couples the lattice and the spin system. Stochastic

Brownian rotational motions of molecules in liquid solutions render the local magnetic fields time-dependent. More precisely, the local fields are composed of a rotationally invariant, and consequently time-independent, component and a rotationally variant, time-dependent component. The time-dependent local magnetic fields can be resolved into components perpendicular and parallel to the main static field. In addition, the fields can be decomposed by Fourier analysis into a superposition of harmonically varying magnetic fields with different frequencies. Thus, the Hamiltonian acting on the spins is given by

$$\begin{aligned} H &= H_z + H_{local}(t) \\ &= H_z + H_{local}^{isotropic} + H_{local}^{anisotropic}(t) \\ &= H_z + H_{local}^{isotropic} + H_{longitudinal}^{anisotropic}(t) + H_{transverse}^{anisotropic}(t) \end{aligned} \qquad [2]$$

in which H_z is the Zeeman Hamiltonian, $H_{local}^{isotropic}$ contains the isotropic chemical shift and scalar coupling interactions and the stochastic, anisotropic Hamiltonians have an ensemble average of zero by construction, Alternatively, the stochastic Hamiltonians average to zero for $t >> \tau_c$ (τ_c being defined as the correlation time of the stochastic process, which in isotropic solution is approximately the rotational correlation time of the molecular species).

Transverse components of the stochastic local field are responsible for *non-adiabatic* contributions to relaxation. If the Fourier spectrum of the fluctuating transverse magnetic fields at the location of a nucleus contains components with frequencies corresponding to the energy differences between eigenstates of the spin system, then transitions between eigenstates can occur. In this case, transition of the spin system from a higher (lower) energy state to a lower (higher) energy state is

accompanied by an energy-conserving transition of the lattice from a lower (higher) to higher (lower) energy state. A transition of the spin system from higher energy to lower energy is more probable because the lattice is always in thermal equilibrium and has a larger population in the lower energy state. Thus, exchange of energy between the spin system and the lattice brings the spin system into thermal equilibrium with the lattice and the populations of the stationary states return to the Boltzmann distribution. Furthermore, transitions between stationary states caused by non-adiabatic processes decrease the lifetimes of these states and introduces uncertainties in the energies of the nuclear spin states through a Heisenberg uncertainty relationship. As a result, the Larmor frequencies of the spins vary randomly and the phase coherence between spins is reduced over time. Consequently, non-adiabatic fluctuations that cause transitions between states result in both thermal equilibration of the spin state populations and decay of off-diagonal coherences.

Fluctuating fields parallel to the main static field are responsible for *adiabatic* contributions to relaxation. The fluctuating fields generate variations in the total magnetic field in the z-direction, and consequently, in the energies in the nuclear spin energy levels. Thus, adiabatic processes cause the Larmor frequencies of the spins to vary randomly. Over time, the spins gradually lose phase coherence and off-diagonal elements of the density matrix decay to zero. The populations of the states are not altered and no energy is exchanged between the spin system and the lattice because transitions between stationary states do not occur.

To illustrate these ideas, the chemical shift anisotropy relaxation mechanism will be investigated. The chemical shift Hamiltonian is defined as

$$H = \gamma \mathbf{I}.\boldsymbol{\sigma}.\mathbf{B} = \sum_{i,j=1}^{3} I_i \sigma_{ij} B_j \qquad [3]$$

in which σ is the nuclear shielding tensor. In a particular molecular frame of reference, called the principal axis system, the shielding tensor is diagonal with elements σ_{xx}, σ_{yy}, and σ_{zz}. For simplicity, the tensor will be assumed to be axially symmetric with $\sigma_{zz} = \sigma_{||}$ and $\sigma_{xx} = \sigma_{yy} = \sigma_{\perp}$. Therefore, in the principal axis system,

$$\mathrm{H} = \gamma(\sigma_{\perp} B_x I_x + \sigma_{\perp} B_y I_y + \sigma_{||} B_z I_z) \qquad [4]$$

which can be written in the form

$$H = \tfrac{1}{3}\gamma\left(\sigma_{||} + 2\sigma_{\perp}\right)\mathbf{B}\cdot\mathbf{I} + \tfrac{1}{3}\gamma\left(\sigma_{||} - \sigma_{\perp}\right)\left(2B_z I_z - B_x I_x - B_y I_y\right) \qquad [5]$$

B_x, B_y and B_z are the projections of the static field, $B_0\,\mathbf{k}$, into the principal axis reference frame and will depend on the orientation of the molecule with respect to the laboratory reference frame. Clearly, for isotropic solution,

$$\langle B_x I_x \rangle = \langle B_y I_y \rangle = \langle B_z I_z \rangle \qquad [6]$$

and the first term in [5] is invariant to rotation and the second term in [5] averages to zero under rotation. The second term is time-dependent as a consequence of rotational diffusion and influences the spins for times on the order of τ_c. To proceed, the Hamiltonian must be transformed back into the laboratory frame to give

$$H = H_{iso} + H_{CSA}(t) \qquad [7]$$

The rotationally invariant term is transformed trivially as

$$H_{iso} = \frac{1}{3}\gamma\left(\sigma_{\parallel} + 2\sigma_{\perp}\right)B_0 I_z = \gamma\sigma_{iso}B_0 I_z \qquad [8]$$

in which $\sigma_{iso} = (\sigma_{||} + 2\sigma_{\perp})/3$. More complicated algebra (or use of Wigner rotation matrices) gives the result for the anisotropic component:

$$H_{CSA}(t) = \sqrt{\tfrac{2}{3}}\gamma\left(\sigma_{\parallel} - \sigma_{\perp}\right)B_0\left\{\sqrt{\tfrac{2}{3}}Y_2^0[\Omega(t)]I_z - \tfrac{1}{2}Y_2^1[\Omega(t)]I^+ + \tfrac{1}{2}Y_2^{-1}[\Omega(t)]I^-\right\} \qquad [9]$$

in which $Y_2^q[\Omega(t)]$ are modified spherical harmonic functions (see Table 1)and $\Omega(t) = \{\theta(t), \phi(t)\}$ are the time-dependent angles defining the orientation of the z-axis of the molecular principal axis system in the laboratory frame. The term proportional to I_z represents the fluctuating longitudinal interactions (giving rise to adiabatic relaxation) and the terms proportional to I^+ and I^- represent the fluctuating transverse field (giving rise to non-adiabatic relaxation). The ensemble average chemical shift Hamiltonian has the expected form:

$$H = H_z + H_{iso} = -\gamma B_0 I_z + \gamma\sigma_{iso}B_0 I_z = -\gamma(1-\sigma_{iso})B_0 I_z \qquad [10]$$

Of course, given the above intuitive model for the origin of spin relaxation, the real problem is to determine theoretically the rate constants for relaxation due to different fluctuating Hamiltonians.

1.1 Relaxation in the Bloch equations

In the simplest theoretical approach to spin relaxation, the relaxation of isolated spins is characterized in the Bloch equations by two phenomenological first order rate constants: the *spin-lattice* or *longitudinal*

relaxation rate constant, R_1, and the *spin-spin* or *transverse* relaxation rate constant, R_2 (*4*),

$$\begin{aligned}\frac{dM_z(t)}{dt} &= \gamma\left(\mathbf{M}(t)\times\mathbf{B}(t)\right)_z - R_1\left(M_z(t)-M_0\right)\\ \frac{dM_x(t)}{dt} &= \gamma\left(\mathbf{M}(t)\times\mathbf{B}(t)\right)_x - R_2 M_x(t)\\ \frac{dM_y(t)}{dt} &= \gamma\left(\mathbf{M}(t)\times\mathbf{B}(t)\right)_y - R_2 M_y(t)\end{aligned} \qquad [11]$$

in which $\mathbf{M}(t)$ is the nuclear magnetization vector (with components $M_x(t)$, $M_y(t)$, and $M_z(t)$) and $\mathbf{B}(t)$ is the applied magnetic field (consisting of the static and rf fields). In the following, rate constants rather than time constants, are utilized; the two quantities are reciprocals of each other (for example $T_1 = 1/R_1$). The spin-lattice relaxation rate constant describes the recovery of the longitudinal magnetization to thermal equilibrium, or, equivalently, return of the populations of the energy levels of the spin system (diagonal elements of the density operator) to the equilibrium Boltzmann distribution. The spin-spin relaxation rate constant describes the decay of the transverse magnetization to zero, or equivalently, the decay of transverse single quantum coherences (off-diagonal elements of the density matrix). Non-adiabatic processes contribute to both spin-lattice and spin-spin relaxation. Adiabatic processes only contribute to spin-spin relaxation; spin-lattice relaxation is not affected because adiabatic processes do not change the populations of stationary states.

The Bloch formulation provides qualitative insights into the effects of relaxation on the NMR experiment, and the phenomenological rate constants can be measured experimentally. For example, the Bloch equations predict that the FID is the sum of exponentially damped

sinusoidal functions and that, following a pulse sequence that perturbs a spins system from equilibrium, R_2 governs the length of time that the FID can be observed and R_1 governs the minimum time required for equilibrium to be restored. The Bloch formulation does not provide a microscopic explanation of the origin or magnitude of the relaxation rate constants, nor is it extendible to more complex, coupled spin systems. For example, in dipolar-coupled two spin systems, multiple spin operators, such as zero-quantum coherence, have relaxation rate constants that differ from both R_1 and R_2.

In the spirit of the Bloch equations, the results for product operator analyses of the evolution of a spin system under a particular pulse sequence in many instances can be corrected approximately for relaxation effects by adding an exponential damping factor for each temporal period *post hoc*. Thus if product operator analysis of a two-dimensional pulse sequence yields a propagator $\mathbf{U} = \mathbf{U}_a(t_2)\mathbf{U}_m\mathbf{U}_e(t_1)\mathbf{U}_p$, in which $\mathbf{U}_p$ is the propagator for the preparation period, etc., relaxation effects approximately can be included by writing,

$$\sigma(t_1, t_2) = \mathbf{U}\sigma(0)\mathbf{U}^{-1}\exp[-R_p t_p - R_e t_1 - R_m t_m - R_a t_2] \qquad [12]$$

in which R_p is the (average) relaxation rate constant for the operators of interest during the preparation time, t_p, etc. Cross-correlation and cross-relaxation effects are assumed to be negligible.

For example, the signal recorded in a ^{1}H-^{15}N HSQC spectrum is proportional to $\cos(\omega_N t_1)\cos(\omega_H t_2)\cos(\pi J_{H^N H^\alpha} t_2)$, in which ω_N and ω_H are the Larmor frequencies of the ^{15}N and ^{1}H, respectively and $J_{H^N H^\alpha}$ is the proton scalar coupling constant between the amide and α protons. The

phenomenological approach modifies this expression to $\cos(\omega_N t_1)\cos(\omega_H t_2)\cos(\pi J_{H^N H^\alpha} t_2)$ $\exp[-R_{2N}t_1 - R_{2H}t_2]$, in which R_{2N} and R_{2H} are the transverse relaxation rate constants for the ^{15}N and ^{1}H operators present during t_1 and t_2, respectively and relaxation during the INEPT sequences has been ignored. Relaxation effects on HSQC spectra are discussed in additional detail in §6.2. As a second example, product operator analysis of the INEPT pulse sequence in the absence of relaxation, yields a density operator term proportional to $-2I_z S_y \sin(2\pi J_{IS}\tau)$. Coherence transfer is maximized for $2\tau = 1/(2J_{IS})$. If relaxation is considered, the result is modified to $-2I_z S_y \sin(2\pi J_{IS}\tau)\exp(-2R_{2I}\tau)$, in which R_{2I} is the relaxation rate of the I spin operators present during the period 2τ. Maximum coherence transfer is obtained for

$$2\tau = (\pi J_{IS})^{-1} \tan^{-1}(\pi J_{IS}/R_{2I}) \leq 1/(2J_{IS}) \qquad [13]$$

1.2 The Solomon equations

Spin-lattice relaxation for interacting spins can be treated theoretically by considering the rates of transitions of the spins between energy levels, as was demonstrated first by Bloembergen, Pound and Purcell (*5*). Figure 1 shows the energy levels for a two spin system with transition frequencies labeled. The four energy levels are labeled in the normal way as $|m_I\, m_S\rangle$. The rate constants for transitions between the energy levels are denoted by W_0, W_I, W_S and W_2 and are distinguished according to which spins change spin state during the transition. Thus, W_I denotes a relaxation process involving an I spin flip, W_S denotes a relaxation process involving an S spin flip, W_0 is a relaxation process in which both spins are flipped in opposite senses (flip-flop transition); W_2 is

a relaxation process in which both spins are flipped in the same sense (flip-flip transition). A differential equation governing the population of the state $|\alpha\alpha>$ can be written by inspection:

$$\frac{dP_{\alpha\alpha}}{dt} = -(W_I + W_S + W_2)P_{\alpha\alpha} + W_I P_{\beta\alpha} + W_S P_{\alpha\beta} + W_2 P_{\beta\beta} + K \qquad [14]$$

in which $P_{\gamma\delta}$ is the population of the state $|\gamma\delta>$ and K is a constant chosen to insure that the population $P_{\gamma\delta}$ returns to the equilibrium value $P^0_{\gamma\delta}$. The value of K can be found by setting the left hand side of [14] equal to zero:

$$K = (W_I + W_S + W_2)P^0_{\alpha\alpha} - W_I P^0_{\beta\alpha} - W_S P^0_{\alpha\beta} - W_2 P^0_{\beta\beta} \qquad [15]$$

Thus, writing $\Delta P_{\gamma\delta} = P_{\gamma\delta} - P^0_{\gamma\delta}$ yields an equation for the deviation of the population of the $|\alpha\alpha>$ state from the equilibrium population,

$$\frac{d\Delta P_{\alpha\alpha}}{dt} = -(W_I + W_S + W_2)\Delta P_{\alpha\alpha} + W_I \Delta P_{\beta\alpha} + W_S \Delta P_{\alpha\beta} + W_2 \Delta P_{\beta\beta} \qquad [16]$$

Similar equations can be written for the other three states:

$$\frac{d\Delta P_{\alpha\beta}}{dt} = -(W_0 + W_I + W_S)\Delta P_{\alpha\beta} + W_0 \Delta P_{\beta\alpha} + W_I \Delta P_{\beta\beta} + W_S \Delta P_{\alpha\alpha}$$

$$\frac{d\Delta P_{\beta\alpha}}{dt} = -(W_0 + W_I + W_S)\Delta P_{\beta\alpha} + W_0 \Delta P_{\alpha\beta} + W_I \Delta P_{\alpha\alpha} + W_S \Delta P_{\beta\beta} \qquad [17]$$

$$\frac{d\Delta P_{\beta\beta}}{dt} = -(W_I + W_S + W_2)\Delta P_{\beta\beta} + W_I \Delta P_{\alpha\beta} + W_S \Delta P_{\beta\alpha} + W_2 \Delta P_{\alpha\alpha}$$

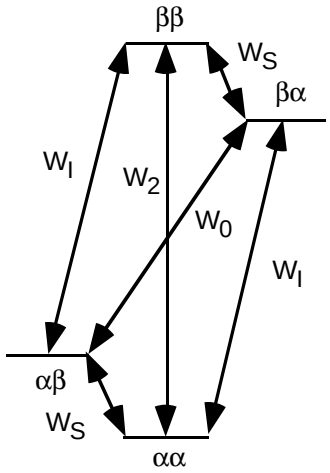

Figure 1. Transitions and associated rate constants for a two spin system.

Now utilizing $\langle I_z \rangle(t) = \mathrm{Tr}\{\sigma(t)\, I_z\} = \sigma_{11} + \sigma_{22} - \sigma_{33} - \sigma_{44} = P_{\alpha\alpha} + P_{\alpha\beta} - P_{\beta\alpha} - P_{\beta\beta}$ and $\langle S_z \rangle(t) = \mathrm{Tr}\{\sigma(t)\, S_z\} = \sigma_{11} - \sigma_{22} + \sigma_{33} - \sigma_{44} = P_{\alpha\alpha} - P_{\alpha\beta} + P_{\beta\alpha} - P_{\beta\beta}$ leads to

$$\begin{aligned} \frac{d\Delta I_z(t)}{dt} &= -(W_0 + 2W_I + W_2)\Delta I_z(t) - (W_2 - W_0)\Delta S_z(t) \\ \frac{d\Delta S_z(t)}{dt} &= -(W_0 + 2W_S + W_2)\Delta S_z(t) - (W_2 - W_0)\Delta I_z(t) \end{aligned} \qquad [18]$$

in which $\Delta I_z(t) = \langle I_z \rangle(t) - \langle I_z^0 \rangle$ and $\langle I_z^0 \rangle$ is the equilibrium magnitude of the I_z operator. Corresponding relationships hold for S_z . Making the identifications $\rho_I = W_0 + 2W_I + W_2$, $\rho_S = W_0 + 2W_S + W_2$, and $\sigma_{IS} = W_2 - W_0$ leads to the Solomon equations for a two spin system (*6*):

$$\begin{aligned} \frac{d\Delta I_z(t)}{dt} &= -\rho_I \Delta I_z(t) - \sigma_{IS}\Delta S_z(t) \\ \frac{d\Delta S_z(t)}{dt} &= -\rho_S \Delta S_z(t) - \sigma_{IS}\Delta I_z(t) \end{aligned} \qquad [19]$$

The rate constants ρ_I and ρ_S are the *auto-relaxation rate constants* (or the spin-lattice relaxation rate constants, R_{1I} and R_{1S}, in the Bloch terminology) for the I and S spins, respectively, and σ_{IS} is the *cross-relaxation rate constant* for exchange of magnetization between the two spins.

The Solomon equations easily can be extended to N interacting spins:

$$\frac{d\Delta I_{kz}(t)}{dt} = -\rho_k \Delta I_{kz}(t) - \sum_{j \neq k} \sigma_{kj} \Delta I_{jz}(t) \qquad [20]$$

in which

$$\rho_k = \sum_{k \neq j} \rho_{kj} \qquad [21]$$

reflects the relaxation of the kth spin by all other spins (in the absence of interference effects, see §2.1 below). Equation [20] written in matrix nomenclature as,

$$\frac{d\Delta \mathbf{M}_z(t)}{dt} = -\mathbf{R} \Delta \mathbf{M}_z(t) \qquad [22]$$

in which $\mathbf{R}$ is a $N \times N$ matrix with elements $R_{kk} = \rho_k$ and $R_{kj} = \sigma_{kj}$, and $\Delta \mathbf{M}_z(t)$ is a $N \times 1$ column vector with entries $\Delta M_k(t) = \Delta I_{kz}(t)$. The Solomon equations in matrix form have the formal solution:

$$\Delta \mathbf{M}_z(t) = e^{-\mathbf{R}t} \Delta \mathbf{M}_z(0) = \mathbf{U}^{-1} e^{-\mathbf{D}t} \mathbf{U} \Delta \mathbf{M}_z(0) \qquad [23]$$

in which $\mathbf{D}$ is a diagonal matrix of the eigenvalues of $\mathbf{R}$, $\mathbf{U}$ is a unitary matrix and,

$$\mathbf{D} = \mathbf{U}\mathbf{R}\mathbf{U}^{-1} \qquad [24]$$

is the similarity transformation that diagonalizes $\mathbf{R}$. These differential equations show that if the populations of the energy levels of the spin system are perturbed from equilibrium, then relaxation of a particular spin is in general a multi-exponential process.

For a two-spin system,

$$\mathbf{R} = \begin{bmatrix} \rho_I & \sigma_{IS} \\ \sigma_{IS} & \rho_S \end{bmatrix}$$

$$\mathbf{D} = \begin{bmatrix} \lambda_+ & 0 \\ 0 & \lambda_- \end{bmatrix}$$

$$\lambda_\pm = \tfrac{1}{2}\left\{ (\rho_I + \rho_S) \pm \left[(\rho_I - \rho_S)^2 + 4\sigma_{IS}^2 \right]^{1/2} \right\}$$

$$\mathbf{U} = \begin{bmatrix} \dfrac{-\sigma_{IS}}{\left[(\rho_I - \lambda_+)^2 + \sigma_{IS}^2 \right]^{1/2}} & \dfrac{-\sigma_{IS}}{\left[(\rho_I - \lambda_-)^2 + \sigma_{IS}^2 \right]^{1/2}} \\ \dfrac{\rho_I - \lambda_+}{\left[(\rho_I - \lambda_+)^2 + \sigma_{IS}^2 \right]^{1/2}} & \dfrac{\rho_I - \lambda_-}{\left[(\rho_I - \lambda_-)^2 + \sigma_{IS}^2 \right]^{1/2}} \end{bmatrix} \qquad [25]$$

and upon substituting into [23], the result obtained is

$$\begin{bmatrix} \Delta I_z(t) \\ \Delta S_z(t) \end{bmatrix} = \begin{bmatrix} a_{II}(t) & a_{IS}(t) \\ a_{SI}(t) & a_{SS}(t) \end{bmatrix} \begin{bmatrix} \Delta I_z(0) \\ \Delta S_z(0) \end{bmatrix} \qquad [26]$$

in which

$$a_{II}(t) = \tfrac{1}{2}\left[\left(1 - \frac{\rho_I - \rho_S}{(\lambda_+ - \lambda_-)} \right) \exp(-\lambda_- t) + \left(1 + \frac{\rho_I - \rho_S}{(\lambda_+ - \lambda_-)} \right) \exp(-\lambda_+ t) \right]$$

$$a_{SS}(t) = \tfrac{1}{2}\left[\left(1 + \frac{\rho_I - \rho_S}{(\lambda_+ - \lambda_-)} \right) \exp(-\lambda_- t) + \left(1 - \frac{\rho_I - \rho_S}{(\lambda_+ - \lambda_-)} \right) \exp(-\lambda_+ t) \right] \qquad [27]$$

$$a_{IS}(t) = a_{SI}(t) = \frac{-\sigma_{IS}}{(\lambda_+ - \lambda_-)} \left[\exp(-\lambda_- t) - \exp(-\lambda_+ t) \right]$$

These equations frequently are written in the form,

$$a_{II}(t) = \tfrac{1}{2}\left[\left(1 - \frac{\rho_I - \rho_S}{R_C}\right) + \left(1 + \frac{\rho_I - \rho_S}{R_C}\right)\exp(-R_C t)\right]\exp(-R_L t)$$

$$a_{SS}(t) = \tfrac{1}{2}\left[\left(1 + \frac{\rho_I - \rho_S}{R_C}\right) + \left(1 - \frac{\rho_I - \rho_S}{R_C}\right)\exp(-R_C t)\right]\exp(-R_L t) \qquad [28]$$

$$a_{IS}(t) = a_{SI}(t) = \frac{-\sigma_{IS}}{R_C}\left[1 - \exp(-R_C t)\right]\exp(-R_L t)$$

by defining the cross rate constant, R_C, and a leakage rate constant, R_L:

$$R_C = \lambda_+ - \lambda_- = [(\rho_I - \rho_S)^2 + 4\sigma_{IS}^2]^{1/2}$$

$$R_L = \lambda_- \qquad [29]$$

If $\rho_I = \rho_S = \rho$, and $\sigma_{IS} = \sigma$, [27] simplifies to:

$$a_{II}(t) = a_{SS}(t) = \tfrac{1}{2}\exp\{-(\rho - \sigma)t\}[1 + \exp(-2\sigma t)]$$

$$a_{IS}(t) = a_{SI}(t) = -\tfrac{1}{2}\exp\{-(\rho - \sigma)t\}[1 - \exp(-2\sigma t)] \qquad [30]$$

The time-dependence of the matrix elements $a_{II}(t)$ and $a_{IS}(t)$ are illustrated in Figure 2.

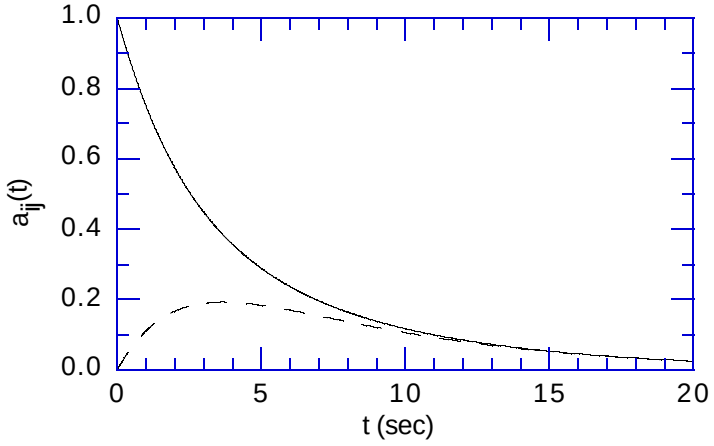

Figure 2. Time dependence of (——) $a_{II}(t)$ and (- - -) $a_{IS}(t)$ calculated using [30] with ρ = 0.30 s^{-1} and σ = -0.15 s^{-1}.

To illustrate aspects of longitudinal relaxation as exemplified by the Solomon equations, four different experiments are analyzed. For simplicity, a homonuclear spin system with $\gamma_I = \gamma_S$, $\rho_I = \rho_S = \rho$, and $\sigma_{IS} = \sigma$ are assumed. The experiments use the pulse sequence:

$$180° - t - 90° - \text{acquire} \qquad [31]$$

The initial state of the longitudinal magnetization is prepared by application of the 180° pulse to thermal equilibrium magnetization. The longitudinal magnetization relaxes according to the Solomon equations during the delay t. The final state of the longitudinal magnetization is converted into transverse magnetization by the 90° pulse and recorded during the acquisition period.

In the *selective inversion recovery* experiment, the 180° pulse is applied selectively to the I spin. The initial conditions are $\Delta I_z(0) = \langle I_z \rangle(0) - \langle I_z^0 \rangle = -2\langle I_z^0 \rangle$, and $\Delta S_z(0) = \langle S_z \rangle(0) - \langle S_z^0 \rangle = 0$. The time decay of the I spin magnetization is given by

$$\langle I_z \rangle(t) \Big/ \langle I_z^0 \rangle = 1 - \exp\{-(\rho - \sigma)t\}[1 + \exp(-2\sigma t)] \qquad [32]$$

and is generally bi-exponential. In the *initial rate regime*, the slope of the recovery curve is given by

$$\left. \frac{d\left(\langle I_z \rangle(t) \Big/ \langle I_z^0 \rangle \right)}{dt} \right|_{t=0} = 2\rho \qquad [33]$$

In the *non-selective inversion recovery* experiment, the 180° pulse is non-selective. The initial conditions are $\Delta I_z(0) = \langle I_z \rangle(0) - \langle I_z^0 \rangle = -2\langle I_z^0 \rangle$ and $\Delta S_z(0)$

= $\langle S_z \rangle(0) - \langle S_z^0 \rangle = -2\langle S_z^0 \rangle$. The time course of the I spin magnetization is given by

$$\begin{aligned} \langle I_z \rangle(t) \Big/ \langle I_z^0 \rangle &= 1 - \exp\{-(\rho - \sigma)t\}[1 + \exp(-2\sigma t)] \\ &\quad + \left(\langle S_z^0 \rangle \Big/ \langle I_z^0 \rangle \right) \exp\{-(\rho - \sigma)t\}[1 - \exp(-2\sigma t)] \\ &= 1 - 2\exp\{-(\rho + \sigma)t\} \end{aligned} \qquad [34]$$

in which the last line is obtained by using $\langle S_z^0 \rangle / \langle I_z^0 \rangle = \gamma_S / \gamma_I = 1$. The recovery curve is mono-exponential with rate constant $\rho + \sigma$. In the initial rate regime,

$$\left. \frac{d\left(\langle I_z \rangle(t) \Big/ \langle I_z^0 \rangle \right)}{dt} \right|_{t=0} = 2(\rho + \sigma) \qquad [35]$$

In the *transient NOE experiment*, the S spin longitudinal magnetization is inverted with a selective 180° pulse to produce initial conditions $\Delta I_z(0) = \langle I_z \rangle(0) - \langle I_z^0 \rangle = 0$ and $\Delta S_z(0) = \langle S_z \rangle(0) - \langle S_z^0 \rangle = -2\langle S_z^0 \rangle$. The time course of the I spin magnetization is given by

$$\begin{aligned} \langle I_z \rangle(t) \Big/ \langle I_z^0 \rangle &= 1 + \left(\langle S_z^0 \rangle \Big/ \langle I_z^0 \rangle \right) \exp\{-(\rho - \sigma)t\}[1 - \exp(-2\sigma t)] \\ &= 1 + \exp\{-(\rho - \sigma)t\}[1 - \exp(-2\sigma t)] \end{aligned} \qquad [36]$$

and is bi-exponential. In the initial-rate regime,

$$\left. \frac{d\left(\langle I_z \rangle(t) \Big/ \langle I_z^0 \rangle \right)}{dt} \right|_{t=0} = 2\sigma \qquad [37]$$

Thus, the initial rate of change of the I spin intensity in the transient NOE experiment is proportional to the cross-relaxation rate, σ. In the *decoupled*

inversion recovery experiment, the S spin is irradiated by a weak selective rf field (so as not to perturb the I spin) throughout the experiment in order to equalize the populations across the S spin transitions. In this situation, $\langle S_z \rangle(t) = 0$ for all t, and the S spins are said to be saturated. Equation [19] reduces to

$$\begin{aligned} \frac{d\langle I_z \rangle(t)}{dt} &= -\rho\left[\langle I_z \rangle(t) - \langle I_z^0 \rangle\right] + \sigma\langle S_z^0 \rangle \\ &= -\rho\left[\langle I_z \rangle(t) - \langle I_z^0 \rangle\left(1 + \frac{\sigma}{\rho}\right)\right] \end{aligned} \qquad [38]$$

Following the 180° pulse, $\Delta I_z(0) = \langle I_z \rangle(0) - \langle I_z^0 \rangle = -2\langle I_z^0 \rangle$ and the time course of the I spin magnetization is given by

$$\langle I_z \rangle(t) \Big/ \langle I_z^0 \rangle = 1 + \frac{\sigma}{\rho} - \left(2 + \frac{\sigma}{\rho}\right)\exp(-\rho t) \qquad [39]$$

In the initial-rate regime,

$$\left.\frac{d\left(\langle I_z \rangle(t) \Big/ \langle I_z^0 \rangle\right)}{dt}\right|_{t=0} = 2\rho + \sigma \qquad [40]$$

In this case, the recovery curve is mono-exponential with rate constant ρ. The above analyses indicate that, even for an isolated two spin system, the time dependence of the longitudinal magnetization usually is bi-exponential. The actual time course observed depends upon the initial condition of the spin system prepared by the NMR pulse sequence. Examples of the time courses of the I spin magnetization for these experiments are given in Figure 3.

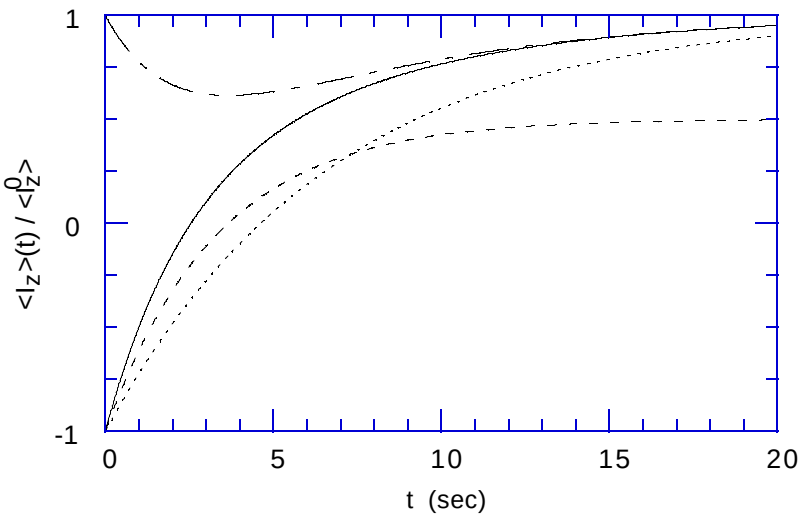

Figure 3. Magnetization decays for inversion recovery experiments. (——) selective inversion recovery calculated using [32]; (· · ·) non-selective inversion recovery calculated using [34]; (– · –) transient NOE recovery calculated using [36]; and (– – –) decoupled inversion recovery calculated using [39]. Calculations were performed for a homonuclear IS spin system with $\gamma_I = \gamma_S$, ρ = 0.30 s^{-1}, and σ = -0.15 s^{-1}.

The present derivation does not provide theoretical expressions for the transition rate constants, W_0 W_I, W_S, and W_2. Bloembergen, et al. (*5*) derived expressions for the transition rate constants; however, herein, the transition rate constants will be calculated using the semi-classical relaxation theory as described in §2. As will be shown, the transition rate constants depend upon the different frequency components of the stochastic magnetic fields [113]. Thus, the transition characterized by W_I is induced by molecular motions that produce fields oscillating at the Larmor frequency of the I spin, and the transition characterized by W_S is induced by molecular motions that produce fields oscillating at the Larmor frequency of the S spin. The W_0 pathway is induced by fields oscillating at the *difference* of the Larmor frequencies of the I and S spins, and the W_2 pathway is induced by fields oscillating at the *sum* of the Larmor frequencies of the two spins. Most importantly, the cross-relaxation rate constant is non-zero only if $W_2 - W_0 \neq 0$; therefore, the relaxation mechanism must generate non-zero rate constants for the flip-flip (double

quantum) and flip-flop (zero-quantum) transitions. For biological macromolecules, dipolar coupling between nuclear spins is the main interaction for which W_2 and W_0 are non-zero. The Solomon equations are central to the study of the NOE and will be discussed in additional detail in §7.

1.3 Bloch, Wangsness and Redfield theory

A microscopic semi-classical theory of spin relaxation was formulated by Bloch, Wangsness and Redfield (BWR) and has proven to be the most useful approach for practical applications (*7*, *8*). In the semi-classical approach the spin system is treated quantum mechanically and the surroundings (the heat bath or lattice) are treated classically. This treatment suffers primarily from the defect that the spin system evolves toward a final state in which energy levels of the spin system are populated equally. Equivalently, the semi-classical theory is formally correct only for an infinite Boltzmann spin temperature; at finite temperatures, an *ad hoc* correction is required to the theory to ensure that the spin system relaxes toward an equilibrium state in which the populations are described by a Boltzmann distribution. A fully quantum mechanical treatment of spin relaxation overcomes this defect and predicts the proper approach to equilibrium; however, the computational details of the quantum mechanical relaxation theory are outside the scope of this text (*2*, *8*).

2 The Master Equation

In the semi-classical theory of spin relaxation, the Hamiltonian for the system is written as the sum of a deterministic quantum-mechanical

Hamiltonian that acts only on the spin system, $H_{det}(t)$ and a stochastic Hamiltonian, $H_1(t)$ that couples the spin system to the lattice:

$$H(t) = H_{det}(t) + H_1(t) = H_0 + H_{rf}(t) + H_1(t) \quad [41]$$

in which H_0 represents the Zeeman and scalar coupling Hamiltonians and $H_{rf}(t)$ is the Hamiltonian for any applied rf fields. The Liouville equation of motion of the density operator is:

$$d\sigma(t)/dt = -i\ [H(t), \sigma(t)] \quad [42]$$

The Hamiltonians $H_{rf}(t)$ and $H_1(t)$ are regarded as time-dependent perturbations acting on the main time-independent Hamiltonian, H_0. The explicit influence of H_0 can be removed by transforming the Liouville equation into a new reference frame, which is called conventionally the *interaction frame*. In the absence of an applied rf field (see §2.3 for the effects of rf fields), the density operator and stochastic Hamiltonian in the interaction frame are defined as

$$\sigma^T(t) = \exp\{iH_0t\}\ \sigma(t)\ \exp\{-iH_0t\} \quad [43]$$

$$H_1^T(t) = \exp\{iH_0t\}\ H_1(t)\ \exp\{-iH_0t\} \quad [44]$$

The form of the transformed Liouville equation is determined as follows:

$$\frac{d\boldsymbol{\sigma}^T(t)}{dt} = i\exp(iH_0t)H_0\boldsymbol{\sigma}(t)\exp(-iH_0t) - i\exp(iH_0t)\boldsymbol{\sigma}(t)H_0\exp(-iH_0t)$$
$$+\exp(iH_0t)\frac{d\boldsymbol{\sigma}(t)}{dt}\exp(-iH_0t)$$
$$= i\exp(iH_0t)[H_0,\boldsymbol{\sigma}(t)]\exp(-iH_0t) - i\exp(iH_0t)[H_0 + H_1(t),\boldsymbol{\sigma}(t)]\exp(-iH_0t)$$
$$= -i\exp(iH_0t)[H_1(t),\boldsymbol{\sigma}(t)]\exp(-iH_0t)$$
$$= -i\exp(iH_0t)H_1(t)\boldsymbol{\sigma}(t)\exp(-iH_0t) + i\exp(iH_0t)\boldsymbol{\sigma}(t)H_1(t)\exp(-iH_0t)$$
$$= -iH_1^T(t)\boldsymbol{\sigma}^T(t) + i\boldsymbol{\sigma}^T(t)H_1^T(t)$$

[45]

with the final result that,

$$d\sigma^T(t)/dt = -i\ [H_1^T(t),\ \sigma^T(t)] \qquad [46]$$

The transformation into the interaction frame is isomorphous to the rotating frame transformation; however, important differences exist between the two. The rotating frame transformation removes the explicit time-dependence of the rf Hamiltonian and renders the Hamiltonian time-independent in the rotating frame. The Hamiltonian H_0 is active in the rotating frame. The interaction frame transformation removes the explicit dependence on H_0; however, $H_1^T(t)$ remains time dependent. As discussed in §2.3, the rotating frame and interaction frame transformations are performed sequentially in some circumstances.

Equation [46] can be solved by successive approximations to second order as illustrated below. First, [46] is formally integrated:

$$\frac{d\boldsymbol{\sigma}^T(t')}{dt'} = -i\left[H_1^T(t'), \boldsymbol{\sigma}^T(t')\right]$$

$$\int_0^t d\boldsymbol{\sigma}^T(t') = -i\int_0^t dt'\left[H_1^T(t'), \boldsymbol{\sigma}^T(t')\right] \qquad [47]$$

$$\boldsymbol{\sigma}^T(t) = \boldsymbol{\sigma}^T(0) - i\int_0^t dt'\left[H_1^T(t'), \boldsymbol{\sigma}^T(t')\right]$$

The last line of [47] can be written equivalently as

$$\boldsymbol{\sigma}^T(t') = \boldsymbol{\sigma}^T(0) - i\int_0^{t'} dt''\left[H_1^T(t''), \boldsymbol{\sigma}^T(t'')\right] \qquad [48]$$

If [48] is substituted for $\sigma^T(t')$ in [47], the result obtained is

$$\boldsymbol{\sigma}^T(t) = \boldsymbol{\sigma}^T(0) - i\int_0^t dt'\left[H_1^T(t'), \boldsymbol{\sigma}^T(0) - i\int_0^{t'} dt''\left[H_1^T(t''), \boldsymbol{\sigma}^T(t'')\right]\right]$$

$$= \boldsymbol{\sigma}^T(0) - i\int_0^t dt'\left[H_1^T(t'), \boldsymbol{\sigma}^T(0)\right] - \int_0^t dt'\int_0^{t'} dt''\left[H_1^T(t'), \left[H_1^T(t''), \boldsymbol{\sigma}^T(t'')\right]\right] \qquad [49]$$

Repeating the above, procedure, [49] can be written as

$$\boldsymbol{\sigma}^T(t'') = \boldsymbol{\sigma}^T(0) - i\int_0^{t''} dt'\left[H_1^T(t'), \boldsymbol{\sigma}^T(0)\right] - \int_0^{t''} dt'\int_0^{t'} dt'''\left[H_1^T(t'), \left[H_1^T(t'''), \boldsymbol{\sigma}^T(t''')\right]\right] \qquad [50]$$

and substituted for $\sigma^T(t'')$ in [49] to yield

$$\boldsymbol{\sigma}^T(t) = \boldsymbol{\sigma}^T(0) - i\int_0^t dt'\left[H_1^T(t'), \boldsymbol{\sigma}^T(0)\right] - \int_0^t dt'\int_0^{t'} dt''\left[H_1^T(t'), \left[H_1^T(t''), \boldsymbol{\sigma}^T(0)\right]\right]$$
$$+ \textit{higher order terms} \qquad [51]$$

If the higher order terms are dropped, then all three terms on the left of the equal sign depend on $\sigma^T(0)$. Having truncated the expansion for $\sigma^T(t)$ to second order, a differential equation for $\sigma^T(t)$ can now be derived. First, [51] is differentiated to yield

$$\frac{\boldsymbol{\sigma}^T(t)}{dt} = -i\left[H_1^T(t), \boldsymbol{\sigma}^T(0)\right] - \int_0^t dt''\left[H_1^T(t), \left[H_1^T(t''), \boldsymbol{\sigma}^T(0)\right]\right] \qquad [52]$$

Next a change of variable $\tau = t - t''$ yields

$$\frac{\boldsymbol{\sigma}^T(t)}{dt} = -i\left[H_1^T(t), \boldsymbol{\sigma}^T(0)\right] - \int_0^t d\tau\left[H_1^T(t), \left[H_1^T(t-\tau), \boldsymbol{\sigma}^T(0)\right]\right] \qquad [53]$$

This equation describes the evolution of the density operator for a particular realization of $H_1(t)$. To obtain the corresponding equation for a macroscopic sample, both sides of the equation must be averaged over the ensemble of subsystems (each described by a particular realization of $H_1(t)$). The ensemble average is performed under the following assumptions:

1. The ensemble average of $H_1^T(t)$ is zero. Any components of $H_1^T(t)$ that do not vanish upon ensemble averaging can be incorporated into H_0.
2. $H_1^T(t)$ and $\sigma^T(t)$ are uncorrelated so that the ensemble average can be taken independently for each quantity.
3. The characteristic correlation time for $H_1^T(t)$, τ_c, is much shorter than t. In liquids, τ_c is on the order of the rotational diffusion correlation time for the molecule, 10^{-12}–10^{-18} s.

The result after performing the ensemble average is

$$\frac{d\boldsymbol{\sigma}^T(t)}{dt} = -\int_0^t d\tau \overline{[H_1^T(t),[H_1^T(t-\tau),\boldsymbol{\sigma}^T(0)]]} \qquad [54]$$

in which the overbar indicates ensemble averaging over the stochastic Hamiltonians and $\sigma^T(t)$ now designates the ensemble average of the density matrix (the overbar is omitted). Equation [54] is converted into a differential equation for $\sigma^T(t)$ by making a number of *a priori* assumptions whose plausibility can be evaluated *post facto*:

1. $\sigma^T(0)$ can be replaced with $\sigma^T(t)$ on the right hand side of [54]. Eventually, the present theory will predict that the relaxation rate constants for the density matrix elements, σ_{ij}, are on the order of $R_{ij} = \overline{H_1^2(t)}\tau_c$. To first order, the fractional change in $\sigma(t)$ is given by $[\sigma(t) - \sigma(0)] / \sigma(0) = -R_{ij}t$. For a time $t << 1/R_{ij}$, $\sigma(t)$ and $\sigma(0)$ differ negligibly and $\sigma^T(t)$ can be substituted for $\sigma^T(0)$ in [54].

2. The limit of the integral can be extended from t to infinity. For times $\tau >> \tau_c$, $H_1^T(t)$ and $H_1^T(t-\tau)$ are uncorrelated and the value of the integrand in [54] is zero. Therefore, if $t >> \tau_c$, extending the limit to infinity does not affect the value of the integral.

3. $\sigma^T(t)$ can be replaced by $\sigma^T(t) - \sigma_0$, in which

$$\sigma_0 = \exp[-i\mathrm{h}H_0/(k_BT)]/\mathrm{Tr}\{\exp[-i\mathrm{h}H_0/(k_BT)]\} \qquad [55]$$

is the equilibrium density operator. By construction, $\sigma_0^T = \sigma_0$. This assumption insures that the spin system relaxes toward

thermal equilibrium. The term σ_0 naturally enters the differential equation in a full quantum mechanical derivation.

More detailed discussion of the range of validity of these assumptions can be found elsewhere (*2*, *3*). The resulting differential equation is

$$\frac{d\boldsymbol{\sigma}^T(t)}{dt} = -\int_0^\infty d\tau \overline{[H_1^T(t),[H_1^T(t-\tau),\boldsymbol{\sigma}^T(t)-\boldsymbol{\sigma}_0]]} \qquad [56]$$

which is valid for a "coarse-grained time scale" given by $\tau_c << t << \left(\overline{H_1^2(t)}\tau_c\right)^{-1}$. The restrictions on t would appear to constitute a fatal weakness because relaxation in NMR experiments normally must be considered for times $T > 1/R_{ij}$. To rectify this, T is defined as $T = nt$, in which n is an integer and t satisfies the above "coarse-grained" temporal restrictions, and relaxation over the period T is calculated by piecewise evaluation of [56] for each of the n intervals in succession.

To proceed further, the stochastic Hamiltonian is decomposed as

$$H_1(t) = \sum_{q=-k}^{k} F_k^q(t)\mathbf{A}_k^q \qquad [57]$$

in which $F_k^q(t)$ is a random function of spatial variables and $\mathbf{A}_k^q$ is a tensor spin operator (*2*, *9*, *10*). Additionally, $\mathbf{A}_k^{-q} \equiv \mathbf{A}_k^{q\dagger}$ and $F_k^{-q}(t) \equiv F_k^{q*}(t)$. For the Hamiltonians of interest in NMR spectroscopy, the rank of the tensor operator, k, is one or two, and the decomposition is always possible. To proceed, the operators $\mathbf{A}_k^q$ are expanded in terms of basis operators,

$$\mathbf{A}_k^q = \sum_p \mathbf{A}_{kp}^q = \sum_p c_p^q H_p \qquad [58]$$

that satisfy the relationship:

$$\left[H_0, H_p\right] = \omega_p H_p \qquad [59]$$

H_p and ω_p are called the eigenfunctions and eigenfrequencies of the Hamiltonian commutation superoperator. Equation [59] implies the additional property,

$$\exp\left(-iH_0 t\right) H_p \exp\left(iH_0 t\right) = \exp\left(-i\omega_p t\right) H_p \qquad [60]$$

which can be proven as follows. First,

$$\begin{aligned} &\frac{d}{dt}\left\{\exp\left(-iH_0 t\right) H_p \exp\left(iH_0 t\right)\right\} \\ &\quad = -i\exp\left(-iH_0 t\right) H_0 H_p \exp\left(iH_0 t\right) + i\exp\left(-iH_0 t\right) H_p H_0 \exp\left(iH_0 t\right) \\ &\quad = -i\exp\left(-iH_0 t\right)\left[H_0, H_p\right]\exp\left(iH_0 t\right) \\ &\quad = -i\omega_p \exp\left(-iH_0 t\right) H_p \exp\left(iH_0 t\right) \end{aligned} \qquad [61]$$

which implies:

$$\frac{d^n}{dt^n}\left\{\exp\left(-iH_0 t\right) H_p \exp\left(iH_0 t\right)\right\} = \left(-i\omega_p\right)^n \exp\left(-iH_0 t\right) H_p \exp\left(iH_0 t\right) \qquad [62]$$

Therefore, the Taylor series expansion of the left hand side of [60] is

$$\begin{aligned} &\exp\left(-iH_0 t\right) H_p \exp\left(iH_0 t\right) \\ &\quad = H_p - i\omega_p t H_p + \tfrac{1}{2}\omega_p^2 t^2 H_p + \ldots \\ &\quad = \left\{1 - i\omega_p t + \tfrac{1}{2}\omega_p^2 t^2 + \ldots\right\} H_p \\ &\quad = \exp\left(-i\omega_p t\right) H_p \end{aligned} \qquad [63]$$

which completes the proof.

For example, if $H_0 = \omega_I I_z + \omega_S S_z$, then the single element operator $2I_zS^+ = I^\alpha S^+ - I^\beta S^+ = |\alpha\alpha><\alpha\beta| - |\beta\alpha><\beta\beta|$ is an eigenoperator with eigenfrequency ω_S:

$$\begin{aligned}
&\left[H_0, I^\alpha S^+ - I^\beta S^+\right] \\
&\quad = \left(\omega_I I_z + \omega_S S_z\right)\left(|\alpha\alpha\rangle\langle\alpha\beta| - |\beta\alpha\rangle\langle\beta\beta|\right) - \left(|\alpha\alpha\rangle\langle\alpha\beta| - |\beta\alpha\rangle\langle\beta\beta|\right)\left(\omega_I I_z + \omega_S S_z\right) \\
&\quad = \omega_I\left(I_z|\alpha\alpha\rangle\langle\alpha\beta| - I_z|\beta\alpha\rangle\langle\beta\beta| - |\alpha\alpha\rangle\langle\alpha\beta|I_z + |\beta\alpha\rangle\langle\beta\beta|I_z\right) \\
&\qquad + \omega_S\left(S_z|\alpha\alpha\rangle\langle\alpha\beta| - S_z|\beta\alpha\rangle\langle\beta\beta| - |\alpha\alpha\rangle\langle\alpha\beta|S_z + |\beta\alpha\rangle\langle\beta\beta|S_z\right) \\
&\quad = \tfrac{1}{2}\omega_I\left(|\alpha\alpha\rangle\langle\alpha\beta| + |\beta\alpha\rangle\langle\beta\beta| - |\alpha\alpha\rangle\langle\alpha\beta| - |\beta\alpha\rangle\langle\beta\beta|\right) \\
&\qquad + \tfrac{1}{2}\omega_S\left(|\alpha\alpha\rangle\langle\alpha\beta| - |\beta\alpha\rangle\langle\beta\beta| + |\alpha\alpha\rangle\langle\alpha\beta| - |\beta\alpha\rangle\langle\beta\beta|\right) \\
&\quad = \omega_S\left(|\alpha\alpha\rangle\langle\alpha\beta| - |\beta\alpha\rangle\langle\beta\beta|\right) \\
&\quad = \omega_S\left(I^\alpha S^+ - I^\beta S^+\right)
\end{aligned} \qquad [64]$$

Applying [60], in the interaction frame,

$$\begin{aligned}
\mathbf{A}_k^{qT} &= \exp\{iH_0t\}\mathbf{A}_k^q\exp\{-iH_0t\} = \sum_p \exp\{iH_0t\}\mathbf{A}_{kp}^q\exp\{-iH_0t\} \\
&= \sum_p \mathbf{A}_{kp}^q\exp\{i\omega_p t\}
\end{aligned} \qquad [65]$$

$$\begin{aligned}
\mathbf{A}_k^{-qT} &= \exp\{iH_0t\}\mathbf{A}_k^{-q}\exp\{-iH_0t\} = \sum_p \exp\{iH_0t\}\mathbf{A}_{kp}^{-q}\exp\{-iH_0t\} \\
&= \sum_p \mathbf{A}_{kp}^{-q}\exp\{-i\omega_p t\}
\end{aligned} \qquad [66]$$

Substituting [57], [65] and [66] into [56] yields

$$\begin{aligned}
\frac{d\boldsymbol{\sigma}^T(t)}{dt} = &-\sum_{q,q'}\sum_{p,p'}\exp\{i(-\omega_{p'}+\omega_p)t\}[\mathbf{A}_{kp'}^{q'},[\mathbf{A}_{kp}^q,\boldsymbol{\sigma}^T(t)-\boldsymbol{\sigma}_0]] \\
&\times\int_0^\infty \overline{F_k^{q'}(t)F_k^q(t-\tau)\exp\{-i\omega_p\tau\}}d\tau
\end{aligned} \qquad [67]$$

The imaginary part of the integral leads to second order frequency shifts of the resonance lines, which are called dynamic frequency shifts; these shifts may be included in H_0 and are not considered further. Considering only the real part of the integral, [67] can be written as

$$\frac{d\boldsymbol{\sigma}^T(t)}{dt} = -\tfrac{1}{2}\sum_q \sum_{p,p'} \exp\{i(-\omega_{p'} + \omega_p)t\}[\mathbf{A}^{-q}_{kp'}, [\mathbf{A}^{q}_{kp}, \boldsymbol{\sigma}^T(t) - \boldsymbol{\sigma}_0]]j^q(\omega_p) \qquad [68]$$

in which the power spectral density function, $j^q(\omega)$, is given by

$$\begin{aligned} j^q(\omega) &= \mathrm{Re}\left\{ \int_{-\infty}^{\infty} \overline{F_k^{-q}(t) F_k^{q}(t-\tau)} \exp\{-i\omega\tau\} d\tau \right\} \\ &= \mathrm{Re}\left\{ \int_{-\infty}^{\infty} \overline{F_k^{q}(t) F_k^{-q}(t+\tau)} \exp\{-i\omega\tau\} d\tau \right\} \end{aligned} \qquad [69]$$

and the random processes $F_k^q(t)$ and $F_k^{q'}(t)$ have been assumed to be statistically independent unless $q' = -q$; therefore, the ensemble average in [67] vanishes if $q' \neq -q$. Terms in [68] in which $|\omega_p - \omega_{p'}| >> 0$ are *non-secular* in the sense of perturbation theory , and do not affect the long-time behavior of $\sigma^T(t)$ because the rapidly oscillating factors $\exp\{i(-\omega_{p'} + \omega_p)\}$ average to zero much more rapidly than relaxation occurs. Furthermore, if none of the eigenfrequencies are degenerate, terms in [68] are *secular* and non-zero only if $p = p'$; thus,

$$\frac{d\sigma^T(t)}{dt} = -\tfrac{1}{2}\sum_q \sum_p [\mathbf{A}^{-q}_{kp}, [\mathbf{A}^{q}_{kp}, \sigma^T(t) - \sigma_0]]j^q(\omega_p) \qquad [70]$$

This equation can be transformed to the laboratory frame to yield the Liouville–von Neuman differential equation for the density operator:

$$\frac{d\boldsymbol{\sigma}(t)}{dt} = -i[H_0, \boldsymbol{\sigma}(t)] - \hat{\boldsymbol{\Gamma}}(\boldsymbol{\sigma}(t) - \boldsymbol{\sigma}_0) \qquad [71]$$

in which the relaxation superoperator is

$$\hat{\boldsymbol{\Gamma}} = \tfrac{1}{2}\sum_q \sum_p j^q(\omega_p)[\mathbf{A}_{kp}^{-q}, [\mathbf{A}_{kp}^{q}, \ ]] \qquad [72]$$

Two critical requirements for a stochastic Hamiltonian to be effective in causing relaxation are encapsulated in [71]: (*i*) the double commutator $[\mathbf{A}_{kp}^{-q}, [\mathbf{A}_{kp}^{q}, \sigma(t) - \sigma_0]]$ must not vanish, and (*ii*) the spectral density function for the random process that modulates the spin interactions must have significant components at the characteristic frequencies of the spin system, ω_p. The former requirement can be regarded as a kind of selection rule for whether the term in the stochastic Hamiltonian that depends upon the operator **A** is effective in causing relaxation of the density operator. In most cases, the stochastic random process is a consequence of molecular reorientational motions. This observation is central to the dramatic differences in spin relaxation and, thus, in NMR spectroscopy, of rapidly rotating small molecules and slowly rotating macromolecules.

Equation [71] can be converted into an equation for product operator, or other basis operators, by expanding the density operator in terms of the basis operators to yield the matrix form of the master equation,

$$db_r(t)/dt = \sum_s \{-i\Omega_{rs} b_s(t) - \Gamma_{rs}[b_s(t) - b_{s0}]\} \qquad [73]$$

in which

$$\Omega_{rs} = <\mathbf{B}_r | [H_0, \mathbf{B}_s] > / <\mathbf{B}_r | \mathbf{B}_r > \qquad [74]$$

is a characteristic frequency,

$$\Gamma_{rs} = <\mathbf{B}_r|\hat{\Gamma}\mathbf{B}_s> / <\mathbf{B}_r|\mathbf{B}_r>$$
$$= \frac{1}{2}\sum_q\sum_p \{<\mathbf{B}_r|[\mathbf{A}_{kp}^{-q},[\mathbf{A}_{kp}^{q},\mathbf{B}_s]]> / <\mathbf{B}_r|\mathbf{B}_r>\} j^q(\omega_p) \quad [75]$$

is the rate constant for relaxation between the operators $\mathbf{B}_r$ and $\mathbf{B}_s$, and

$$b_j(t) = <\mathbf{B}_j|\sigma(t)> \quad [76]$$

For normalized basis operators with $\mathrm{Tr}\{\mathbf{B}_r{}^2\} = \mathrm{Tr}\{\mathbf{B}_s{}^2\}$, $\Gamma_{rs} = \Gamma_{rs}$. Equations [73]-[76] are the main results of this section for relaxation in the laboratory reference frame. As shown by [73], the evolution of the base operators for a spin system is described by a set of coupled differential equations. Diagonal elements Γ_{rr} are the rate constants for auto- or self-relaxation of $\mathbf{B}_r$; off-diagonal elements Γ_{rs} are the rate constants for cross-relaxation between $\mathbf{B}_r$ and $\mathbf{B}_s$. Cross-relaxation between operators with different coherence orders is precluded as a consequence of restricting [73] to secular contributions; for example, cross-relaxation does not occur between zero and single quantum coherence. Furthermore, if none of the transitions in the spin system are degenerate (to within approximately a linewidth), then cross-relaxation rate constants between off-diagonal elements of the density operator in the laboratory reference frame are also zero. Consequently, the matrix of relaxation rate constants between operators has a characteristic block diagonal form, known as the Redfield kite, illustrated in Figure 4.

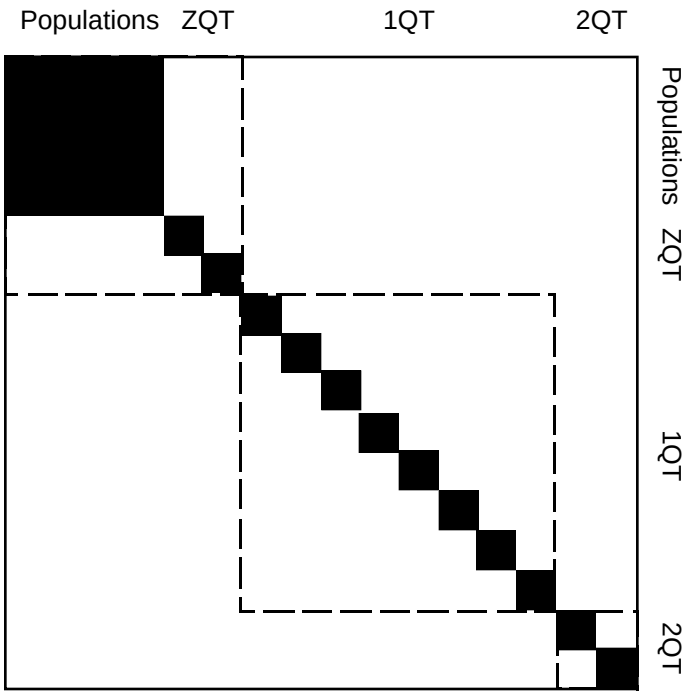

Figure 4. Redfield kite. Solid blocks indicate non-zero relaxation rate constants between operators in the absence of degenerate transitions. Populations have non-zero cross relaxation rate constants, but all other coherences relax independently. If transitions are degenerate, the dashed blocks indicate the additional non-zero cross relaxation rate constants observed between coherences with the same coherence level.

Calculation of relaxation rate constants involves two steps: (*i*) calculation of the double commutator and trace formation over the spin variables, and (*ii*) calculation of the spectral density function. These two calculations are pursued in the following sections.

2.1 Interference effects

In many instances, more than one stochastic Hamiltonian capable of causing relaxation of a given spin may be operative. In this circumstance, equation [57] is generalized to

$$H_1(t) = \sum_m \sum_{q=-k}^{k} F^q_{mk}(t)\,\mathbf{A}^q_{mk} \qquad [77]$$

in which the summation over the index m refers to the different relaxation interactions or stochastic Hamiltonians. Using [77] rather than [57] in the above derivation leads once more to [73] with Γ_{rs} given by a generalization of [75]

$$\Gamma_{rs} = \frac{1}{2}\sum_m \sum_q \sum_p \{< \mathbf{B}_r | [\mathbf{A}^{-q}_{mkp}, [\mathbf{A}^{q}_{mkp}, \mathbf{B}_s]] > / < \mathbf{B}_r | \mathbf{B}_r >\} j^q(\omega_p)$$

$$+ \frac{1}{2} \sum_{\substack{m,n \\ m \neq n}} \sum_q \sum_p \{< \mathbf{B}_r | [\mathbf{A}^{-q}_{mkp}, [\mathbf{A}^{q}_{nkp}, \mathbf{B}_s]] > / < \mathbf{B}_r | \mathbf{B}_r >\} j^q_{mn}(\omega_p) \qquad [78]$$

$$= \sum_m \Gamma^m_{rs} + \sum_{\substack{m,n \\ m \neq n}} \Gamma^{mn}_{rs}$$

in which the cross-spectral density is

$$j^q_{mn}(\omega) = \mathrm{Re}\left\{ \int_{-\infty}^{\infty} \overline{F^q_{mk}(t) F^{-q}_{nk}(t+\tau)} \exp\{-i\omega\tau\} d\tau \right\} \qquad [79]$$

Γ^m_{rs} is the relaxation rate due to the mth relaxation mechanism and Γ^{mn}_{rs} is the relaxation rate constant arising from interference or cross-correlation between the mth and nth relaxation mechanisms.

Clearly, $j^q_{mn}(\omega) = 0$ unless the random processes $F^q_{mk}(t)$ and $F^q_{nk}(t)$ are correlated. In the absence of correlation between the different relaxation mechanisms, $\Gamma^{mn}_{rs} = 0$ for all m and n and each mechanism contributes additively to relaxation of the spin system.

The two most frequently encountered interference or cross-correlation effects in biological macromolecules are interference between dipolar and anisotropic chemical shift (CSA) interactions; and interference between the dipolar interactions of different pairs of spins. The prototypical example of the former is the interference between the dipolar and CSA interactions for ^{15}N (*11*). The prototypical example of the latter is the interference between the dipolar interactions in a I_2S or I_3S spin system such as a methylene (I_2 represents the two methylene protons; S represents either a remote proton or the methylene ^{13}C) or methyl group

(I_3 represents the three methyl protons; S represents either a remote proton or the methyl ^{13}C) (*12*). Most importantly, interference effects can result in cross relaxation between pairs of operators for which cross relaxation would not be observed otherwise. Thus, the observation of otherwise "forbidden" cross relaxation pathways is one of the hallmarks of interference effects (*13*).

2.2 Like and unlike spins

A distinction frequently is made between like and unlike spins and relaxation rate constants are derived independently for each case (*2*). Like spins are defined as spins with identical Larmor frequencies and unlike spins are defined as spins with widely different Larmor frequencies. Such distinctions can obscure the generality of the theory embodied in [73]. In actuality, the presence of spins with degenerate Larmor frequencies has straightforward consequences for relaxation. First, particular operators $\mathbf{A}_{kp}^{q}$ in [57] may become degenerate (i.e. have the same eigenfrequency, ω_p) and are therefore secular with respect to each other. Thus, prior to applying the secular condition, the set of $\mathbf{A}_{kp}^{q}$ must be redefined as

$$\mathbf{A}_{kp}^{q} = \sum_{m} \mathbf{A}_{km}^{q} \qquad [80]$$

in which the summation extends over the operators for $\mathbf{A}_{km}^{q}$ for which $\omega_p = \omega_m$. For example, operators $\mathbf{A}_{km}^{q}$ with eigenfrequencies of 0 and ω_I - ω_S belong to different orders p for unlike spins; the eigenfrequencies are degenerate for like spins and the corresponding operators would be summed to yield a single operator with eigenfrequency of zero. Second, for spins that are magnetically equivalent, such as the three protons in a methyl group, basis operators that exhibit the maximum symmetry of the

chemical moiety can be derived using group theoretical methods (*9, 14*). Although such basis operators simplify the resulting calculations, the group theoretical treatment of relaxation of magnetically equivalent spins is beyond the scope of the present text; the interested reader is referred to the original literature (*9, 14*). As the distinction between like and unlike spins is artificial within the framework of the semi-classical relaxation theory, the following discussions will focus on spin systems without degenerate transitions; results of practical interest that arise as a consequence of degeneracy will be presented as necessary.

2.3 Relaxation in the rotating frame

In the presence of an applied rf field (for example in a ROESY or TOCSY experiment), the transformation into the interaction frame involves first a transformation into a rotating frame to remove the time dependence of $H_{RF}(t)$ followed by transformation into the interaction frame of the resulting time independent Hamiltonian. If $H_0 \approx H_z$, that is if the Zeeman Hamiltonian is dominant (i.e. ignoring the scalar coupling Hamiltonian), then the interaction frame is equivalent to a doubly rotating tilted frame. For macromolecules with $\omega_1 \tau_c << 1$, in which $\omega_1 = -\gamma B_1$ is the strength of the applied rf field and τ_c is the rotational correlation time of the molecule, $j^q(\omega + \omega_1) \approx j^q(\omega)$, and approximate values for the relaxation rate constants in the rotating frame can be calculated using [76] in which the operators $\mathbf{B}_r$ and $\mathbf{B}_s$ are replaced by the corresponding operators in the tilted frame, $\mathbf{B}'_r$ and $\mathbf{B}'_s$. Thus,

$$\begin{aligned} \Gamma'_{rs} &= < \mathbf{B}'_r | \hat{\Gamma} \mathbf{B}'_s > / < \mathbf{B}'_r | \mathbf{B}'_r > \\ &= \frac{1}{2} \sum_q \sum_p \{ < \mathbf{B}'_r | [\mathbf{A}^{-q}_{kp}, [\mathbf{A}^{q}_{kp}, \mathbf{B}'_s]] > / < \mathbf{B}'_r | \mathbf{B}'_r > \} j^q(\omega_p) \end{aligned} \qquad [81]$$

For an rf field applied with x-phase, the Cartesian operators are transformed as

$$\begin{bmatrix} I'_x \\ I'_y \\ I'_z \end{bmatrix} = \begin{bmatrix} \cos\theta_I & 0 & -\sin\theta_I \\ 0 & 1 & 0 \\ \sin\theta_I & 0 & \cos\theta_I \end{bmatrix} \begin{bmatrix} I_x \\ I_y \\ I_z \end{bmatrix} \qquad [82]$$

in which

$$\tan\theta_I = \omega_1/(\omega_I - \omega_0) \qquad [83]$$

and $\omega_I - \omega_0$ is the resonance offset frequency in the rotating reference frame (if $\mathbf{B}_r$ and $\mathbf{B}_s$ refer to different spins, then θ_I may differ for each spin). The relative orientation of the tilted and untilted reference frames are illustrated in Figure 5. If $\theta_I = 0$, either because $\omega_1 = 0$ or because $\omega_1 << |\omega_I - \omega_0|$, [81] reduces to [76]; if the rf field is applied on-resonance ($\omega_I = \omega_0$), $\theta_I = \pi/2$. If the rf field is applied midway between the Larmor frequencies of two spins, or if $\omega_1 >> \omega_I - \omega_0$ for the spins of interest, then the effective frequencies in the rotating frame are degenerate, and the relaxation superoperator in the rotating frame is calculated as for like spins (§2.2).

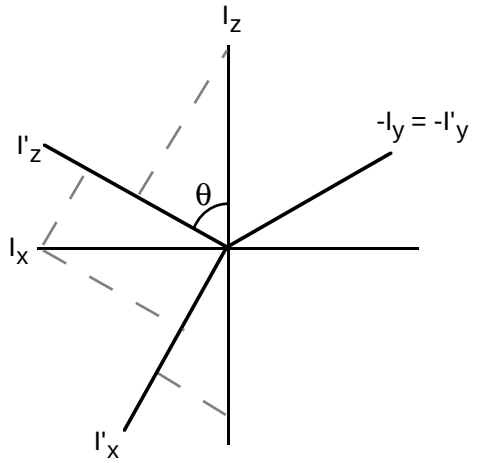

Figure 5. Relative orientations of the laboratory and tilted reference frames used to determine the transformation [82].

In general, operators that do not commute with the Hamiltonian in the rotating frame decay rapidly as a consequence of rf inhomogeneity. Thus, if a CW rf field is applied, as in a ROESY experiment, only operators with effective frequencies in the rotating frame equal to zero must be considered; such operators are usually limited to longitudinal operators and homonuclear zero quantum operators. If the rf field is phase modulated to compensate for resonance offset and rf inhomogeneity, e.g. by applying the DIPSI-2 or other coherent decoupling scheme, single and multiple quantum operators also must be considered (*15*). For operators containing transverse components in the rotating frame, the relaxation rate constant given by [81] is an instantaneous rate constant; the effective average rate constant is obtained by averaging the rate constant over the trajectory followed by the operator under the influence of the Hamiltonian in the rotating frame (*16*).

3 Spectral density functions

A general expression for the spectral density function is given by [69]. For relaxation in isotropic liquids in the high-temperature limit (*17*),

$$j^q(\omega) = (-1)^q j^0(\omega) \equiv (-1)^q j(\omega) \qquad [84]$$

therefore, only one auto-spectral density function need be calculated. The relaxation mechanisms of interest in the present context arise from tensorial operators of rank $k = 2$. The random functions $F_2^0(t)$ can be written in the form

$$F_2^0(t) = c_0(t)\, Y_2^0[\Omega(t)] \qquad [85]$$

and, consequently,

$$j(\omega) = \mathrm{Re}\left\{ \int_{-\infty}^{\infty} \overline{c_0(t)c_0(t+\tau)Y_2^0[\Omega(t)]Y_2^0[\Omega(t+\tau)]} \exp(-i\omega\tau)\, d\tau \right\}$$
$$= \mathrm{Re}\left\{ \int_{-\infty}^{\infty} C(\tau) \exp(-i\omega\tau)\, d\tau \right\} \qquad [86]$$

in which the *stochastic correlation function* is given by

$$C(\tau) = \overline{c_0(t)c_0(t+\tau)Y_2^0[\Omega(t)]Y_2^0[\Omega(t+\tau)]} \qquad [87]$$

$c_0(t)$ is a function of physical constants and spatial variables, $Y_2^0[\Omega(t)]$ is a modified second order spherical harmonic function, $\Omega(t) = \{\theta(t), \phi(t)\}$ are polar angles in the laboratory reference frame. The polar angles define the orientation of a unit vector that points in the principal direction for the interaction. For the dipolar interaction, the unit vector points along the line between the two nuclei (or between the nucleus and the electron for paramagnetic relaxation). For CSA interaction with an axially symmetric chemical shift tensor, the unit vector is collinear with the symmetry axis of the tensor. For the quadrupolar interaction, the unit vector is collinear with the symmetry axis of the electric field gradient tensor. The modified spherical harmonics are given in Table 1 (*18*). The functions $c_0(t)$ for dipolar, CSA and quadrupolar interactions are given in Table 2.

Table 1: Modified Second Order Spherical Harmonics

q	Y_2^q	$Y_2^{-q} = Y_2^{q*}$
0	$(3\ \cos^2\theta\ -\ 1)/2$	$(3\ \cos^2\theta\ -\ 1)/2$
1	$\sqrt{3/2}\ \sin\theta\ \cos\theta\ e^{i\phi}$	$\sqrt{3/2}\ \sin\theta\ \cos\theta\ e^{-i\phi}$
2	$\sqrt{3/8}\ \sin^2\theta\ \ e^{i2\phi}$	$\sqrt{3/8}\ \sin^2\theta\ \ e^{-i2\phi}$

The modified spherical harmonic functions are normalized (to give the conventional spherical harmonic functions) by multiplying by $[5/(4\pi)]^{1/2}$.

Table 2: Spatial Functions for Relaxation Mechanisms

Interaction	$c(t)$
Dipolar	$\sqrt{6}\ (\mu_0/4\pi)\hbar\ \gamma_I\gamma_S\ r_{IS}(t)^{-3}$
CSA[1]	$\sqrt{2/3}\ (\sigma_{\parallel}\ -\ \sigma_{\perp})\ \gamma_I B_0$
Quadrupolar[2]	$e^2qQ\ /\ [4\hbar I(2I-1)]$

[1]The chemical shift tensor is assumed to be axially symmetric with principal values $\sigma_{zz} = \sigma_{||}$ and $\sigma_{xx} = \sigma_{yy} = \sigma_{\perp}$.

[2]Q is the nuclear quadrupole moment and e is the charge of the electron. The electric field gradient tensor is assumed to be axially symmetric with principal value $V_{zz} = eq$, and $V_{xx} = V_{yy}$.

The power spectral density function measures the contribution to orientational (rotational) dynamics of the molecule from motions with frequency components in the range ω to$\omega + d\omega$. Not surprisingly, as a molecule rotates stochastically in solution due to Brownian motion, the

oscillating magnetic fields produced are not distributed uniformly over all frequencies. A small organic molecule tumbles at a greater rate than a biological macromolecule in the same solvent, and the distribution of oscillating magnetic fields resulting from rotational diffusion of the two molecules will be different.

For a rigid spherical molecule undergoing rotational Brownian motion, $c_0(t) = c_0$ is a constant and the auto-spectral density function is

$$j(\omega) = d_{00} J(\omega) \qquad [88]$$

in which the orientational spectral density function is

$$J(\omega) = \mathrm{Re}\left\{ \int_{-\infty}^{\infty} C_{00}^2(\tau) \exp\{-i\omega\tau\} d\tau \right\} \qquad [89]$$

the orientational correlation function is

$$C_{00}^2(\tau) = \overline{Y_2^0[\Omega(t)] Y_2^0[\Omega(t+\tau)]} \qquad [90]$$

and $d_{00} = c_0^2$. For *isotropic* rotational diffusion of a rigid rotor or spherical top, the correlation function is given by (*12*),

$$C_{00}^2(\tau) = \tfrac{1}{5} \exp\left[-\tau / \tau_c\right] \qquad [91]$$

in which the *correlation time*, τ_c, is approximately the average time for the molecule to rotate by one radian. The correlation time varies due to molecular size, solvent viscosity and temperature, but generally τ_c is of the order of picoseconds for small molecules and of the order of nanoseconds for biological macromolecules in aqueous solution (§6.1). The corresponding spectral density function is,

$$J(\omega) = \frac{2}{5}\frac{\tau_c}{(1+\omega^2\tau_c^2)} \qquad [92]$$

The functional form of the spectral density function for a rigid rotor is Lorentzian; a graph of $J(\omega)$ versus ω is shown in Figure 6. The plot of $J(\omega)$ is relatively constant for $\omega^2\tau_c^2 << 1$ and then begins to decrease rapidly at $\omega^2\tau_c^2$ 1. If molecular motion is sufficiently rapid to satisfy $\omega^2\tau^2_c << 1$, then the *extreme narrowing* condition obtains and $J(\omega) \approx J(0)$. For sufficiently slow molecular motion, $\omega^2\tau_c^2 >> 1$, $J(\omega) \propto \omega^{-2}$, and the slow tumbling regime or *spin diffusion* limit is reached.

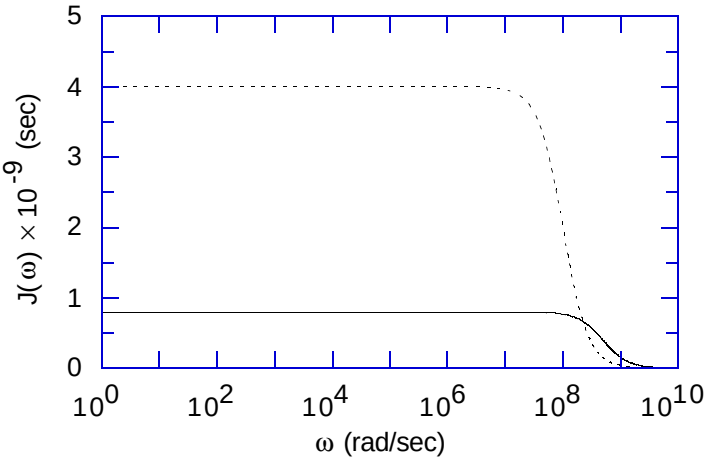

Figure 6. Spectral density functions for an isotropic rotor. Calculations were performed using [92] with (——) τ_C = 2 ns and (· · ·) τ_C = 10 ns.

Local fields are modulated stochastically by relative motions of nuclei in a molecular reference frame as well as by overall rotational Brownian motion. Rigorously for isotropic rotational diffusion and approximately for anisotropic rotational diffusion, the total correlation function is factored as (*19*),

$$C(\tau) = C_O(\tau)C_I(\tau) \qquad [93]$$

The correlation function for overall motion, $C_O(\tau)$, is given by [91]. The correlation function for internal motions, $C_I(\tau)$, is given by [87], in which the orientational variables are defined in a fixed molecular reference frame, rather than the laboratory reference frame, Calculations of $C_I(\tau)$ have been performed for a number of diffusion and lattice jump models for internal motions. N-site lattice jump models assume that the nuclei of the relevant spins jump between N allowed conformations. The jumps are assumed to be instantaneous; therefore the transition rates reflect the lifetimes of each conformation.

Rather than describing in detail calculations of spectral density functions for diffusion and jump models of intramolecular motions, two useful limiting cases of N-site models are given without proof (see (*10*) for a more extensive review). The spectral density function depends upon the time scale of the variation in the spatial variables, $c_0(t)$. If the transition rates between sites approaches zero, then

$$j(\omega) = J(\omega) \sum_{\kappa=1}^{N} p_\kappa c_{0\kappa}^2 = J(\omega) \overline{c_0^2} \qquad [94]$$

in which p_κ is the population and $c_{0\kappa}$ is the value of the spatial function for site κ. If the transition rates between sites approaches infinity, then

$$j(\omega) = J(\omega) \sum_{q=-2}^{q} \left| \sum_{\kappa=1}^{N} p_\kappa c_{0\kappa} Y_2^q(\Omega_k) \right|^2 = J(\omega) \sum_{m=-2}^{2} \left| \overline{c_0 Y_2^q(\Omega)} \right|^2 \qquad [95]$$

in which Ω_k are the polar angles for site k.

An extremely useful treatment that incorporates intramolecular motions in addition to overall rotational motion is provided by the Lipari-

Szabo model free formalism (*19*, *20*). In this treatment, the spectral density function is given by

$$j(\omega) = \frac{2}{5}\overline{c_0^2}\left[\frac{S^2\tau_c}{1+(\omega\tau_c)^2} + \frac{(1-S^2)\tau}{1+(\omega\tau)^2}\right] \qquad [96]$$

in which $\tau^{-1} = \tau_c^{-1} + \tau_e^{-1}$, S^2 is the square of the generalized order parameter that characterizes the amplitude of the intramolecular motion in a molecular reference frame, and τ_e is the effective correlation time for internal motions. The order parameter is defined by

$$S^2 = \left[\overline{c_0^2}\right]^{-1} \sum_{q=-2}^{2} \left|\overline{c_0 Y_2^q(\Omega)}\right|^2 \qquad [97]$$

in which the overbar indicates an ensemble average performed over the equilibrium distribution of orientations Ω in the molecular reference frame. The order parameter satisfies the inequality, $0 \le S^2 \le 1$, in which lower values indicate larger amplitudes of internal motions. A significant advantage of the Lipari-Szabo formalism is that specification of the microscopic motional model is not required. If τ_e approaches infinity, [96] reduces to the same form as [94]; if τ_e approaches zero, [96] reduces to the same form as [95]. Equation [96] has been used extensively to analyze spin relaxation in proteins (*21*, *22*).

The expressions given in [94], [95], and [96] are commonly encountered in discussions of dipolar relaxation between two spins, *I* and *S*. Using $c_0(t)$ from Table 2 gives:

$$j(\omega) = \zeta J(\omega)\overline{r_{IS}^{-6}} \qquad [98]$$

$$j(\omega) = \zeta J(\omega) \sum_{q=-2}^{2} \left| \overline{\frac{Y_2^q(\Omega_k)}{r_{IS}^3}} \right|^2 \qquad [99]$$

$$j(\omega) = \frac{2}{5} \zeta \overline{r_{IS}^{-6}} \left[\frac{S^2 \tau_c}{1+(\omega\tau_c)^2} + \frac{(1-S^2)\tau}{1+(\omega\tau)^2} \right] \qquad [100]$$

$$S^2 = \left[\overline{r_{IS}^{-6}} \right]^{-1} \sum_{q=-2}^{2} \left| \overline{\frac{Y_2^q(\Omega)}{r_{IS}^3}} \right|^2 \qquad [101]$$

in which

$$\zeta = 6\left[(\mu_0 / 4\pi) \hbar \gamma_I \gamma_S \right]^2 \qquad [102]$$

Equation [98] (slow internal motion) is called "r^{-6} averaging" and [99] (fast internal motion) is called "r^{-3} averaging" with respect to the conformations of the molecule. The former equation is appropriate for treating the effects of aromatic ring flips and the latter equation is appropriate for treating methyl group rotations in proteins (*23*, *24*).

The Lipari-Szabo model free formalism can be modified in a straightforward fashion to account for cross-correlations between relaxation interactions with fixed relative orientations (*25*). The cross-spectral density function is given by

$$j_{mn}(\omega) = \frac{2}{5} \overline{c_0^m c_0^n} \left[\frac{S_{mn}^2 \tau_c}{1+(\omega\tau_c)^2} + \frac{\left\{ P_2(\cos\theta_{mn}) - S_{mn}^2 \right\} \tau}{1+(\omega\tau)^2} \right] \qquad [103]$$

in which $\tau^{-1} = \tau_c^{-1} + \tau_e^{-1}$,

$$S_{mn}^2 = \left[\overline{c_0^m c_0^n} \right]^{-1} \sum_{q=-2}^{2} \left| \overline{c_0^m Y_2^q(\Omega_m)} \right| \left| \overline{c_0^n Y_2^q(\Omega_n)} \right| \qquad [104]$$

$P_2(x)$ = $(3x^2$ - 1)/2, and θ_{mn} is the angle between the principal axes for the two interactions.

Other expressions for $j(\omega)$ have been derived for molecules that exhibit anisotropic rotational diffusion or specific internal motional models; although, the resulting expressions are often cumbersome (*12*).

4 Relaxation mechanisms

A very large number of physical interactions give rise to stochastic Hamiltonians capable of mediating spin relaxation. In the present context, only the intramolecular magnetic dipolar, anisotropic chemical shift (CSA), quadrupolar, and scalar coupling interactions will be discussed. Intramolecular paramagnetic relaxation has the same Hamiltonian as for nuclear dipolar relaxation, except that the interaction occurs between a nucleus and an unpaired electron. Other relaxation mechanisms are of minor importance for macromolecules or are only of interest in very specialized cases. For spin 1/2 nuclei in diamagnetic biological macromolecules, the dominant relaxation mechanisms are the magnetic dipolar and anisotropic chemical shift mechanisms. For nuclei with spin > 1/2, notably ^{14}N and ^{2}H in proteins, the dominant relaxation mechanism is the quadrupolar interaction.

Relaxation rate constants for nuclei in proteins depend upon a large number of factors, including: overall rotational correlation times, internal motions, the geometrical arrangement of nuclei, and the relative strengths of the applicable relaxation mechanisms. If the overall correlation time and the three-dimensional structural coordinates of the protein are known, relaxation rate constants can be calculated in a relatively straightforward

manner using expressions derived in the following sections. In general, ^{1}H relaxation in proteins is dominated by dipolar interactions with other protons (within approximately 5Å) and by interactions with directly bonded heteronuclei. The latter arise from dipolar interactions with ^{13}C and ^{15}N in labeled proteins or from scalar relaxation of the second kind between the quadrupolar ^{14}N nuclei and amide protons. Relaxation of protonated ^{13}C and ^{15}N heteronuclei is dominated by dipolar interactions with the directly bonded protons, and secondarily by CSA (for ^{15}N spins and aromatic ^{13}C spins). Relaxation of unprotonated heteronuclei, notably carbonyl ^{13}C and unprotonated aromatic ^{13}C spins, is dominated by CSA interactions.

4.1 Intramolecular dipolar relaxation for IS spin system

Any magnetic nucleus in a molecule generates an instantaneous magnetic dipolar field that is proportional to the magnetic moment of the nucleus. As the molecule tumbles in solution, this field fluctuates and constitutes a mechanism for relaxation of nearby spins. Most importantly for structure elucidation, the efficacy of dipolar relaxation depends on the nuclear moments and on the *inverse sixth power of the distance between the interacting nuclei*. As a result, nuclear spin relaxation can be used to determine distances between nuclei. Protons have a large gyromagnetic ratio; therefore, dipole-dipole interactions cause the most efficient relaxation of proton spins and constitute a sensitive probe for internuclear distances.

Initially, a two spin system, *IS*, will be considered with $\omega_I >> \omega_S$ and scalar coupling constant $J_{IS} = 0$. The energy levels of the spin system and

the associated transition frequencies are shown in Figure 7. The terms $\mathbf{A}_{2p}^{q}$ are given in Table 3. The spatial functions for the different interactions are given in Tables 1 and 2.

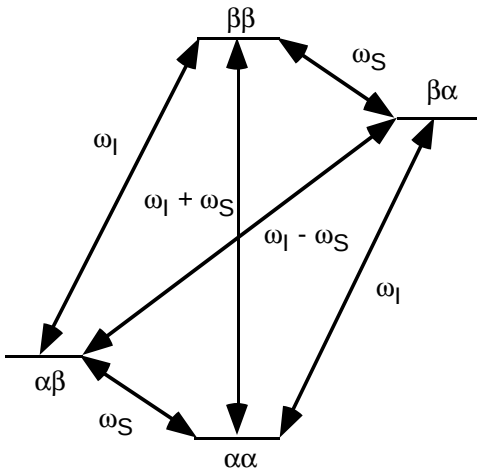

Figure 7. Transitions and associated eigenfrequencies for a two spin system.

Table 3: Tensor Operators for the Dipolar Interaction

q	p	A_{2p}^{q}	$A_{2p}^{-q} = A_{2p}^{q\dagger}$	ω_p
0	0	$(2/\sqrt{6})I_zS_z$	$(2/\sqrt{6})I_zS_z$	0
0	1	$-1/(2\sqrt{6})\ I^+S^-$	$-1/(2\sqrt{6})\ I^-S^+$	$\omega_I - \omega_S$
1	0	$-(1/2)\ I_zS^+$	$(1/2)\ I_zS^-$	ω_S
1	1	$-(1/2)\ I^+S_z$	$(1/2)\ I^-S_z$	ω_I
2	0	$(1/2)\ I^+S^+$	$(1/2)\ I^-S^-$	$\omega_I + \omega_S$

The relaxation rate constants are calculated using [75]. To aid in the calculation of the double commutators, the commutation relations given in Table 4 are useful. To begin, the identity operator can be disregarded because it has no effect on the relaxation equations. Next, the block structure of the relaxation matrix can be derived from the coherence

orders of the operators and the secular condition. The zero order block consists of the operators with coherence order equal to zero for both the I and S spins: I_z, S_z and $2I_zS_z$. Each of the other operators consists of a unique combination of coherence order for the I and S spins; consequently, each of these operators comprises a block of dimension one and each operator relaxes independently of the others.

Table 4: Commutator Relationships[1]

$[I_x, I_y] = iI_z$
$[I_\alpha, 2I_\beta S_\gamma] = 2[I_\alpha, I_\beta]S_\gamma$
$[2I_\alpha S_\gamma, 2I_\beta S_\varepsilon] = [I_\alpha, I_\beta]\delta_{\gamma\varepsilon}$

[1] $I_\alpha = I_x$, I_y, or I_z; $S_\gamma = S_x$, S_y, or S_z. Equivalent expressions for S operators are obtained by exchanging I and S labels. $\delta_{\gamma\varepsilon}$ is the Kronecker delta.

The relaxation matrix for the zero order block has dimensions 3×3, with individual elements, Γ_{rs}, giving the rate constant for relaxation between operators $\mathbf{B}_r$ and $\mathbf{B}_s$ for r, s = 1, 2, and 3 and $\mathbf{B}_1 = I_z$, $\mathbf{B}_2 = S_z$, and $\mathbf{B}_3 = 2I_zS_z$. The double commutators $[\mathbf{A}_{2p}^{-q}, [\mathbf{A}_{2p}^{q}, I_z]]$ are calculated as follows for each combination of p and q in Table 3:

$$[\mathbf{A}^{0}_{20}, [\mathbf{A}^{0}_{20}, I_z]] = (2/3)\ [I_zS_z, [I_zS_z, I_z]] = 0$$

$$[\mathbf{A}^{-0}_{21}, [\mathbf{A}^{0}_{21}, I_z]] = (1/24)\ [I^-S^+, [I^+S^-, I_z]] = -(1/24)\ [I^-S^+, I^+S^-]$$

$$= (1/12)\ \{I^-I^+S_z - S^-S^+I_z\}$$

$$= (1/24)\ \{I_z - S_z\}$$

$$[\mathbf{A}^{0}_{21}, [\mathbf{A}^{-0}_{21}, I_z]] = (1/24)\ [I^+S^-, [I^-S^+, I_z]] = (1/24)\ [I^+S^-, I^-S^+]$$

$$= (1/12)\ \{I^+I^-S_z - S^+S^-I_z\}$$

$$= (1/24)\ \{I_z - S_z\}$$

$$[\mathbf{A}^{-1}_{20}, [\mathbf{A}^{1}_{20}, I_z]] = -(1/4)\ [I_zS^-, [I_zS^+, I_z]] = 0$$

$$[\mathbf{A}^{1}_{20}, [\mathbf{A}^{-1}_{20}, I_z]] = -(1/4)\ [I_zS^+, [I_zS^-, I_z]] = 0$$

$$[\mathbf{A}^{-1}_{21}, [\mathbf{A}^{1}_{21}, I_z]] = -(1/4)\ [I^-S_z, [I^+S_z, I_z]] = (1/4)\ S_z^2[I^-, I^+]$$

$$= -(1/2)\ S_z^2I_z = -(1/8)\ I_z$$

$$[\mathbf{A}^{1}_{21}, [\mathbf{A}^{-1}_{21}, I_z]] = -(1/4)\ [I^+S_z, [I^-S_z, I_z]] = -(1/4)\ S_z^2[I^+, I^-]$$

$$= -(1/2)\ S_z^2I_z = -(1/8)\ I_z$$

$$[\mathbf{A}^{-2}_{20}, [\mathbf{A}^{2}_{20}, I_z]] = (1/4)\ [I^-S^-, [I^+S^+, I_z]] = -(1/4)\ [I^-S^-, I^+S^+]$$

$$= (1/2)\ \{I^+I^-S_z + S^-S^+I_z\}$$

$$= (1/4)\ \{S_z + I_z\}$$

$$[\mathbf{A}^{2}_{20}, [\mathbf{A}^{-2}_{20}, I_z]] = (1/4)\ [I^+S^+, [I^-S^-, I_z]] = (1/4)\ [I^+S^+, I^-S^-]$$

$$= (1/2)\ \{I^+I^-S_z + S^-S^+I_z\}$$

$$= (1/4)\ \{S_z + I_z\} \qquad [105]$$

For auto-relaxation of the I_z operator, the above operators are premultiplied by I_z and the trace operation performed:

$$(1/24)\ \langle I_z|\{I_z - S_z\}\rangle = (1/24)\ \langle I_z^2 - I_zS_z\rangle$$

$$= (1/24)\ \{\langle\alpha\alpha|I_z^2 - I_zS_z|\alpha\alpha\rangle + \langle\alpha\beta|I_z^2 - I_zS_z|\alpha\beta\rangle$$

$$+ \langle\beta\alpha|I_z^2 - I_zS_z|\beta\alpha\rangle + \langle\beta\beta|I_z^2 - I_zS_z|\beta\beta\rangle\}$$

$$= 1/24$$

$$-(1/8)\ \langle I_z|I_z\rangle = -(1/8)\ \langle I_z^2\rangle$$

$$= -(1/8)\ \{\langle\alpha\alpha|I_z^2|\alpha\alpha\rangle + \langle\alpha\beta|I_z^2|\alpha\beta\rangle$$

$$+ \langle\beta\alpha|I_z^2|\beta\alpha\rangle + \langle\beta\beta|I_z^2|\beta\beta\rangle\}$$

$$= -1/8$$

$$(1/4)\ \langle I_z|\{S_z + I_z\}\rangle = (1/4)\ \langle I_z^2 + I_zS_z\rangle$$

$$= (1/4)\ \{\langle\alpha\alpha|I_z^2 + I_zS_z|\alpha\alpha\rangle + \langle\alpha\beta|I_z^2 + I_zS_z|\alpha\beta\rangle$$

$$+ \langle\beta\alpha|I_z^2 + I_zS_z|\beta\alpha\rangle + \langle\beta\beta|I_z^2 + I_zS_z|\beta\beta\rangle\}$$

$$= 1/4 \qquad [106]$$

For cross-relaxation between the S_z and the I_z operator, the above operators are premultiplied by S_z and the trace operation performed:

$$(1/24)\ \langle S_z|\{I_z - S_z\}\rangle = (1/24)\ \langle I_zS_z - S_z^2\rangle$$

$$= (1/24)\ \{<\alpha\alpha|I_zS_z\text{-}S_z^2|\alpha\alpha> + <\alpha\beta|I_zS_z\text{-}S_z^2|\alpha\beta>$$

$$+ <\beta\alpha|I_zS_z\text{-}S_z^2|\beta\alpha> + <\beta\beta|I_zS_z\text{-}S_z^2|\beta\beta>\}$$

$$= \ \text{-}1/24$$

$$\text{-}(1/8)\ <S_z|I_z> = \text{-}(1/8)\ <I_zS_z>$$

$$= \text{-}(1/8)\ \{<\alpha\alpha|I_zS_z|\alpha\alpha> + <\alpha\beta|I_zS_z|\alpha\beta>$$

$$+ <\beta\alpha|I_zS_z|\beta\alpha> + <\beta\beta|I_zS_z|\beta\beta>\}$$

$$= 0$$

$$(1/4)\ <S_z|\{S_z + I_z\}> = (1/4)\ <S_z^2+I_zS_z>$$

$$= (1/4)\ \{<\alpha\alpha|S_z^2+I_zS_z|\alpha\alpha> + <\alpha\beta|S_z^2+I_zS_z|\alpha\beta>$$

$$+ <\beta\alpha|S_z^2+I_zS_z|\beta\alpha> + <\beta\beta|S_z^2+I_zS_z|\beta\beta>\}$$

$$= \ 1/4 \qquad [107]$$

For cross-relaxation between the $2I_zS_z$ operator and the I_z operator, the above operators are premultiplied by $2I_zS_z$ and the trace operation performed:

$$(1/24)\ <2I_zS_z\ |\{I_z\ \text{-}\ S_z\}> = (1/12)\ <I_z^2S_z\ \text{-}I_zS_z^2>$$

$$= (1/12)\ \{<\alpha\alpha|I_z^2S_z\ \text{-}I_zS_z^2|\alpha\alpha> + <\alpha\beta|I_z^2S_z\ \text{-}I_zS_z^2|\alpha\beta>$$

$$+ <\beta\alpha|I_z^2S_z\ \text{-}I_zS_z^2|\beta\alpha> + <\beta\beta|I_z^2S_z\ \text{-}I_zS_z^2|\beta\beta>\}$$

$$= 0$$

$$\text{-}(1/8)\ <2I_zS_z\ |I_z> = \text{-}(1/4)\ <I_z^2S_z>$$

$$= -(1/4)\ \{<\alpha\alpha|I_z^2S_z\ |\alpha\alpha> + <\alpha\beta|I_z^2S_z\ |\alpha\beta>$$

$$+ <\beta\alpha|I_z^2S_z\ |\beta\alpha> + <\beta\beta|I_z^2S_z\ |\beta\beta>\}$$

$$= 0$$

$$(1/4)\ <2I_zS_z\ |\{S_z + I_z\}> = (1/2)\ <I_z^2S_z + I_zS_z^2>$$

$$= (1/2)\ \{<\alpha\alpha|I_z^2S_z + I_zS_z^2|\alpha\alpha> + <\alpha\beta|I_z^2S_z + I_zS_z^2|\alpha\beta>$$

$$+ <\beta\alpha|I_z^2S_z + I_zS_z^2|\beta\alpha> + <\beta\beta|I_z^2S_z + I_zS_z^2|\beta\beta>\}$$

$$= 0 \qquad [108]$$

Autorelaxation and cross-relaxation of the S_z operator can be obtained by exchanging I and S operators in the above expressions. Substituting the values of the trace operations above into [75] (and using $<I_z|I_z> = 1$) yields

$$\Gamma_{11} = (1/24)\ \{j(\omega_I - \omega_S) + 3j(\omega_I) + 6j(\omega_I + \omega_S)\}$$

$$\Gamma_{22} = (1/24)\ \{j(\omega_I - \omega_S) + 3j(\omega_S) + 6j(\omega_I + \omega_S)\}$$

$$\Gamma_{12} = (1/24)\ \{-j(\omega_I - \omega_S) + 6j(\omega_I + \omega_S)\}$$

$$\Gamma_{13} = 0$$

$$\Gamma_{23} = 0 \qquad [109]$$

If the I and S spins are separated by a constant distance, r_{IS}, then,

$$\Gamma_{11} = (d_{00}/4)\ \{J(\omega_I - \omega_S) + 3J(\omega_I) + 6J(\omega_I + \omega_S)\}$$

$$\Gamma_{22} = (d_{00}/4)\ \{J(\omega_I - \omega_S) + 3J(\omega_S) + 6J(\omega_I + \omega_S)\}$$

$$\Gamma_{12} = (d_{00}/4)\ \{-J(\omega_I - \omega_S) + 6J(\omega_I + \omega_S)\} \qquad [110]$$

in which

$$d_{00} = \left(\mu_0/4\pi\right)^2 \hbar^2 \gamma_I^2 \gamma_S^2 r_{IS}^{-6} \qquad [111]$$

Dipolar cross relaxation between the operators $2I_zS_z$ and I_z does not occur; therefore, the $2I_zS_z$ operator relaxes independently of the I_z and S_z operators. This result can be anticipated using symmetry and group theoretical arguments beyond the scope of this text (*9*, *14*, *12*). Cross-relaxation between these operators does arise due to interference between dipolar and CSA relaxation mechanisms (*11*).

Thus, the evolution of the longitudinal operators, I_z and S_z, are governed by

$$d(\langle I_z\rangle(t) - \langle I_z^0\rangle)/dt = -\Gamma_{11}\,(\langle I_z\rangle(t) - \langle I_z^0\rangle) - \Gamma_{12}(\langle S_z\rangle(t) - \langle S_z^0\rangle)$$

$$d(\langle S_z\rangle(t) - \langle S_z^0\rangle)/dt = -\Gamma_{22}(\langle S_z\rangle(t) - \langle S_z^0\rangle) - \Gamma_{12}(\langle I_z\rangle(t) - \langle I_z^0\rangle) \qquad [112]$$

Making the identification $\Gamma_{11} = \rho_I$ (= R_{1I}), $\Gamma_{22} = \rho_S$ (= R_{1S}) and $\Gamma_{12} = \sigma_{IS}$ puts [112] into the form of the Solomon equations [19] in which ρ_I and ρ_S are the auto-relaxation rate constants and σ_{IS} is the cross-relaxation rate constant. The Solomon transition rate constants (§1.2) are

$$W_0 = j(\omega_I - \omega_S)/24$$

$$W_I = j(\omega_I)/16$$

$$W_S = j(\omega_S)/16$$

$$W_2 = j(\omega_I + \omega_S)/4 \qquad [113]$$

Now consider the relaxation of the transverse I^+ operator; as a consequence of the secular approximation, this operator is immediately seen to relax independently of all other operators except, potentially, for $2I^+S_z$. The double commutators $[\mathbf{A}_{2p}^{-q}, [\mathbf{A}_{2p}^{q}, I^+]]$ are calculated as follows for each combination of p and q in Table 3:

$$[\mathbf{A}_{20}^{0}, [\mathbf{A}_{20}^{0}, I^+] = (2/3)\ [I_zS_z, [I_zS_z, I^+]] = (2/3)\ I^+S_z^2 = (1/6)\ I^+$$

$$[\mathbf{A}_{21}^{-0}, [\mathbf{A}_{21}^{0}, I^+] = (1/24)\ [I^-S^+, [I^+S^-, I^+] = 0$$

$$[\mathbf{A}_{21}^{0}, [\mathbf{A}_{21}^{-0}, I^+]] = (1/24)\ [I^+S^-, [I^-S^+, I^+]] = -(1/12)\ [I^+S^-, I_zS^+]$$

$$= (1/6)\ I^+I_zS_z^- + (1/12)\ I^+S^+S^- = (1/24)I^+$$

$$[\mathbf{A}_{20}^{-1}, [\mathbf{A}_{20}^{1}, I^+]] = -(1/4)\ [I_zS^-, [I_zS^+, I^+]] = (1/8)\ [I_zS^-, I^+S^+] = -(1/8)\ I^+$$

$$[\mathbf{A}_{20}^{1}, [\mathbf{A}_{20}^{-1}, I^+]] = -(1/4)\ [I_zS^+, [I_zS^-, I^+]] = -(1/8)\ [I_zS^+, I^+S^-] = -(1/8)\ I^+$$

$$[\mathbf{A}_{21}^{-1}, [\mathbf{A}_{21}^{1}, I^+]] = -(1/4)\ [I^-S_z, [I^+S_z, I^+]] = 0$$

$$[\mathbf{A}_{21}^{1}, [\mathbf{A}_{21}^{-1}, I^+]] = -(1/4)\ [I^+S_z, [I^-S_z, I^+]] = (1/2)\ S_z^2[I^+, I_z] = -(1/8)\ I^+$$

$$[\mathbf{A}_{20}^{-2}, [\mathbf{A}_{20}^{2}, I^+]] = (1/4)\ [I^-S^-, [I^+S^+, I^+]] = 0$$

$$[\mathbf{A}_{20}^{2}, [\mathbf{A}_{20}^{-2}, I^+]] = (1/4)\ [I^+S^+, [I^-S^-, I^+]] = -(1/2)\ [I^+S^+, I_zS^-] = (1/4)\ I^+$$

[114]

Note that all non-zero results are proportional to I^+; therefore, since the operator basis is orthogonal, no operator cross-relaxes with I^+. For auto-relaxation of the I_+ operator, the above operators are premultiplied by I^+ and the trace operation performed:

$$<I^+|I^+> = <I^-I^+> =$$

$$= \{<\alpha\alpha|I^-I^+|\alpha\alpha> + <\alpha\beta|I^-I^+|\alpha\beta>$$

$$+ <\beta\alpha|I^-I^+|\beta\alpha> + <\beta\beta|I^-I^+|\beta\beta>\}$$

$$= 2 \qquad [115]$$

This same factor is the normalization in the denominator of [75]. Thus,

$$R_{2I} = (1/48)\ \{4j(0) + j(\omega_I - \omega_S) + 3j(\omega_I) + 6j(\omega_S) + 6j(\omega_I + \omega_S)\} \qquad [116]$$

and

$$d<I^+>/dt = -i\omega_I<I^+> - R_{2I}<I^+> \qquad [117]$$

If r_{IS} is constant:

$$R_{2I} = (d_{00}/8)\{4J(0) + J(\omega_I - \omega_S) + 3J(\omega_I) + 6J(\omega_S) + 6J(\omega_I + \omega_S)\} \qquad [118]$$

Analogous equations can be written by inspection for the I^-, S^+ and S^- operators. The complete set of dipolar relaxation rate constants for the basis operators for the two spin system are given in Table 5.

The dependence of R_1 and R_2 on τ_c for a rigid molecule is illustrated in Figure 8. R_1 has a maximum for $\omega_0\tau_c = 1$ whereas R_2 increases monotonically with τ_c.

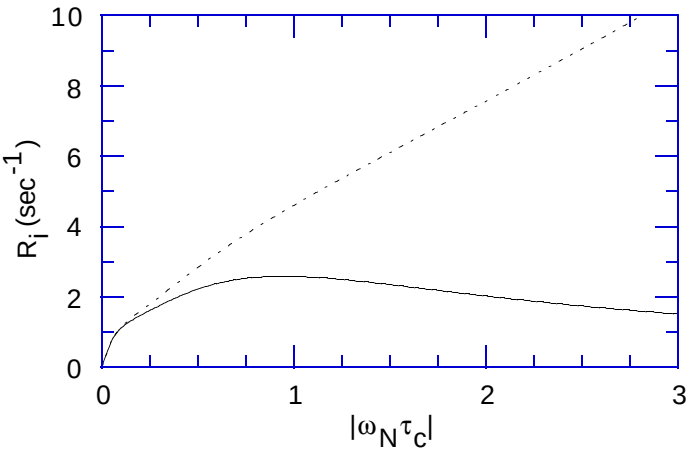

Figure 8. Relaxation rate constants for ^{1}H-^{15}N dipolar spin system. (——) ^{15}N R_1 spin-lattice rate constants. (· · ·) ^{15}N R_2 spin-spin rate constants. Calculations were performed using expressions given in Table 5 together with [111] and [92]. Parameters used were B_0 = 11.74 T, $\gamma_I = 2.675 \times 10^8$ T^{-1} s^{-1} (^{1}H), γ_S = -2.712 × 10^7 T^{-1} s^{-1} (^{15}N), and r_{IS} = 1.02 Å.

Table 5: Relaxation Rate Constants for *IS* Dipolar Interaction

Coherence Level	Operator[1]	Relaxation Rate Constant[2]
Populations	I_z	$(d_{00}/4)\ \{J(\omega_I - \omega_S) + 3J(\omega_I) + 6J(\omega_I + \omega_S)\}$
	S_z	$(d_{00}/4)\ \{J(\omega_I - \omega_S) + 3J(\omega_S) + 6J(\omega_I + \omega_S)\}$
	$I_z \leftrightarrow S_z$	$(d_{00}/4)\ \{-J(\omega_I - \omega_S) + 6J(\omega_I + \omega_S)\}$
0	$2I_zS_z$	$(3d_{00}/4)\ \{J(\omega_I) + J(\omega_S)\}$
	ZQ_x, ZQ_y	$(d_{00}/8)\ \{2J(\omega_I - \omega_S) + 3J(\omega_I) + 3J(\omega_S)\}$
± 1	I^+, I^-	$(d_{00}/8)\ \{4J(0) + J(\omega_I - \omega_S) + 3J(\omega_I) + 6J(\omega_S) + 6J(\omega_I + \omega_S)\}$
	S^+, S^-	$(d_{00}/8)\ \{4J(0) + J(\omega_I - \omega_S) + 3J(\omega_S) + 6J(\omega_I) + 6J(\omega_I + \omega_S)\}$
	$2I^+S_z, 2I^-S_z$	$(d_{00}/8)\ \{4J(0) + J(\omega_I - \omega_S) + 3J(\omega_I) + 6J(\omega_I + \omega_S)\}$
	$2I_zS^+, 2I_zS^-$	$(d_{00}/8)\ \{4J(0) + J(\omega_I - \omega_S) + 3J(\omega_S) + 6J(\omega_I + \omega_S)\}$
± 2	DQ_x, DQ_y	$(d_{00}/8)\ \{3J(\omega_I) + 3J(\omega_S) + 12J(\omega_I + \omega_S)\}$

[1]Cross relaxation only occurs between I_z and S_z.

[2]$d_{00} = (\mu_0/4\pi)^2 \hbar^2 \gamma_I^2 \gamma_S^2\ r_{IS}^{-6}$.

4.2 Intramolecular dipolar relaxation for scalar coupled IS spin system

The I_z and S_z operators both commute with the scalar coupling Hamiltonian; consequently dipolar spin-lattice relaxation is unaffected by the scalar coupling interaction and the expressions given in [109] and [112] remain valid. The in-phase and anti-phase transverse operators, I^+ and $2I^+S_z$ are coupled together by the scalar coupling Hamiltonian. Applying [73] yields the following equations in the laboratory frame:

$$d\langle I^+\rangle(t)/dt = -i\omega_I\langle I^+\rangle(t) - i\pi J_{IS}\langle 2I^+S_z\rangle(t) - R_{2I}\langle I^+\rangle(t)$$

$$d\langle 2I^+S_z\rangle(t)/dt = -i\omega_I\langle 2I^+S_z\rangle(t) - i\pi J_{IS}\langle I^+\rangle(t) - R_{IS}\langle 2I^+S_z\rangle(t) \qquad [119]$$

in which R_{2I} and R_{IS} are given in Table 5. These equations are written in matrix form as

$$\begin{bmatrix} \langle I^+\rangle(t) \\ \langle 2I^+S_z\rangle(t) \end{bmatrix} = -\begin{bmatrix} i\omega_I + R_{2I} & i\pi J_{IS} \\ i\pi J_{IS} & i\omega_I + R_{2IS} \end{bmatrix}\begin{bmatrix} \langle I^+\rangle(t) \\ \langle 2I^+S_z\rangle(t) \end{bmatrix} \qquad [120]$$

and are solved by analogy to [23] to yield:

$$\langle I^+\rangle(t) = \tfrac{1}{2}\left[\left(1-\frac{R_{2I}-R_{2IS}}{(\lambda_+-\lambda_-)}\right)\exp(-\lambda_- t)+\left(1+\frac{R_{2I}-R_{2IS}}{(\lambda_+-\lambda_-)}\right)\exp(-\lambda_+ t)\right]\langle I^+\rangle(0)$$
$$-\frac{i\pi J_{IS}}{(\lambda_+-\lambda_-)}\left[\exp(-\lambda_- t)-\exp(-\lambda_+ t)\right]\langle 2I^+S_z\rangle(0)$$

$$\langle 2I^+S_z\rangle(t) = \tfrac{1}{2}\left[\left(1+\frac{R_{2I}-R_{2IS}}{(\lambda_+-\lambda_-)}\right)\exp(-\lambda_- t)+\left(1-\frac{R_{2I}-R_{2IS}}{(\lambda_+-\lambda_-)}\right)\exp(-\lambda_+ t)\right]\langle 2I^+S_z\rangle(0)$$
$$-\frac{i\pi J_{IS}}{(\lambda_+-\lambda_-)}\left[\exp(-\lambda_- t)-\exp(-\lambda_+ t)\right]\langle I^+\rangle(0)$$

[121]

in which

$$\lambda_{\pm} = i\omega + \left(R_{2I} + R_{2IS} \right) / 2 \pm \left[\left(\left(R_{2I} - R_{2IS} \right) / 2 \right)^2 - \left(\pi J_{IS} \right)^2 \right]^{1/2} \qquad [122]$$

If $(2\pi J_{IS})^2 >> (R_{2I} - R_{2IS})^2$, then

$$\left\langle I^+ \right\rangle(t) = \tfrac{1}{2}\left[\exp\left\{ -\left(i\omega - i\pi J_{IS} + R_{ave} \right) t \right\} + \exp\left\{ -\left(i\omega + i\pi J_{IS} + R_{ave} \right) t \right\} \right] \left\langle I^+ \right\rangle(0)$$
$$- \left[\exp\left\{ -\left(i\omega - i\pi J_{IS} + R_{ave} \right) t \right\} - \exp\left\{ -\left(i\omega + i\pi J_{IS} + R_{ave} \right) t \right\} \right] \left\langle 2 I^+ S_z \right\rangle(0)$$
$$\left\langle 2 I^+ S_z \right\rangle(t) = \tfrac{1}{2}\left[\exp\left\{ -\left(i\omega - i\pi J_{IS} + R_{ave} \right) t \right\} + \exp\left\{ -\left(i\omega + i\pi J_{IS} + R_{ave} \right) t \right\} \right] \left\langle 2 I^+ S_z \right\rangle(0)$$
$$- \left[\exp\left\{ -\left(i\omega - i\pi J_{IS} + R_{ave} \right) t \right\} - \exp\left\{ -\left(i\omega + i\pi J_{IS} + R_{ave} \right) t \right\} \right] \left\langle I^+ \right\rangle(0) \qquad [123]$$

with

$$R_{ave} = (R_{2I} + R_{2IS})/2 = (1/48)\ \{4j(0) + j(\omega_I - \omega_S) + 3j(\omega_I) + 3j(\omega_S) + 6j(\omega_I + \omega_S)\} \qquad [124]$$

Equation [123] predicts that the signal arising from I^+ has the expected form of a doublet with linewidth R_{ave}/π. The doublet is in-phase if $\langle 2I^+S_z \rangle(0) = 0$ and anti-phase if $\langle I^+ \rangle(0) = 0$. Evolution of the scalar coupling interaction on a faster time scale than the relaxation processes averages the two relaxation rate constants because coherence is rapidly exchanged between the I^+ and $2I^+S_z$ operators.

For the purely dipolar *IS* interaction in the spin diffusion limit,

$$R_{2I} - R_{2IS} = 3\, d_{00}\, J(\omega_S) / 8 = \frac{3\mu_0^2 \hbar^2 \gamma_I^2}{320\, \pi^2 B_0^2 r_{IS}^6 \tau_c} \qquad [125]$$

normally is quite small. For example, if $I = {}^{15}\text{N}$, $S = {}^{1}\text{H}$, and τ_c = 5 ns, then $R_{2I} - R_{2IS}$ = 0.016 s^{-1}, compared with J_{IS} = 92 Hz. However, the S_z operator may have relaxation pathways other than the IS dipolar interaction. In the cited example, the proton S_z operator would be dipolar coupled to other protons, and the relaxation rate constant for the $2I^+S_z$ operator contains a contribution, R_{ext}, from proton dipolar longitudinal relaxation. Ignoring cross-correlation and cross-relaxation effects, R_{ext} is simply additive to R_{2IS}. The additional contribution from R_{ext} has two important effects. First, R_{ave} is increased by $R_{ext}/2$, as seen from [124]. Practical consequences of the increased linewidth in heteronuclear NMR spectra are discussed in §6.2. Second, if R_{ext} is sufficiently large, then $(R_{2I} - R_{2IS} - R_{ext})^2 \quad R_{ext}^2 \gg (2\pi J_{IS})^2$, $\lambda_+ = i\omega + R_{2I}$, $\lambda_- = i\omega + R_{2IS} + R_{ext}$, and [121] reduces to:

$$\left\langle I^+ \right\rangle(t) = \left\langle I^+ \right\rangle(0) \exp\left[-\left(i\omega + R_{2I}\right)t\right]$$
$$\left\langle 2I^+S_z \right\rangle(t) = \left\langle 2I^+S_z \right\rangle(0) \exp\left[-\left(i\omega + R_{2IS} + R_{ext}\right)t\right] \qquad [126]$$

The expected doublet has been reduced to a singlet resonance in a process commonly called *self-decoupling*, which is similar both to scalar relaxation of the second kind (§4.5) and chemical exchange (§5.2). For $(R_{2I} - R_{2IS} - R_{ext})^2 \quad (2\pi J_{IS})^2$, the doublet is partially decoupled and broadened as for intermediate chemical exchange (§5.2). Self-decoupling can complicate the measurement of scalar coupling constants (*26*).

A similar set of equations can obtained for the S^+ and $2S^+I_z$ coherences by interchanging the I and S labels. Notice that for an uncoupled IS spin system, $R_{2I} \neq R_{2S}$, but for a scalar coupled spin system undergoing free precession, R_{ave} is identical for the I and S spins.

4.3 Intramolecular dipolar relaxation for IS spin system in the rotating frame

An *IS* homonuclear spin system, in which the two spins interact through the dipolar interaction but are not scalar coupled, will be treated. The spin lock field is assumed to be applied along with *x*-phase. The auto-relaxation rate constant of the I'_z operator and the cross-relaxation rate constant between the I'_z and S'_z operators will be calculated in the tilted rotating frame. As discussed in §2.3, in the presence of the spin lock field the *I* and *S* spins are degenerate and are treated as like spins; thus, the components of the dipolar interaction listed in Table 3 must be redefined according to [80] as

$$\mathbf{A}_2^0 = \mathbf{A}_{20}^0 + \mathbf{A}_{21}^{-0} + \mathbf{A}_{21}^0$$

$$\mathbf{A}_2^{\pm 1} = \mathbf{A}_{20}^{\pm 1} + \mathbf{A}_{21}^{\pm 1}$$

$$\mathbf{A}_2^{\pm 2} = \mathbf{A}_{20}^{\pm 2} \qquad [127]$$

From [82],

$$I'_z = \sin\theta_I I_x + \cos\theta_I I_z,$$

$$S'_z = \sin\theta_S S_x + \cos\theta_S S_z, \qquad [128]$$

Applying [81], the double commutators $[\mathbf{A}_2^{-q}, [\mathbf{A}_2^q, I'_z]]$ are calculated first. Straightforward, but tedious, calculations yield

$$[\mathbf{A}_2^0, [\mathbf{A}_2^0, I'_z]] = \sin\theta_I(5I_x + 4S_x)/24 + \cos\theta_I(I_z - S_z)/6$$

$$[\mathbf{A}_2^{-1}, [\mathbf{A}_2^1, I'_z]] = [\mathbf{A}_2^1, [\mathbf{A}_2^{-1}, I'_z]]$$

$$= -\sin\theta_I(2I_x + 2S_x + 2I^-)/8 - \cos\theta_I I_z /8$$

$$[\mathbf{A}_2^{-2}, [\mathbf{A}_2^2, I'_z]] = [\mathbf{A}_2^2, [\mathbf{A}_2^{-2}, I'_z]]$$

$$= -\sin\theta_I I^-/8 - \cos\theta_I(I_z + S_z)/8 \qquad [129]$$

The auto-relaxation rate constant is determined by premultiplying the above expressions by I'_z and forming the trace:

$$<\sin\theta_I I_x + \cos\theta_I I_z|\sin\theta_I(5I_x + 4S_x)/24 + \cos\theta_I(I_z - S_z)/6>$$

$$= (5/24)\ \sin^2\theta_I + (1/12)\ \cos^2\theta_I$$

$$<\sin\theta_I I_x + \cos\theta_I I_z|-\sin\theta_I(2I_x + 2S_x + 2I^-)/8 - \cos\theta_I I_z /8>$$

$$= -(3/16)\ \sin^2\theta_I - (1/8)\ \cos^2\theta_I$$

$$<\sin\theta_I I_x + \cos\theta_I I_z|-\sin\theta_I I^-/8 - \cos\theta_I(I_z + S_z)/8>$$

$$= (1/8)\ \sin^2\theta_I + (1/4)\ \cos^2\theta_I \qquad [130]$$

Thus, the auto-relaxation rate, $R_1(\theta_I)$ (which commonly is called $R_{1\rho}$) is given by

$$R_1(\theta_I) = (1/48)\ \{(2\cos^2\theta_I + 5\sin^2\theta_I)\, j(0) +$$

$$(6\cos^2\theta_I + 9\sin^2\theta_I)\, J(\omega_0) + (12\cos^2\theta_I + 6\sin^2\theta_I)\, j(2\omega_0)\ \}$$

$$= R_{1I}\cos^2\theta_I + \mathrm{R}_{2I}\sin^2\theta_I \qquad [131]$$

Similarly, the cross-relaxation rate constant is found by premultiplying the expressions in [129] by S'_z and forming the trace:

$$<\sin\theta_S\, S_x + \cos\theta_S\, S_z|\sin\theta_I\ (5I_x + 4S_x)/24 + \cos\theta_I\ (I_z - S_z)/6>$$

$$= (1/6)\ \sin\theta_S \sin\theta_I - (1/12)\ \cos\theta_S\ \cos\theta_I$$

$$<\sin\theta_S\ S_x + \cos\theta_S\ S_z | -\sin\theta_I\ (2I_x + 2S_x + 2I^-)/8 - \cos\theta_I\ I_z\ /8>$$

$$= -(1/8)\ \sin\theta_S \sin\theta_I$$

$$<\sin\theta_S\ S_x + \cos\theta_S\ S_z | -\sin\theta_I\ I^-/8 - \cos\theta_I\ (I_z + S_z)/8>$$

$$= (1/4)\ \cos\theta_S\ \cos\theta_I \qquad [132]$$

Thus, the cross-relaxation rate, $R_{IS}(\theta_I, \theta_S)$ is given by

$$R_{IS}(\theta_I, \theta_S) = (1/24)\ \{(-\cos\theta_S\ \cos\theta_I + 2\sin\theta_S \sin\theta_I)\ j(0)$$

$$+ 3\sin\theta_S \sin\theta_I\ j(\omega_0) + 6\cos\theta_S\ \cos\theta_I\ j(2\omega_0)\ \}$$

$$= \cos\theta_I \cos\theta_S \sigma_{IS}^{NOE} + \sin\theta_I \sin\theta_S \sigma_{IS}^{ROE} \qquad [133]$$

in which pure laboratory frame cross-relaxation rate constant, σ_{IS}^{NOE}, is given in [109] and the pure rotating frame cross-relaxation rate constant is given by (*27*):

$$\sigma_{IS}^{ROE} = (1/24)\{2\,j(0) + 3\,j(\omega_0)\} \qquad [134]$$

For both auto-relaxation and cross-relaxation, the effect of the tilted field is to average laboratory (longitudinal) and rotating frame (transverse) relaxation rate constants by the projection of the spin operators onto the tilted reference frame.

4.4 Chemical shift anisotropy and quadrupolar relaxation

Chemical shifts are reflections of the electronic environments that modify the local magnetic fields experienced by different nuclei. These

local fields are anisotropic; consequently, the components of the local fields in the laboratory reference frame vary as the molecule re-orients due to molecular motion. These varying magnetic fields are a source of relaxation. Very approximately, the maximum CSA for a particular nucleus is of the order of the chemical shift range for the nucleus. CSA is important as a relaxation mechanism only for nuclei with a large chemical shift range. In the NMR spectroscopy of biological molecules, carbon, nitrogen and phosphorous have significant CSA contributions to relaxation. CSA is generally a negligible effect for proton relaxation. CSA rate constants have a quadratic dependence on the applied magnetic field strength. Thus, use of higher magnetic field strengths does not always increase the achievable signal-to-noise ratio as much as expected theoretically, because increased CSA relaxation broadens the resonance linewidths.

Nuclei with $I > 1/2$ also possess nuclear electric quadrupole moments. The quadrupole moment is a characteristic of the particular nucleus and represents a departure of the nuclear charge distribution from spherical symmetry. The interaction of the quadrupole moment with local oscillating electric field gradients (due to electrons) provide a relaxation mechanism. Quadrupolar interactions can be very large and efficient for promoting relaxation. Quadrupolar nuclei display broad resonance lines in NMR spectra, unless the nuclei are in highly symmetric electronic environment (which reduces the magnitudes of the electric field gradients at the locations of the nuclei). As discussed in more detail elsewhere, Bloch spin-lattice and spin-spin relaxation rate constants can only be defined for quadrupolar nuclei under extreme narrowing conditions or for quadrupolar nuclei with $I = 1$ (*2*).

The terms $\mathbf{A}_{2p}^{q}$ for the CSA and quadrupolar interactions are given in Tables 6 and 7. The spherical harmonic and spatial functions for the different interactions are given in Tables 1 and 2. Relaxation rate constants are calculated for a single spin I by using the basis operators, I_z, I^-, I^+. Spin-lattice and spin-spin relaxation rate constants for the CSA and quadrupolar interactions are calculated by the same procedure as for the dipolar interactions and are given in Table 8. The results are calculated for axially symmetric chemical shift and electric field gradient tensors (i.e. $\sigma_{xx} = \sigma_{yy} \neq \sigma_{zz}$ and $V_{xx} = V_{yy} \neq V_{zz}$). Extensions to these results for anisotropic tensors are given elsewhere (*2*).

Table 6: Tensor Operators for the CSA Interaction

CSA				
q	p	A_{2p}^{q}	$A_{2p}^{-q} = A_{2p}^{q\dagger}$	ω_p
0	0	$(2/\sqrt{6})\ I_z$	$(2/\sqrt{6})\ I_z$	0
1	0	$-(1/2)\ I^+$	$(1/2)\ I^-$	ω_I
2	0	—	—	$2\omega_I$

Table 7: Tensor Operators for the Quadrupolar Interaction

Quadrupolar				
q	p	A^{q}_{2p}	$A^{-q}_{2p} = A^{q}_{2p}\dagger$	ω_p
0	0	$(1/2\sqrt{6})\ [4I_z^2 - I^+I^- - I^-I^+]$	$(1/2\sqrt{6})\ [4I_z^2 - I^+I^- - I^-I^+]$	0
1	0	$-(1/2)\ (I_zI^+ + I^+I_z)$	$-(1/2)\ (I_zI^- + I^-I_z)$	ω_I
2	0	$(1/2)\ I^+I^+$	$(1/2)\ I^-I^-$	$2\omega_I$

Table 8: CSA and Quadrupolar Relaxation Rate Constants

Rate Constant	CSA[1]	Quadrupolar[2]
R_1	$d_{00}\ J(\omega_I)$	$3d_{00}\ \{J(\omega_I) + 2J(2\omega_I)\}$
R_2	$(d_{00}/6)\ \{4J(0) + 3J(\omega_I)\}$	$(3d_{00}/2)\ \{3J(0) + 5J(\omega_I) + 2J(2\omega_I)\}$

[1] $d_{00} = (\sigma_{\|} - \sigma_{\perp})^2\, \gamma_I^2 B_0^2 / 3 = (\sigma_{\|} - \sigma_{\perp})^2\, \omega_I^2 / 3.$

[2] A spin-1 quadrupolar nucleus is assumed. $d_{00} = \left[e^2 qQ / (4\hbar)\right]^2.$

4.5 Scalar relaxation

The isotropic scalar coupling Hamiltonian, $H_J = 2\pi J_{IS}\, \mathbf{I}\cdot\mathbf{S}$, slightly perturbs the Zeeman energy levels of the coupled spins; the resonances thereby are split into characteristic multiplet patterns. Spin I experiences a local magnetic field that depends on the value of the coupling constant and the state of spin S. The local magnetic field becomes time-dependent if the value of J_{IS} is time-dependent or if state of the S spin varies rapidly. The former relaxation mechanism is termed *scalar relaxation of the first kind*;

the latter mechanism is termed *scalar relaxation of the second kind*. Scalar relaxation of the first kind results from transitions of the spin system between environments with different values of J_{IS}. For example, the three-bond scalar coupling constant for a pair of protons depends upon the intervening dihedral angle according to the Karplus relationship. If the dihedral angle is time-dependent, the consequent time-dependence of J_{IS} can lead to scalar relaxation. Scalar relaxation of the second kind results if the S spin relaxes rapidly (e.g. S is a quadrupolar nucleus) or is involved in rapid chemical exchange. Scalar relaxation of the second kind also can be significant if the S spin is a proton nucleus in a macromolecule, in which case the homonuclear relaxation rate constants (reflecting the dipolar interaction of the S spin with protons other than the I spin) can be large. Normally field fluctuations produced by this mechanism are not fast enough for effective longitudinal relaxation, but transverse relaxation may be induced.

In contrast to earlier sections, the relaxation rate constants for scalar relaxation will not be explicitly calculated; instead, the appropriate expressions for R_1^{sc} and R_2^{sc} are given by (*2*):

$$R_1^{sc} = \frac{2A^2}{3} S(S+1) \frac{\tau_2}{1+(\omega_I - \omega_S)^2 \tau_2^2}$$

$$R_2^{sc} = \frac{A^2}{3} S(S+1) \left[\frac{\tau_2}{1+(\omega_I - \omega_S)^2 \tau_2^2} + \tau_1 \right] \qquad [135]$$

for τ_1, $\tau_2 << 1/A$. For scalar relaxation of the first kind, $A = 2\pi(p_1 p_2)^{1/2}(J_1 - J_2)$, in which J_1 and J_2 are the scalar coupling constants, p_1 and p_2 are the relative populations ($p_1 + p_2 = 1$), and $\tau_1 = \tau_2 = \tau_e$ are the exchange time

constants for the two environments. For scalar relaxation of the second kind, $A = 2\pi J_{IS}$, in which τ_1 and τ_2 are the spin-lattice and spin-spin relaxation time constants for the S spin, respectively. If the S spin is a quadrupolar nucleus, then the relaxation time constants can be calculated using the expressions given in Table 8. A more general treatment of scalar relaxation has been given by London (*28*).

5 Chemical exchange effects in NMR spectroscopy

NMR spectroscopy provides an extremely powerful and convenient method for monitoring the *exchange* of a nucleus between environments due to chemical reactions or conformational transitions. In the first instance, the nucleus exchanges intermolecularly between sites in different molecules; in the second, the nucleus exchanges intramolecularly between conformations. The exchange process can be monitored by NMR spectroscopy even if the sites are chemically equivalent provided that the sites are magnetically distinct. Nuclear spins can be manipulated during the NMR experiment without affecting the chemical states of the system, because of the weak coupling between the spin system and the lattice. Thus, chemical reactions and conformational exchange processes can be studied by NMR spectroscopy while the system remains in chemical equilibrium.

To establish a qualitative picture of the effects of exchange on an NMR spectrum, suppose that a given nucleus exchanges with rate constant k between two magnetically distinct sites with resonance frequencies that differ by $\Delta\omega$. On average, the resonance frequency of the spin in each site can only be observed for a time of the order of $1/k$ before the spin jumps

to the other site and begins to precess with a different frequency. The finite observation time places a lower limit on the magnitude of $\Delta\omega$ required to distinguish the two sites. If the exchange rate is *slow* ($k << \Delta\omega$), then distinct signals are observed from the nuclei in the two sites; in contrast, if the exchange rate is *fast* ($k >> \Delta\omega$) then a single resonance is observed at the population-weighted average chemical shift of the nuclei in the two sites. *Coalescence* between the two signals occurs for intermediate exchange ($k = \Delta\omega$). *The NMR chemical shift timescale is defined by the difference between the frequencies of the two exchanging resonances.*

In addition, chemical exchange can contribute to spin relaxation. As a consequence of exchange, the resonance frequency (or effective Zeeman Hamiltonian) of the affected nuclear spin fluctuates stochastically by $\pm\Delta\omega/2$. The fluctuating longitudinal field constitutes an adiabatic relaxation mechanism and consequently contributes to transverse relaxation (see §1). The magnitude of the relaxation rate constant depends on the value of $J(\Delta\omega)$ for the exchange process. If $J(\omega)$ is assumed to be Lorentzian [92], then the relaxation contributions from exchange are small for $k << \Delta\omega$ (slow exchange) or $k >> \Delta\omega$ (fast exchange) and are maximal for $k = \Delta\omega$ (intermediate exchange).

5.1 Chemical exchange for isolated spins

For simplicity, only the case of chemical exchange in spin systems without scalar coupling interactions will be treated. In this situation, the exchange process can be treated using an extension of the Bloch equations (§1.1). An alternative derivation is given by Wennerström (*29*).

A first order chemical reaction (or two-site chemical exchange) between two chemical species, A_1 and A_2, is described by the reaction

$$A_1 \underset{k_{-1}}{\overset{k_1}{\rightleftharpoons}} A_2 \qquad [136]$$

in which k_1 is the reaction rate constant for the forward reaction and k_{-1} is the reaction rate constant for the reverse reaction. The chemical kinetic rate laws for this system can be written in matrix form as

$$\frac{d}{dt}\begin{bmatrix}[A_1](t)\\ [A_2](t)\end{bmatrix} = \begin{bmatrix}-k_1 & k_{-1}\\ k_1 & -k_{-1}\end{bmatrix}\begin{bmatrix}[A_1](t)\\ [A_2](t)\end{bmatrix} \qquad [137]$$

For a coupled set of N first-order chemical reactions between N chemical species, this equation can be generalized to

$$\frac{d\mathbf{A}(t)}{dt} = \mathbf{K}\mathbf{A}(t) \qquad [138]$$

in which the matrix elements of the rate matrix, $\mathbf{K}$, are given by

$$\begin{aligned} K_{ij} &= k_{ji} \qquad (i \neq j)\\ K_{ii} &= -\sum_{\substack{j=1\\ j\neq i}}^{N} k_{ij} \end{aligned} \qquad [139]$$

and the chemical reaction between the ith and jth species is

$$A_i \underset{k_{ji}}{\overset{k_{ij}}{\rightleftharpoons}} A_j \qquad [140]$$

The modified Bloch equations can be written in matrix form for the jth chemical species as

$$\frac{d\mathbf{M}_{jz}(t)}{dt} = \gamma(1-\sigma_j)[\mathbf{M}_j(t)\times\mathbf{B}(t)]_z - \mathbf{R}_{1j}\left\{\mathbf{M}_{jz}(t)-\mathbf{M}_{j0}(t)\right\} + \sum_{k=1}^{N} K_{jk}\mathbf{M}_{kz}(t)$$

$$\frac{d\mathbf{M}_{jx}(t)}{dt} = \gamma(1-\sigma_j)[\mathbf{M}_j(t)\times\mathbf{B}(t)]_x - \mathbf{R}_{2j}\mathbf{M}_{jx}(t) + \sum_{k=1}^{N} K_{jk}\mathbf{M}_{kx}(t)$$

$$\frac{d\mathbf{M}_{jy}(t)}{dt} = \gamma(1-\sigma_j)[\mathbf{M}_j(t)\times\mathbf{B}(t)]_y - \mathbf{R}_{2j}\mathbf{M}_{jy}(t) + \sum_{k=1}^{N} K_{jk}\mathbf{M}_{ky}(t)$$

[141]

with

$$\mathbf{M}_{j0}(t) = \mathbf{M}_0[A_j](t) \Big/ \sum_{j=1}^{N} [A_j](t) \qquad [142]$$

The modified Bloch equations for chemical reactions are called the McConnell equations (*30*). If the system is in chemical equilibrium, then $[A_j](t) = [A_j]$. The index j in [141] and [142] refer to the same spin in different chemical environments, not to different nuclear spins (cf. §1.2).

The above equations can be generalized to the case of higher-order chemical reactions by defining the pseudo-first order rate constants:

$$k_{ij} = \frac{\xi_{ij}(t)}{[A_i](t)} \qquad [143]$$

in which $\xi_{ij}(t)$ is the rate law for conversion of the *i*th species containing the nuclear spin of interest into the *j*th species containing the nuclear spin of interest. The effect of the chemical reactions is to shift the spin of interest between molecular environments. For example, consider the elementary reaction

$$A_1 + B \underset{k_{-1}}{\overset{k_1}{\rightleftharpoons}} A_2 + C \qquad [144]$$

in which a spin in species A_1 is transferred to species A_2 as a result of the chemical reaction. The chemical kinetic rate laws for this system can be written in matrix form as

$$\frac{d}{dt}\begin{bmatrix}[A_1](t)\\ [A_2](t)\end{bmatrix}=\begin{bmatrix}-k_1[B](t) & k_{-1}[C](t)\\ k_1[B](t) & -k_{-1}[C](t)\end{bmatrix}\begin{bmatrix}[A_1](t)\\ [A_2](t)\end{bmatrix} \qquad [145]$$

which has the same form as [138] in which the elements of **K** are defined using [139] and [143]. Importantly, the rate expressions for [B](t) and [C](t) are not included in [145] because the spin of interest is not contained in either species.

In the absence of applied rf fields, the equation governing the evolution of longitudinal magnetization becomes

$$\frac{d\mathbf{M}_{jz}(t)}{dt}=-\mathbf{R}_{1j}\left\{\mathbf{M}_{jz}(t)-\mathbf{M}_{j0}(t)\right\}+\sum_{k=1}^{N}K_{jk}\mathbf{M}_{kz}(t) \qquad [146]$$

Defining

$$\mathbf{M}_z(t)=\begin{bmatrix}\mathbf{M}_{1z}(t)\\ \vdots\\ \mathbf{M}_{Nz}(t)\end{bmatrix} \qquad [147]$$

yields the compact expression,

$$\frac{d\mathbf{M}_z(t)}{dt}=(-\mathbf{R}+\mathbf{K})\left\{\mathbf{M}_z(t)-\mathbf{M}_0(t)\right\}+\mathbf{K}\mathbf{M}_0(t) \qquad [148]$$

in which the elements of **R** are given by $R_{ij} = \delta_{ij} R_{1j}$ (for simplicity, the possibility of simultaneous dipolar cross-relaxation and chemical exchange is not considered). If the system is in chemical equilibrium, $\mathbf{K}\mathbf{M}_0(t) = \mathbf{K}\mathbf{M}_0 = 0$ and

$$\frac{d\Delta\mathbf{M}_z(t)}{dt} = (-\mathbf{R} + \mathbf{K})\Delta\mathbf{M}_z(t) \qquad [149]$$

The equation of motion for the transverse magnetization can be written in the rotating frame as

$$\frac{d\mathbf{M}^+(t)}{dt} = (i\mathbf{\Omega} - \mathbf{R} + \mathbf{K})\mathbf{M}^+(t) \qquad [150]$$

in which the elements of Ω are given by $\Omega_{ij} = \delta_{ij}\,\Omega_j$, and the elements of $\mathbf{R}$ are given by $R_{ij} = \delta_{ij}\,R_{2j}$.

Equations [149] and [150] have the same functional form as [22] and can be solved by the same methods [23]. For example, the rate matrix for longitudinal relaxation in a system undergoing two-site exchange is given by,

$$\mathbf{R} - \mathbf{K} = \begin{bmatrix} \rho_1 + k_1 & -k_{-1} \\ -k_1 & \rho_2 + k_{-1} \end{bmatrix} \qquad [151]$$

with eigenvalues

$$\lambda_{\pm} = \tfrac{1}{2}\left\{(\rho_1 + \rho_2 + k_1 + k_{-1}) \pm \left[(\rho_1 - \rho_2 + k_1 - k_{-1})^2 + 4\,k_1 k_{-1}\right]^{1/2}\right\} \qquad [152]$$

The time course of the magnetization is given by

$$\begin{bmatrix} \Delta M_1(t) \\ \Delta M_2(t) \end{bmatrix} = \begin{bmatrix} a_{11}(t) & a_{12}(t) \\ a_{21}(t) & a_{22}(t) \end{bmatrix} \begin{bmatrix} \Delta M_1(0) \\ \Delta M_2(0) \end{bmatrix} \qquad [153]$$

in which

$$a_{11}(t) = \tfrac{1}{2}\left[\left(1 - \frac{\rho_1 - \rho_2 + k_1 - k_{-1}}{(\lambda_+ - \lambda_-)}\right)\exp(-\lambda_- t) + \left(1 + \frac{\rho_1 - \rho_2 + k_1 - k_{-1}}{(\lambda_+ - \lambda_-)}\right)\exp(-\lambda_+ t)\right]$$

$$a_{22}(t) = \tfrac{1}{2}\left[\left(1 + \frac{\rho_1 - \rho_2 + k_1 - k_{-1}}{(\lambda_+ - \lambda_-)}\right)\exp(-\lambda_- t) + \left(1 - \frac{\rho_1 - \rho_2 + k_1 - k_{-1}}{(\lambda_+ - \lambda_-)}\right)\exp(-\lambda_+ t)\right]$$

$$a_{12}(t) = \frac{k_{-1}}{(\lambda_+ - \lambda_-)}\left[\exp(-\lambda_- t) - \exp(-\lambda_+ t)\right]$$

$$a_{21}(t) = \frac{k_1}{(\lambda_+ - \lambda_-)}\left[\exp(-\lambda_- t) - \exp(-\lambda_+ t)\right]$$

[154]

To obtain some insight in to the form of these equations, assume that $\rho_1 = \rho_2 = \rho$, and that exchange is symmetrical with $k_1 = k_{-1} = k$. Under these conditions, the time-dependence of the longitudinal magnetization is given by,

$$a_{11}(t) = a_{22}(t) = \tfrac{1}{2}\left[1 + \exp(-2kt)\right]\exp(-\rho t)$$
$$a_{12}(t) = a_{21}(t) = \tfrac{1}{2}\left[1 - \exp(-2kt)\right]\exp(-\rho t) \qquad [155]$$

The homology between [30] and [155] illustrates the fundamental similarity between the effects of cross-relaxation and chemical exchange on longitudinal magnetization. Indeed, similar experimental techniques are utilized to study both phenomena (such as NOESY and ROESY experiments, §7).

The rate matrix for transverse relaxation in a system undergoing two-site exchange is given by,

$$-i\Omega + \mathbf{R} - \mathbf{K} = \begin{bmatrix} -i\Omega_1 + \rho_1 + k_1 & -k_{-1} \\ -k_1 & -i\Omega_2 + \rho_2 + k_{-1} \end{bmatrix} \qquad [156]$$

with eigenvalues

$$\lambda_{\pm} = \frac{1}{2}\left\{\left(-i\Omega_1 - i\Omega_2 + \rho_1 + \rho_2 + k_1 + k_{-1}\right)\right.$$
$$\left.\pm\left[\left(-i\Omega_1 + i\Omega_2 + \rho_1 - \rho_2 + k_1 - k_{-1}\right)^2 + 4\,k_1 k_{-1}\right]^{1/2}\right\} \qquad [157]$$

The time course of the magnetization is given by

$$\begin{bmatrix} M_1^+(t) \\ M_2^+(t) \end{bmatrix} = \begin{bmatrix} a_{11}(t) & a_{12}(t) \\ a_{21}(t) & a_{22}(t) \end{bmatrix} \begin{bmatrix} M_1^+(0) \\ M_2^+(0) \end{bmatrix} \qquad [158]$$

in which

$$a_{11}(t) = \frac{1}{2}\left[\left(1 - \frac{-i\Omega_1 + i\Omega_2 + \rho_1 - \rho_2 + k_1 - k_{-1}}{\left(\lambda_+ - \lambda_-\right)}\right)\exp(-\lambda_- t)\right.$$
$$\left.+\left(1 + \frac{-i\Omega_1 + i\Omega_2 + \rho_1 - \rho_2 + k_1 - k_{-1}}{\left(\lambda_+ - \lambda_-\right)}\right)\exp(-\lambda_+ t)\right]$$

$$a_{22}(t) = \frac{1}{2}\left[\left(1 + \frac{-i\Omega_1 + i\Omega_2 + \rho_1 - \rho_2 + k_1 - k_{-1}}{\left(\lambda_+ - \lambda_-\right)}\right)\exp(-\lambda_- t)\right.$$
$$\left.+\left(1 - \frac{-i\Omega_1 + i\Omega_2 + \rho_1 - \rho_2 + k_1 - k_{-1}}{\left(\lambda_+ - \lambda_-\right)}\right)\exp(-\lambda_+ t)\right]$$

$$a_{12}(t) = \frac{k_{-1}}{\left(\lambda_+ - \lambda_-\right)}\left[\exp(-\lambda_- t) - \exp(-\lambda_+ t)\right] \qquad [159]$$

$$a_{21}(t) = \frac{k_1}{\left(\lambda_+ - \lambda_-\right)}\left[\exp(-\lambda_- t) - \exp(-\lambda_+ t)\right]$$

To obtain some insight in to the form of these equations, assume that $\Omega_1 = -\Omega_2 = \Omega$ (i.e. the reference frequency in the rotating frame is midway between the frequencies of the two sites), that $\rho_1 = \rho_2 = \rho$, and that

exchange is symmetrical with $k_1 = k_{-1} = k$. Under these conditions, the time-dependence of the transverse magnetization is given by

$$a_{11}(t) = \tfrac{1}{2}\left[\left(1+\frac{i\Omega}{\Delta}\right)\exp\left\{-(\rho+k-\Delta)t\right\}+\left(1-\frac{i\Omega}{\Delta}\right)\exp\left\{-(\rho+k+\Delta)t\right\}\right]$$

$$a_{22}(t) = \tfrac{1}{2}\left[\left(1-\frac{i\Omega}{\Delta}\right)\exp\left\{-(\rho+k-\Delta)t\right\}+\left(1+\frac{i\Omega}{\Delta}\right)\exp\left\{-(\rho+k+\Delta)t\right\}\right] \qquad [160]$$

$$a_{12}(t) = a_{21}(t) = \frac{k}{2\Delta}\left[\exp\left\{-(\rho+k-\Delta)t\right\} - \exp\left\{-(\rho+k+\Delta)t\right\}\right]$$

in which $\Delta = (k^2 - \Omega^2)^{1/2}$. In the slow exchange limit, $\Omega >> k$ and

$$a_{11}(t) = \exp\left\{-(\rho+k-i\Omega)t\right\}$$

$$a_{22}(t) = \exp\left\{-(\rho+k+i\Omega)t\right\} \qquad [161]$$

$$a_{12}(t) = a_{21}(t) = 0$$

Two resonances are observed at $\Omega_1 = \Omega$ and $\Omega_2 = -\Omega$ with linewidths equal to $(\rho + k)/\pi$. In the fast exchange limit, $\Omega << k$ and,

$$a_{11}(t) = a_{22}(t) = \tfrac{1}{2}\left[1+\exp(-2kt)\right]\exp(-\rho t)$$

$$a_{12}(t) = a_{21}(t) = \tfrac{1}{2}\left[1-\exp(-2kt)\right]\exp(-\rho t) \qquad [162]$$

In this case, [162] are purely real. Consequently, a single resonance line is observed at a shift of $(\Omega_1+\Omega_2)/2 = 0$. The observed signal is equal to

$$\begin{aligned} M_1^+(t) + M_2^+(t) &= a_{11}(t)M_1^+(0) + a_{12}(t)M_2^+(0) + a_{22}(t)M_2^+(0) + a_{21}(t)M_1^+(0) \\ &= \left[a_{11}(t) + a_{12}(t) + a_{22}(t) + a_{21}(t)\right]M^+(0)/2 \\ &= M^+(0)\exp(-\rho t) \end{aligned} \qquad [163]$$

and has a linewidth equal to ρ/π. Equations [161] and [163] confirm the qualitative conclusions about the slow and fast exchange regimes stated above.

For two site exchange, lineshapes expected for various exchange rates can be calculated by Fourier transformation of [159] or [160]. Figure 9 shows calculated spectra in several exchange regimes. Figure 9a shows the case of slow exchange. As expected from [161], two resonance lines are observed. As the exchange rate increases, the resonance lines broaden as shown in Figure 9b. When the exchange rate is of the order of the chemical shift separation between the two sites, the lines become very broad and begin to coalesce (Figure 9c). This is known as the *intermediate exchange* regime or *coalescence*. Intermediate exchange processes can cause peaks to disappear in spectra because the broadening becomes so great that the resonance line becomes indistinguishable from the baseline noise. Increasing the exchange rate for the system above the coalescence point drives the system into fast exchange (Figure 9d,e). As expected from [163] a single resonance is observed at the average resonance frequency for the two sites and the linewidths become narrower.

5.2 Qualitative effects of chemical exchange in scalar coupled systems

Multiplet structure due to scalar couplings is affected by chemical exchange. Detailed theoretical treatment using the density matrix formalism is beyond the subject matter of this text (*31*); instead, the present discussion will present qualitatively the most important effects.

Formally, scalar relaxation (§4.5) and chemical exchange in scalar coupled systems are homologous. Two different cases must be considered: intermolecular (homologous to scalar relaxation of the second kind) and intramolecular exchange (homologous to scalar relaxation of the first kind).

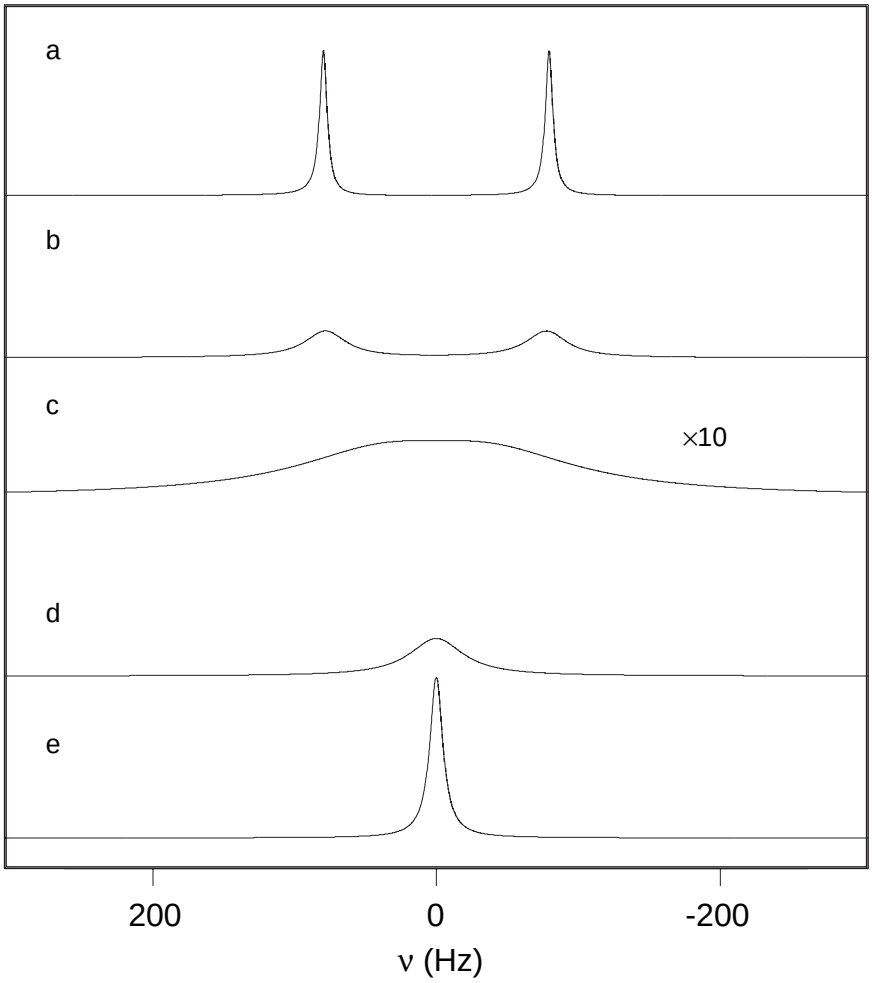

Figure 9. Chemical exchange for a two-site system. Shown are the Fourier transformations of FIDs calculated by using [160]. The calculations used Ω = 80 Hz and ρ = 10 s^{-1}. Calculations were performed for values of the exchange rate, k, equal to (a) 10 s^{-1}, (b) 100 s^{-1}, (c) 450 s^{-1}, (d) 1000 s^{-1} and (e) 5000 s^{-1}. The spectrum for (c) has been expanded vertically by a factor of 10 for clarity.

Intermolecular chemical exchange in scalar coupled systems is encountered frequently in biological NMR applications. For example, exchange between labile amide protons and solvent protons perturbs the

NH to H^{α} scalar coupling interaction. In an *IS* spin system, the *I* spin resonance is a doublet, with the lines separated by J_{IS}. One line of the doublet is associated with the *S* spin in the α state, and the other line is associated with the *S* spin in the β state. Suppose that a given *I* spin is coupled to an *S* spin in the α state. If the *S* spin exchanges with another *S* spin originating from the solvent (intermolecular exchange), then after the exchange the *I* spin has equal probability of being coupled to an *S* spin in the α and β states because the incoming spin has a 50% chance of either being in its α state or in its β state. Similar considerations hold for an *I* spin initially coupled to an *S* spin in the β state. Consequently, the *I* spin sees the *S* spin state constantly changing due to exchange and thus the frequency of the *I* spin resonance constantly changes between the frequencies of the two lines of the doublet. This phenomenon constitutes a two-site exchange process and exhibits properties of slow, intermediate and fast exchange. If the exchange is fast compared to the difference in frequency between the two lines (i.e. compared to the scalar coupling constant), a single line is observed at the mean frequency (the Larmor frequency of the *I* spin). Since homonuclear scalar couplings constants tend to be small, relatively slow exchange processes, that would minimally perturb the chemical shifts of the exchanging spins, can result in collapse of multiplet structure. Indeed, the broadening of multiplets and the disappearance of multiplet structure are the first clues to the existence of exchange phenomena in NMR spectra.

Intramolecular exchange constitutes a slightly different situation. Consider a system in which spin *I* is scalar coupled to spin *S*, but due to the presence of multiple conformers, spin *S* can be in *n* environments, S^1, S^2, ...

S^n, with different scalar coupling constants. For simplicity, the chemical shift of the I spin is assumed to be identical in all conformers. If the conformers interconvert on a time scale long compared to the scalar coupling constants, the I spin multiplet is a superposition of n doublets arising from the IS^1, IS^1, ..., IS^n scalar coupling interactions. On the other hand, if the conformers interconvert at a rate much larger than the scalar coupling constants, the I spin resonance is a doublet with an effective scalar coupling constant that is a population weighted average of the n scalar coupling constants. An example of this effect arises for the scalar coupling between H^α and H^β protons in amino acids. If the conformations of the H^β protons are fixed relative to the H^α proton, then the H^α multiplet is split by two coupling constants, one from each of the H^β protons to the H^α proton (e.g. 12 Hz and 3 Hz for a trans, gauche conformation). On the other hand, if the H^β protons exchange between trans, gauche$^+$ and gauche$^-$ rotomeric sites due to free-rotation about the C^α-C^β bond, then the H^α multiplet is split by a single average coupling constant (with a value (12 + 3 + 3)/3 = 6 Hz) due to the H^β protons.

6 Some practical aspects of NMR spin relaxation

6.1 Linewidth

The phenomenological linewidth is defined as the full-width-at-half-height of the resonance lineshape and is a primary factor affecting both resolution and signal-to-noise ratio of NMR spectra. For a Lorentzian lineshape, the homogeneous linewidth is given by $\Delta\nu_{FWHH} = R_2/\pi$ in Hertz (or $\Delta\omega_{FWHH} = 2R_2$ in rad/s) and the inhomogeneous linewidth is $\Delta\nu_{FWHH} = R_2^*/\pi$ in which $R_2^* = R_2 + R_{inhom}$ and R_{inhom} represents the broadening of

the resonance signal due to inhomogeneity of the magnetic field. In modern NMR spectrometers R_{inhom}/π is on the order of 1 Hertz. Values of R_2 (and hence homogenous linewidths) are approximately proportional to the overall rotational correlation time of the protein and thus depend on molecular mass and shape of the molecule.

The correlation time for Brownian rotational diffusion can be measured experimentally by using time-resolved fluorescence spectroscopy, light scattering and NMR spin relaxation spectroscopy, or calculated by using a variety of hydrodynamic theories (that unfortunately require detailed information on the shape of the molecule) (*32*). In the absence of more accurate information, the simplest theoretical approach for approximately spherical globular proteins calculates the isotropic rotational correlation time from Stokes Law:

$$\tau_c = \frac{4\pi\eta_w r_H^3}{3k_B T} \qquad [164]$$

in which η_w is the viscosity of the solvent, r_H is the effective hydrodynamic radius of the protein, k_B is Boltzmann's constant and T is the temperature. The hydrodynamic radius can be very roughly estimated from the molecular mass of the protein by assuming that the specific volume of the protein is $\overline{V}$ = 0.73 cm^3/g and that a hydration layer of r_w = 1.6 to 3.2 Å (corresponding to one-half to one hydration shell) surrounds the protein (*33*):

$$r_H = \left[3\overline{V}M_r / (4\pi N_A)\right]^{1/3} + r_w \qquad [165]$$

For the protein ubiquitin (M_r =8565 Da), [164] and [165] yield r_H = 16.5 Å, and τ_c = 3.8 ns at 300 K, compared with a value of 4.1 ns determined from

NMR spectroscopy . Rotational correlation times in D_2O solution are approximately 25% greater than in H_2O solution because of the larger viscosity of D_2O.

Given theoretical or experimental estimates of τ_c, the theoretical equations presented in §4 and §6 can be used to calculate approximate values of resonance linewidths. The resulting curves are shown in Figure 10. The principle uncertainties in the calculation are due to the following factors: (*i*) anisotropic rotational diffusion of non-spherical molecules, (*ii*) differential contributions from internal motions (particularly in loops or for side chains), (*iii*) cross-correlation effects, (*iv*) ^1H dipolar interactions with all nearby protons (which depends on detailed structures of the proteins), and (*v*) incomplete knowledge of fundamental parameters (such as chemical shift anisotropies). In light of these uncertainties, the results presented in the Figure should be regarded as approximate guidelines. For example, ^1H (in an unlabeled sample), $^{13}C^{\alpha}$ and ^{15}N linewidths in ubiquitin are ~6-9 Hz, ~7 Hz, and ~3 Hz. These values are consistent with values of 5 Hz, 6 Hz and 2 Hz from Figure 10. Observed linewidths significantly larger than expected based on the molecular mass of the protein imply that aggregation is increasing the apparent rotational correlation time or that chemical exchange effects (§5) contribute significantly to the inhomogeneous linewidth.

6.2 Relaxation during HMQC and HSQC experiments

Two-dimensional HMQC and HSQC experiments are integral components of all heteronuclear multidimensional NMR experiments. The effective F_1 linewidths of resonance signals in HMQC and HSQC spectra

depend upon the transverse relaxation rates of the coherences present during the chemical shift evolution period plus the contributions from inhomogeneous broadening (*35, 36*). Therefore, the linewidth in the F_1 dimension of a HMQC spectrum is determined by the relaxation rate of the heteronuclear MQ coherence, $2I_xS_y$, the F_1 linewidth of a HSQC spectrum is determined by the relaxation rate of the heteronuclear SQ coherence under conditions of free precession during t_1, and the F_1 linewidth of a decoupled HSQC spectrum is determined by the relaxation rate of in-phase SQ coherence in the absence of *IS* scalar coupling. The F_1 linewidth of a constant-time HSQC spectrum is determined only by inhomogenous broadening. Pulse sequences for these heteronuclear correlation experiments are illustrated in Figure 11. In the following, the appropriate relaxation rate constants for the heteronuclear SQ and MQ operators are calculated using methods outlined in §4.

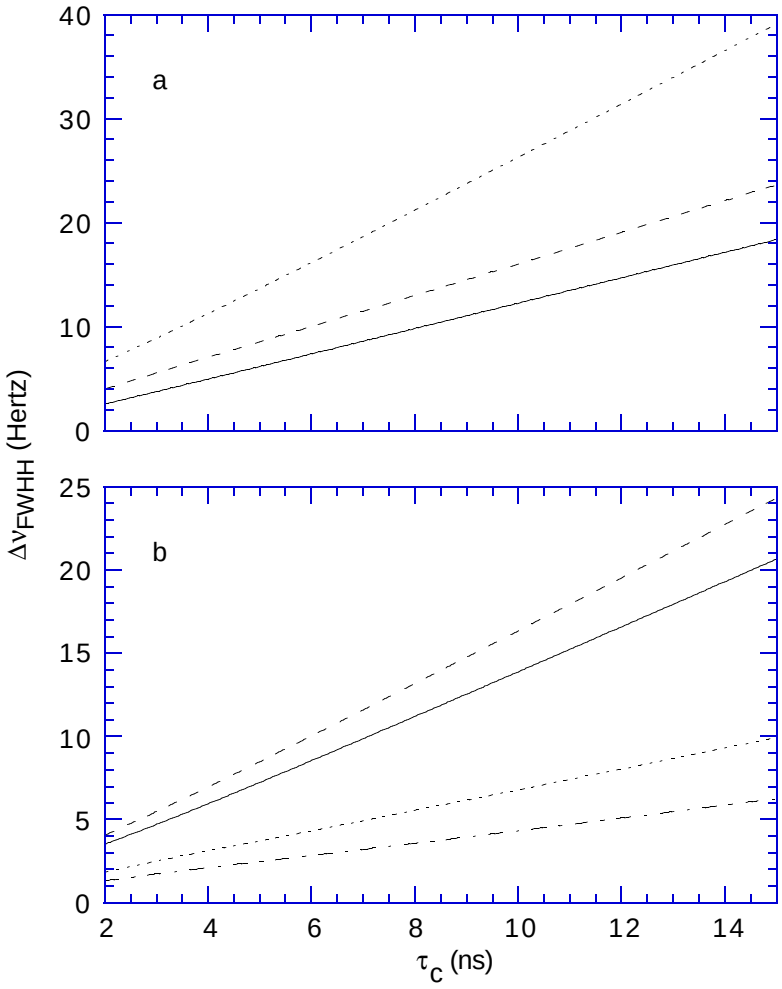

Figure 10. Resonance linewidths. Protein resonance linewidths are shown as a function of rotational correlation time. (a) Linewidths for (——) ^{1}H spins, (····) ^{1}H spins covalently bonded to ^{13}C, (– – –) ^{1}H spins covalently bonded to ^{15}N nuclei. (b) Heteronuclear linewidths for (——) proton-decoupled ^{13}C, (– – –) proton-coupled ^{13}C, (· – · – ·) proton-decoupled ^{15}N and (····) proton-coupled ^{15}N spins. Calculations included dipolar relaxation of all spins, and CSA relaxation of ^{15}N spins. For ^{1}H-^{1}H dipolar interactions, $\sum_j r_{ij}^{-6}$ = 0.027 Å^{-6} (*34*).

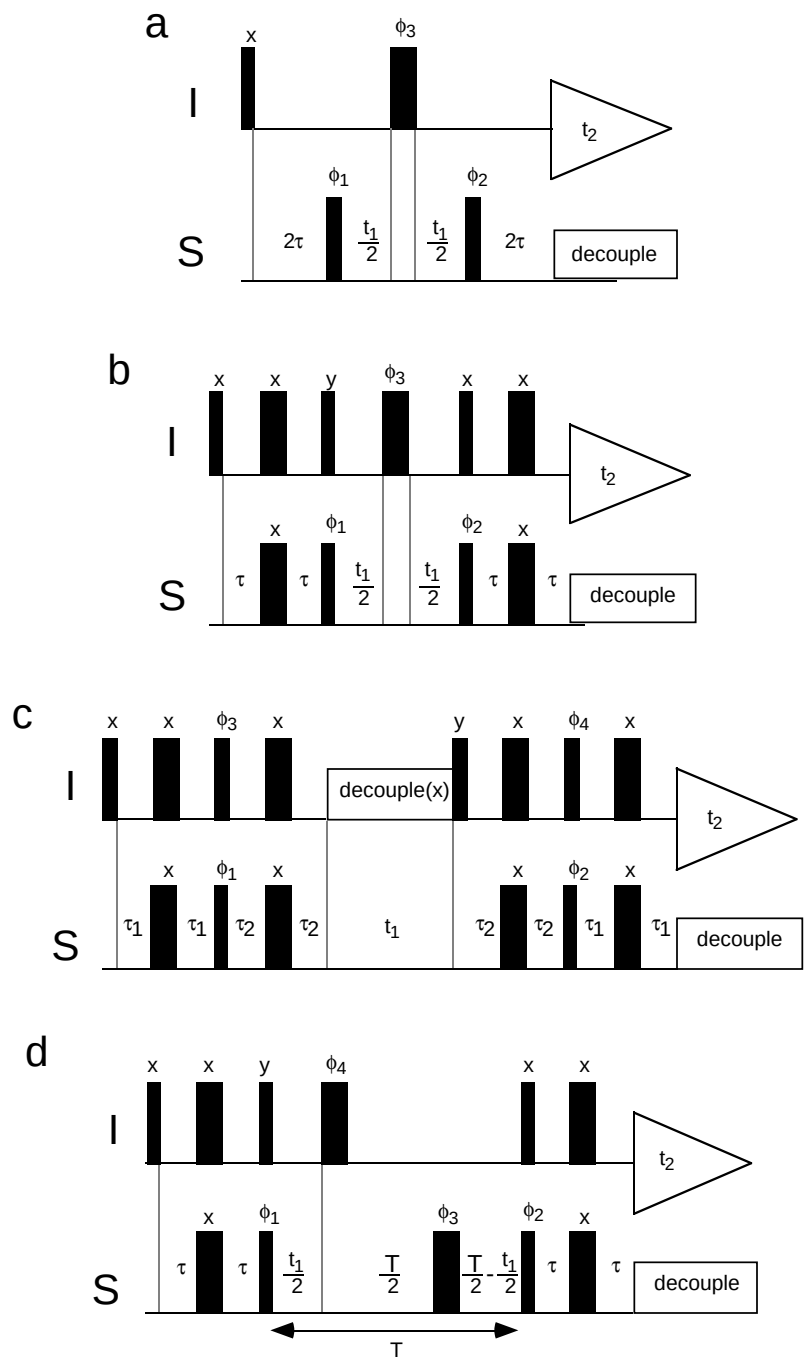

Figure 11. Pulse sequences for the ^{1}H-detected heteronuclear correlation experiments. In all pulse sequence figures, thin bars represent 90° pulses and thick bars represent 180° pulses. The phase of each pulse is indicated above the bar. (a) The HMQC experiment, in which the phase cycling is $\phi_1 = x, -x$; $\phi_2 = 8(x), 8(-x)$; $\phi_3 = 2(x), 2(y), 2(-x), 2(-y)$; and receiver = $2(x, -x, -x, x), 2(-x, x, x, -x)$. (b) The HSQC experiment, in which the phase cycling is $\phi_1 = x, -x$; $\phi_2 = 2(x), 2(-x)$; $\phi_3 = 4(y), 4(-y)$; and receiver = $2(x, -x, -x, x)$. This phase cycle can be further extended by the inclusion of independent cycling of the 90°(^{1}H) pulses on either side of the t_1 period as in the decoupled-HSQC experiment. (c) The decoupled-HSQC experiment, in which the phase cycling is $\phi_1 = 2(x), 2(-x)$; $\phi_2 = 8(x), 8(-x)$; $\phi_3 = y, -y$; $\phi_4 = 4(x), 4(-x)$; and receiver = $x, -x, -x, x, 2(-x, x, x, -x), x, -x, -x, x$. (d) The constant-time HSQC experiment, in which the phase cycling is $\phi_1 = x, -x$; $\phi_2 = 8(x), 8(-x)$; $\phi_3 = 2(x), 2(y), 2(-x), 2(-y)$; $\phi_4 = 16(y), 16(-y)$; and receiver = $2(x, -x, -x, x), 2(-x, x, x, -x)$. If desired, this 32 step phase cycle can be reduced to 8 steps by eliminating the cycling of ϕ_2 and using only the first 4 steps of the phase cycle of ϕ_3; an additional reduction by a factor of two can be obtained by eliminating cycling of ϕ_4. In each case the optimal value for 2τ is $1/(2J_{IS})$. Decoupling during t_2 can be achieved by using either GARP-1 or WALTZ-16 decoupling sequences. Decoupling during the t_1 evolution period of scheme c is achieved using WALTZ-16 or DIPSI-2 sequences.

The average transverse relaxation rates of the S spin SQ coherence (during coherent decoupling), S spin SQ coherence (during free-precession), heteronuclear MQ coherence (during free-precession), and I spin SQ coherence (during free-precession) are given by,

$$\begin{aligned} R_{2S} &= R_2^{IS}(S) + R_2^{CSA}(S) \\ &= \frac{d_{IS}}{24}\left\{4J(0) + J(\omega_I - \omega_S) + 3J(\omega_S) + 3J(\omega_I) + 6J(\omega_I + \omega_S)\right\} \\ &\quad + \frac{d_{CSA}}{6}\left\{4J(0) + 3J(\omega_S)\right\} \end{aligned} \quad [166]$$

$$\begin{aligned} \overline{R}_{2S} &= \tfrac{1}{2}\left[R_2^{IS}(2I_zS^+) + R_2^{IS}(S) + R_1^{IK}(I)\right] + R_2^{CSA}(S) \\ &= \frac{d_{IS}}{24}\left\{4J(0) + J(\omega_I - \omega_S) + 3J(\omega_S) + 3J(\omega_I) + 6J(\omega_I + \omega_S)\right\} \\ &\quad + \frac{d_{CSA}}{6}\left\{4J(0) + 3J(\omega_S)\right\} + \frac{1}{24}\sum_k d_{Ik}\left\{J(0) + 3J(\omega_I) + 6J(2\omega_I)\right\} \end{aligned} \quad [167]$$

$$\begin{aligned} R_{2MQ} &= \tfrac{1}{2}\left[R_2^{IS}(ZQ) + R_2^{IS}(DQ)\right] + R_2^{IK}(I) + R_2^{CSA}(S) \\ &= \frac{d_{IS}}{24}\left\{J(\omega_I - \omega_S) + 3J(\omega_I) + 3J(\omega_S) + 6J(\omega_I + \omega_S)\right\} \\ &\quad + \frac{d_{CSA}}{6}\left\{4J(0) + 3J(\omega_S)\right\} + \frac{1}{24}\sum_k d_{Ik}\left\{5J(0) + 9J(\omega_I) + 6J(2\omega_I)\right\} \end{aligned} \quad [168]$$

$$\begin{aligned} \overline{R}_{2I} &= \tfrac{1}{2}\left[R_2^{IS}(2I^+S_z) + R_2^{IS}(I)\right] + R_2^{IK}(I) \\ &= \frac{d_{IS}}{24}\left\{4J(0) + J(\omega_I - \omega_S) + 3J(\omega_S) + 3J(\omega_I) + 6J(\omega_I + \omega_S)\right\} \\ &\quad + \frac{1}{24}\sum_k d_{Ik}\left\{5J(0) + 9J(\omega_I) + 6J(2\omega_I)\right\} \end{aligned} \quad [169]$$

respectively, in which the individual relaxation rate constants are obtained from Tables 5 and 8, $J(\omega)$ is given by [92], and the summations, Σ, include

all the homonuclear k I spins. Equations [166] - [169] are subject to the following assumptions: (*i*) the S spin relaxes by dipole-dipole interactions with the directly attached I spin and through chemical shift anisotropy, (*ii*) the I spins relax through dipole-dipole interactions with the S spins and with k additional remote protons, (*iii*) evolution of the scalar coupling interaction during free-precession averages the relaxation rates of in-phase and anti-phase operators as described in §4.2 (indicated by overbars), (*iv*) coherent decoupling suppresses averaging by the scalar coupling interaction, and (*v*) ω_I ω_K. The terms containing d_{IS} arise from heteronuclear dipolar coupling between the scalar coupled I and S spins, terms containing d_{CSA} arise from chemical shift anisotropy of the S spin, and the terms containing d_{Ik} reflect the homonuclear dipolar coupling between I spins (§4.1 and §4.4). In ^{13}C or ^{13}C/^{15}N labeled samples, the S spin (either ^{13}C or ^{15}N) has additional dipolar interactions with nearby, predominantly directly bonded, ^{13}C spins, designated as R spins. These interactions are smaller than the dipolar IS interaction by a factor of,

$$\frac{d_{RS}}{d_{IS}} = \frac{\gamma_R^2 r_{IS}^6}{\gamma_I^2 r_{RS}^6} \qquad [170]$$

and are neglected in the following discussion.

In the limit of slow overall tumbling, which typically applies for proteins, $\omega_I\tau_c >> \omega_S\tau_c >> 1$, and $J(0) >> J(\omega_S) >> J(\omega_I)$ $J(\omega_I \pm \omega_S)$. The relaxation rates are approximated by

$$R_{2S} = \frac{\tau_c}{15}\left[d_{IS} + 4\, d_{CSA} \right] \qquad [171]$$

$$\overline{R}_{2S} = \frac{\tau_c}{15}\left[d_{IS} + 4\, d_{CSA} + \frac{1}{4}\sum_k d_{Ik} \right] \qquad [172]$$

$$R_{2MQ} = \frac{\tau_c}{3}\left[\frac{4}{5}d_{CSA} + \frac{1}{4}\sum_k d_{Ik}\right] \quad [173]$$

$$\overline{R}_{2I} = \frac{\tau_c}{3}\left[\frac{d_{IS}}{5} + \frac{1}{4}\sum_k d_{Ik}\right] \quad [174]$$

For backbone amide moieties in proteins, d_{CSA}/d_{IS} = 0.055 (assuming $\Delta\sigma$ = -160 ppm for ^{15}N and B_0 = 11.74 T), $d_{IS}/\sum d_{Ik} \approx 0.3$. Therefore, $\overline{R}_{2I} > R_{2MQ} \quad \overline{R}_{2S} \quad R_{2S}$, and linewidths are narrower in the F_1 dimension of a ^{1}H-^{15}N HSQC spectrum than of a HMQC spectrum. Decoupling of the I and S spins during t_1 eliminates broadening due to longitudinal relaxation of I_z, and consequently results in even narrower linewidths in decoupled ^{1}H-^{15}N HSQC spectra. For ^{1}H-^{13}C methine moieties, d_{CSA}/d_{IS} = 0.002 (assuming $\Delta\sigma$ = 25 ppm for ^{13}C and B_0 = 11.74 T) and $d_{IS}/\sum d_{Ik} \approx 1.4$. Therefore, $\overline{R}_{2I} > R_{2MQ} \quad \overline{R}_{2S} \quad R_{2S}$, and linewidth differences in ^{1}H-^{13}C HSQC and ^{1}H-^{13}C HMQC spectra are not as pronounced.

The different relaxation properties of the HMQC and HSQC experiments are emphasized in Figure 12, which shows the t_1 interferograms through a selected amide proton resonance of ^{1}H-^{15}N HSQC spectra of ubiquitin, and the corresponding Fourier transforms. The observed linewidths in Figures 12a-c are consistent with values of 4.9 Hz, 3.0 Hz, and 2.0 Hz calculated from [173], [172], and [171] by using τ_c = 4.1 ns. The dispersive contribution associated with the homonuclear scalar coupling is clearly visible in the HMQC spectrum (Figure 12a). As expected, the interferogram for the constant-time HSQC experiment (Figure 12d) exhibits very little decay, and the linewidth in the transformed spectrum is dominated by the apodization applied during processing.

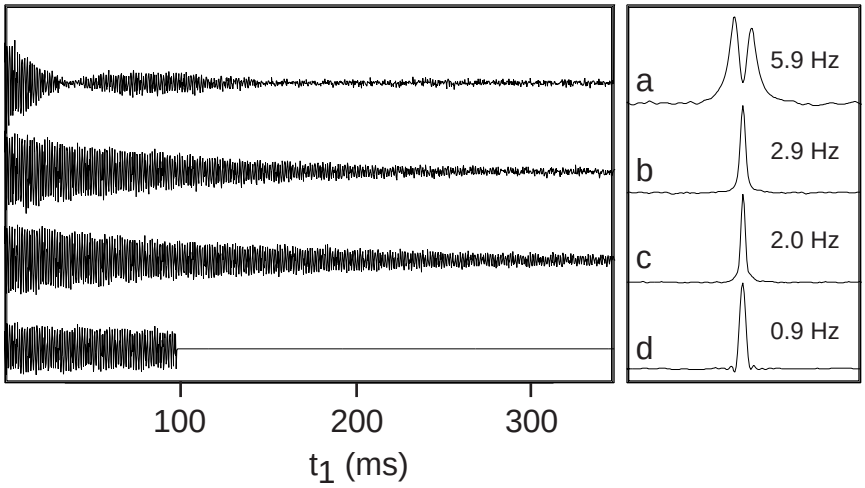

Figure 12. The t_1 interferograms, and their resulting Fourier transforms, taken through the amide proton resonance of Ile36 in the ^1H-^{15}N heteronuclear correlation spectra of ubiquitin. The F_1 linewidth at half-height is indicated beside each peak. Linewidths were measured by curve fitting the decay of the t_1 interferograms. For (d) the indicated linewidth represents inhomogenous broadening.

7 Nuclear Overhauser effect

By far the most important manifestation of the prediction [112] that dipolar coupled spins do not relax independently is the nuclear Overhauser effect (NOE). The Solomon equations [19] are extremely useful for explication of NOE experiments. The NOE is characterized by the cross relaxation rate constant, σ_{IS}^{NOE}, defined by [109], or the steady-state *NOE enhancement*, η_{IS}, which will be defined below. These two quantities naturally arise in transient or steady-state NOE experiments, respectively. The NOE is without doubt one of the most important effects in NMR spectroscopy; more detailed discussions can be found in monographs devoted to the subject (*37, 38*).

The principal use of the NOE in biological NMR spectroscopy is the determination of distances between pairs of protons (*39*). The NOE

enhancements of interest arise from slowly tumbling biological macromolecules in the spin diffusion limit. For such molecules, relatively large transient homonuclear proton NOE (or ROE) enhancements build up quickly and are detected most effectively by transient NOE and NOESY (or transient ROE and ROESY) methods.

7.1 Steady state and transient NOE experiments

The steady state NOE experiment will be illustrated by using a two spin system as an example. If the *S* spin is irradiated by a weak rf field (so as not to perturb the *I* spin) for a lengthy period of time $t >> 1/\rho_S,\ 1/\rho_I$, then the populations across the *S* spin transitions are equalized and the *I* spin magnetization evolves to a steady-state value, $\left\langle I_z^{ss} \right\rangle$. In this situation, the *S* spins are said to be saturated. Setting $d\Delta I_z(t)/dt = 0$ and $<S_z>(t) = 0$ in [19] and solving for $\left\langle I_z^{ss} \right\rangle / \left\langle I_z^0 \right\rangle$ yields:

$$\frac{d < I_z^{ss} >}{dt} = -\rho_I \left(< I_z^{ss} > - < I_z^0 > \right) + \sigma_{IS}^{NOE} < S_z^0 > = 0$$

$$< I_z^{ss} > / < I_z^0 > = 1 + \sigma_{IS}^{NOE} < S_z^0 > / \left(\rho_I < I_z^0 > \right) \qquad [175]$$

$$< I_z^{ss} > / < I_z^0 > = 1 + \frac{\sigma_{IS}^{NOE} \gamma_S}{\rho_I \gamma_I} = 1 + \eta_{IS}$$

in which

$$\eta_{IS} \equiv \frac{\sigma_{IS}^{NOE} \gamma_S}{\rho_I \gamma_I} \qquad [176]$$

As shown, the value of the longitudinal magnetization (or population difference) for the *I* spin is altered by saturating (equalizing the population difference) the *S* spin. If η_{IS} is positive, then the population differences across the *I* spin transitions are increased by reducing the

population differences across the *S* spin transitions. Since the equilibrium population differences are inversely proportional to temperature, this result appears to indicate that heating the *S* spins (reducing the population difference) has the effect of cooling the *I* spins (increasing the population difference). This conclusion would appear to violate the Second Law of Thermodynamics; however, if coupling between the spin system and the lattice is properly taken into account, then no inconsistency with thermodynamics exists.

The value of the NOE enhancement, η_{IS}, can be measured using the *steady-state NOE difference experiment*. In this experiment, two spectra are recorded. In the first spectrum, the *S* spin is saturated for a period of time sufficient to establish the NOE enhancement of the *I* spin, a 90° pulse is applied to the system, and the FID recorded. The intensity of the *I* spin resonance in the spectrum is proportional to $<I_z^{SS}>$. In the second experiment, the *S* spin is not saturated. Instead a 90° pulse is applied to the system at equilibrium and the FID is recorded. The intensity of the *I* spin resonance in this spectrum is proportional to $<I_z^0>$. The value of η_{IS} can then be calculated from [176]. In practice, the steady-state NOE difference experiment is performed somewhat differently than described in order to maximize the accuracy of the results; such complications are not relevant to the present discussion (*38*).

Measurements of σ_{IS}^{NOE} can be made by use of the one-dimensional *transient NOE experiment*, discussed in §1.2 or the two-dimensional *NOESY experiment* (§7.2). These laboratory frame relaxation transient NOE experiments have rotating frame analogs: the *transient ROE experiment*

and the two dimensional *ROESY experiment* (§7.3) in which the rotating frame cross relaxation rate constant, σ_{IS}^{ROE}, is given by [134].

Using the isotropic rotor spectral density function [92], the cross-relaxation rate constants for a homonuclear spin system ($\gamma_I = \gamma_S = \gamma$) are given by

$$\sigma_{IS}^{NOE} = \frac{\hbar^2 \mu_0^2 \gamma^4 \tau_c}{10\pi^2 r_{IS}^6}\left\{-1 + \frac{6}{1+4\omega_0^2\tau_c^2}\right\}$$
$$\sigma_{IS}^{ROE} = \frac{\hbar^2 \mu_0^2 \gamma^4 \tau_c}{10\pi^2 r_{IS}^6}\left\{2 + \frac{3}{1+\omega_0{}^2\tau_c^2}\right\} \qquad [177]$$

and the NOE enhancement is given by

$$\eta_{IS} = \left\{-1 + \frac{6}{1+4\omega_0^2\tau_c^2}\right\} \Big/ \left\{1 + \frac{3}{1+\omega_0{}^2\tau_c^2} + \frac{6}{1+4\omega_0^2\tau_c^2}\right\} \qquad [178]$$

The cross relaxation rate constants are proportional to the inverse sixth power of the distance between the two dipolar interacting spins but η_{IS} does not depend upon the distance r_{IS} between the two spins. Thus, a measurement of η_{IS} can indicate that two spins are close enough in space to experience dipolar cross-relaxation, but a quantitative estimate of the distance separating the spins cannot be obtained. To estimate the distance between two nuclei, σ_{IS}^{NOE} or σ_{IS}^{ROE} must be measured directly (or η_{IS} measured in one experiment and ρ_I in a second experiment).

In the extreme narrowing limit ($\omega_0\tau_c$ <<1), [177] and [178] reduce to

$$\sigma_{IS}^{NOE} = \sigma_{IS}^{ROE} = \frac{\hbar^2 \mu_0^2 \gamma^4 \tau_c}{2\pi^2 r_{IS}^6}$$
$$\eta_{IS} = \frac{1}{2} \qquad [179]$$

and in the spin-diffusion limit ($\omega_0\tau_c$ >>1),

$$\sigma_{IS}^{NOE} = -\frac{\hbar^2\mu_0^2\gamma^4\tau_c}{10\pi^2 r_{IS}^6}$$
$$\sigma_{IS}^{ROE} = \frac{\hbar^2\mu_0^2\gamma^4\tau_c}{5\pi^2 r_{IS}^6} \qquad [180]$$
$$\eta_{IS} = -1$$

In the slow tumbling regime , the laboratory and rotating frame cross relaxation rate constants are related by

$$\sigma_{ROE} = -2\sigma_{NOE} \qquad [181]$$

This relationship has been used to compensate approximately for cross-relaxation effects in NMR spectra (*40, 41*). The values of σ_{IS}^{NOE} and η_{IS} are zero if $\omega\tau_c$ = 1.12, whereas, σ_{IS}^{ROE} > 0 for all τ_c.

7.2 NOESY

The pulse sequence for the NOESY (Nuclear Overhauser Effect Spectroscopy) experiment is shown in Figure 13. Initially, a 90°-t_1-90° period frequency labels the spins and returns the magnetization to the z-axis. Magnetization transfer occurs via dipolar coupling for a period τ_m before observable transverse magnetization is created by the final 90° pulse. The final pulse can be replaced by a Hahn-echo sequence with a concomitant improvement in the flatness of the baseline. A coherence level diagram for this pulse sequence is presented in Figure 13.

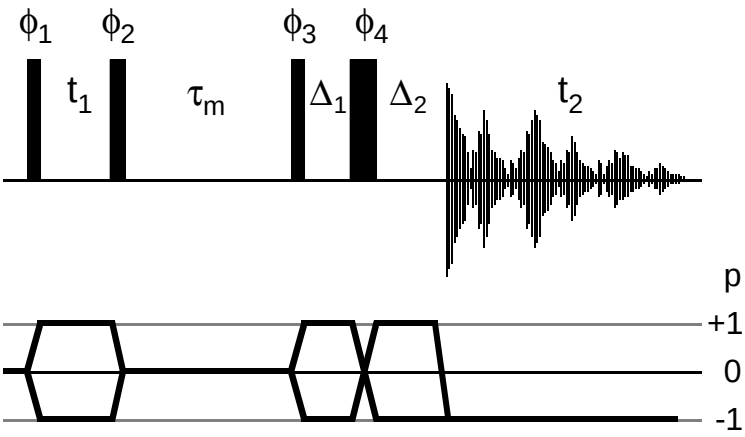

Figure 13. Pulse sequence and coherence level diagram for the NOESY experiment. A Hahn-echo sequence is included prior to detection. The basic phase cycle is four steps (ϕ_1 = *x*, -*x*, -*x*, *x*; ϕ_2 = *x*, *x*, -*x*, -*x*; and receiver = *x*, -*x*, *x*, -*x*). Alternatively, both pulses can be phase cycled in synchrony to select Δp =0. EXORCYCLE phase cycling is used for the Hahn echo and CYCLOPS is applied to all pulses. Bodenhausen and coworkers have discussed phase cycles for NOESY experiments (*42*).

For a two spin system, initial I_{1z} magnetization evolves through the the 90°_x-t_1-90°_x pulse sequence element as:

$$I_{1z} \xrightarrow{\left(\frac{\pi}{2}\right)_x - t_1 - \left(\frac{\pi}{2}\right)_x} -I_{1z}\cos(\Omega_1 t_1)\cos(\pi J_{12} t_1) - 2I_{1x}I_{2y}\cos(\Omega_1 t_1)\sin(\pi J_{12} t_1) + I_{1x}\sin(\Omega_1 t_1)\cos(\pi J_{12} t_1) - 2I_{1z}I_{2y}\sin(\Omega_1 t_1)\sin(\pi J_{12} t_1) \quad [182]$$

in which $\left(\frac{\pi}{2}\right)_x$ represent non-selective rf pulses with *x*-phase applied to the *I* spins, the chemical shift of the spin I_1 is Ω_1, and the scalar coupling constant between the I_1 and I_2 spins is J_{12} (assumed to represent a three-bond scalar interaction). . Parallel evolution beginning with I_{2z} magnetization is exhibited by exchanging I_1 and I_2 labels.

Evolution of the I_{1z} term in [182] during τ_m is governed by the Solomon equations in which the initial condition is $-I_{1z}\cos(\Omega_1 t_1)\cos(\pi J_{12} t_1)$ and the equilibrium magnetization, I^0_{1z}, is rejected by phase cycling for axial peak suppression. If *K*-1 spins (I_k for *k* = 2, ... *K*) are close in space to spin I_1 (this notation allows for the possibility that the scalar coupled spin,

I_2, is dipolar coupled to I_1 as well), then the resulting evolution during τ_m is:

$$-I_{1z}\cos(\Omega_I t_1)\cos(\pi J t_1) \xrightarrow{\tau_m} -\sum_{k=1}^{K} I_{kz} a_{1k}(\tau_m)\cos(\Omega_1 t_1)\cos(\pi J_{12} t_1) \qquad [183]$$

in which $a_{1k}(\tau_\mathrm{m}) = [\exp(-\mathbf{R}\,\tau_m)]_{1k}$ is the (1, k)th element of the matrix exponential and **R** is the matrix of rate constants ρ_i and σ_{ij} (§1.2). After the final 90° pulse and Hahn echo, the density operator terms that result from the longitudinal magnetization are given by

$$\sum_{k=1}^{K} I_{ky} a_{1k}(\tau_m)\cos(\Omega_1 t_1)\cos(\pi J_{12} t_1) \qquad [184]$$

The final spectrum contains I_1 diagonal peaks (the k = 1 term in [184]) and $I_1 \rightarrow I_k$ NOE cross-peaks for k > 1. All of the peaks are in-phase with respect to homonuclear scalar coupling in F_1 and F_2, and also can be phased to absorption in both dimensions.

The longitudinal magnetization that will give rise to the NOE cross-peaks has coherence level p = 0) during τ_m, and the phase cycle rejects other coherence levels during this period, including the single quantum terms I_{1x} and $2I_{1x}I_{2z}$ in [182]. The second term of [182] is a mixture of ZQ_y^{12} (p = 0) and DQ_y^{12} (p = 2) coherences. The double-quantum operator is suppressed by the phase cycling; however, the zero-quantum term survives. During τ_m the zero quantum term will precess according to the difference in chemical shift of I_1 and I_2. The following terms will be generated by the final 90° pulse and Hahn echo:

$$-ZQ_y^{12}\cos(\Omega_1 t_1)\sin(\pi J_{12} t_1) \xrightarrow{\tau_m-(\pi/2)_x-\Delta_1-\pi_y-\Delta_2}$$

$$+\frac{1}{2}\left[2I_{1x}I_{2x}-2I_{1z}I_{2z}\right]\cos(\Omega_1 t_1)\sin(\pi J_{12} t_1)\sin\left[(\Omega_1-\Omega_2)\tau_m\right] \quad [185]$$

$$-\frac{1}{2}\left[2I_{1z}I_{2x}-2I_{1x}I_{2z}\right]\cos(\Omega_1 t_1)\sin(\pi J_{12} t_1)\cos\left[(\Omega_1-\Omega_2)\tau_m\right]$$

The last line of [185] contains observable terms and therefore must be considered in an analysis of the NOESY spectrum. Such artifacts arise via a zero-quantum pathway and are referred to as *zero-quantum* peaks. These peaks are in anti-phase in both dimensions, and are also in dispersion when the normal NOE peaks [184] are phased to absorption.

The NOE and zero-quantum peaks between two coupled spins appear at identical chemical shifts in F_1 and F_2. Although the net integrated intensity of the dispersive zero-quantum component is zero, accurately integrating the contributions from the dispersive tails of this component may not be possible, and errors in the measurement of the NOE cross-peak volume result; in addition, the anti-phase dispersive tails can interfere with the integration of other cross-peaks in crowded regions of the spectrum. The magnitude of the zero quantum component varies as $\cos[(\Omega_1\text{-}\Omega_2)\tau_m]$ which depends on the chemical shifts of the spins involved and the mixing time. In addition, because the zero-quantum terms have transverse components during τ_m, relaxation is faster than for longitudinal magnetization, and the zero-quantum component is reduced in intensity relative to the true NOE peak when a long mixing time is employed.

The theoretical time dependence of the NOE cross-peaks in the NOESY experiment (§1.2) suggests that the mixing time should be on the order of $1/R_1$ to maximize the intensities of NOE cross peaks. A long mixing time

also has the advantage that zero-quantum artifacts will be of low intensity. However, long mixing times will also allow multiple magnetization transfers, or *spin diffusion*, to contribute substantially to the cross-peak intensity. The origins and consequences of spin diffusion are illustrated for a three-spin system with the following relaxation rate matrix:

$$\mathbf{R} = \begin{bmatrix} \rho_1 & \sigma_{12} & 0 \\ \sigma_{12} & \rho_2 & \sigma_{23} \\ 0 & \sigma_{23} & \rho_3 \end{bmatrix} \qquad [186]$$

By construction, spins I_1 and I_3 are too far apart to have an appreciable dipolar coupling (σ_{13} = 0); thus direct magnetization transfer between I_1 and I_3 is not possible. The time dependence of the I_1 magnetization is given to third-order in time by,

$$\begin{aligned}
\langle I_{1z}\rangle(\tau_m) &= \sum_{k=1}^{3}\left[\exp(-\mathbf{R}\tau_m)\right]_{1k}\langle I_{kz}\rangle(0) \\
&\approx \sum_{k=1}^{3}\left[E_{1k} - R_{1k}\tau_m + \tfrac{1}{2}R_{1k}^2\tau_m^2 - \tfrac{1}{6}R_{1k}^3\tau_m^3\right]\langle I_{kz}\rangle(0) \\
&= \langle I_{1z}\rangle(0)\left\{1-\rho_1\tau_m + \tfrac{1}{2}\left(\rho_1^2+\sigma_{12}^2\right)\tau_m^2 - \tfrac{1}{6}\left(\rho_1^3+2\rho_1\sigma_{12}^2+\rho_2\sigma_{12}^2\right)\tau_m^3\right\} \\
&\quad + \langle I_{2z}\rangle(0)\left\{-\sigma_{12}\tau_m + \tfrac{1}{2}(\rho_1+\rho_2)\sigma_{12}\tau_m^2\right. \\
&\qquad\qquad \left. - \tfrac{1}{6}\left[\left(\rho_1^2+\sigma_{12}^2\right)\sigma_{12} + (\rho_1+\rho_2)\rho_2\sigma_{12} + \sigma_{12}\sigma_{23}^2\right]\tau_m^3\right\} \\
&\quad + \langle I_{3z}\rangle(0)\left\{\tfrac{1}{2}\sigma_{12}\sigma_{23}\tau_m^2 - \tfrac{1}{6}(\rho_1+\rho_2+\rho_3)\sigma_{12}\sigma_{23}\tau_m^3\right\}
\end{aligned} \qquad [187]$$

Each of the terms in [187] can be assigned a physical interpretation; however only three terms will be discussed in detail. The first order term $-\sigma_{12}\tau_m\langle I_{2z}\rangle(0)$ represents direct transfer of magnetization from spin I_2 to spin I_1 and gives rise to a cross peak in the NOESY spectrum. In the initial rate regime, only this term contributes to the cross peak intensity and the

cross peak intensity is proportional to the cross-relaxation rate constant, σ_{12}. The second order term $(1/2)\sigma_{12}\sigma_{23}\tau_m^2\langle I_{3z}\rangle(0)$ exemplifies spin diffusion. This term gives rise to a cross peak between spins I_1 and I_3 by an indirect two step transfer from $I_3 \rightarrow I_2 \rightarrow I_1$. In the quadratic time regime, the intensity of the spin-diffusion cross peak depends on the product of the individual cross-relaxation rate constants. Finally, the third order term $\rho_2\sigma_{12}^2\tau_m^3\langle I_{1z}\rangle(0)$ represents a back transfer pathway $I_1 \rightarrow I_2 \rightarrow I_1$. The back transfer has the effect of reducing the intensity of the cross peak that would otherwise result from cross-relaxation between I_1 and I_2. Spin diffusion is illustrated graphically for a three spin system in Figure 14. Even for a two spin system, outside of the initial rate regime, NOE cross-peak intensities are not proportional to the cross-relaxation rate constants. The assumed linearity between the NOE cross peak intensities and cross-relaxation rate constants sometimes is called “the isolated two-spin approximation”; as the present discussion shows, this phrase is a misnomer.

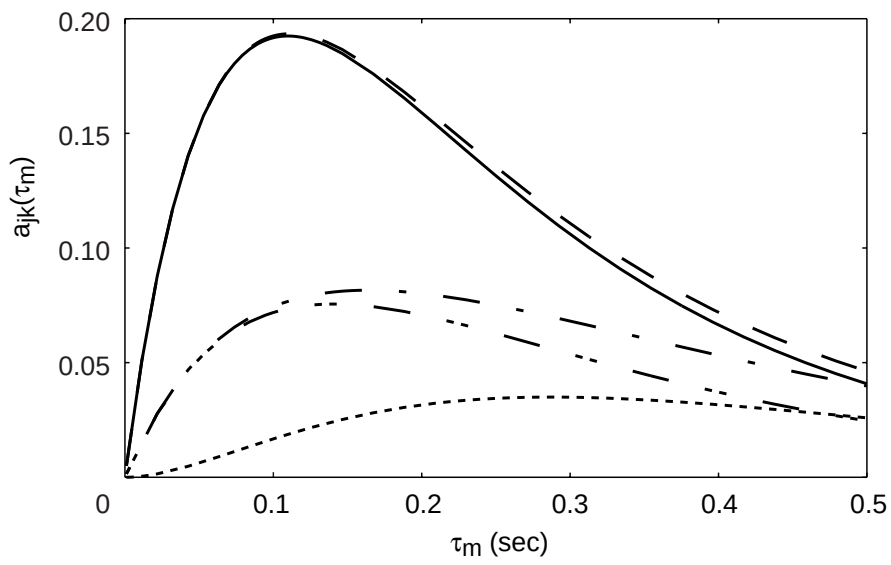

Figure 14. Amplitudes of the NOESY cross peaks are shown as a function of mixing time for a three spin system. (– –) $I_1 \rightarrow I_2$, (– - –) $I_2 \rightarrow I_3$, (- - -) $I_1 \rightarrow I_3$. Calculations were performed using ρ_1 = 10 s^{-1}, ρ_2 = 10 s^{-1}, ρ_5 = 5 s^{-1}, σ_{12} = -5 s^{-1}, σ_{13} = 0 s^{-1}, σ_{23} = -1.5 s^{-1}. For comparison, (—) $I_1 \rightarrow I_2$ with σ_{23} = 0 s^{-1}, and (– - – –) $I_2 \rightarrow I_3$ with σ_{12} = 0 s^{-1} are also shown.

As a consequence of spin diffusion, cross-peaks between pairs of protons that are far apart will gain intensity from magnetization that has been transferred via intervening spins whilst cross-peak between pairs of protons that are close together will be decreased by the loss of magnetization to other nearby protons. Failure to adequately account for spin-diffusion results in the derivation of inaccurate distance constraints between pairs of protons; overly tight constraints derived from NOE cross peaks dominated by spin diffusion leads to overly constrained and incorrect protein structures. Spin-diffusion effects may be minimized by using a short mixing time, but in these experiments all cross-peak intensities will be low, and zero-quantum artifacts will be emphasized. A compromise with mixing times of 50-150 ms provides reasonable cross-peak intensities that are not overly influenced by spin-diffusion or zero-quantum contributions. Dipolar relaxation is more efficient in systems with

long rotational correlation times, hence a shorter mixing time is required to limit spin-diffusion in large proteins.

NOESY spectra provide a powerful means of elucidating conformational details of molecules in solution. The requirement that two protons be separated by less than 5 Å (or so) in order to give rise to an NOE immediately allows a loose restraint to be placed on their separation. Furthermore, the size of the NOE depends inversely on the distance, hence the restraint can be shorter than 5 Å if the NOE is intense. In order to calculate the structure of a protein, many such restraints must be identified in an unambiguous fashion. In most applications, NOE cross-peaks simply are placed into one of several size categories associated with an upper bound for the proton separation. More accurate calibration is difficult because of the complex relationship between NOE build-up, local correlation time and the distribution of neighboring protons. Analysis of NOESY spectra with different mixing times (called a build-up or τ_m-series) allows the initial slope of the NOE build up to be estimated and facilitates calibration. A variety of methods have been proposed to improve the quality of cross-peak volume extraction from NOESY spectra (*43-46*).

Besides cross-relaxation, chemical exchange can also lead to cross-peaks in NOESY spectra. In cases of slow exchange (on the chemical shift time scale) between two species (§5.1), a cross-peak is observed at the frequencies of a particular nucleus in the two different sites if the exchange rate between the species is not slow compared to τ_m. For proteins, the chemical exchange peaks have the same sign as NOE cross-peaks (the same sign as the diagonal peaks, formally negative), hence discrimination of the two can be difficult. Very complicated spectra can

result due to peaks arising from combinations of exchange and cross-relaxation; in effect, these are spin-diffusion peaks involving two transfer steps.

7.3 ROESY

Rotating frame Overhauser effect spectroscopy (ROESY) was first developed by Bothner-By and co-workers and was initially known by the acronym CAMELSPIN (cross-relaxation appropriate for mini-molecules emulated by locked spins) (*27*). As both names suggest, the experiment monitors cross-relaxation between spins that are spin-locked by the application of rf pulses (*27*, *47*). ROESY has the advantage that the rotating frame Overhauser effect (ROE) cross-relaxation rate constant is positive for *all* rotational correlation times: the maximum size of the ROE varies from 0.38 for $\omega_0\tau_c$ <<1 to 0.68 for $\omega_0\tau_c$ >> 1. Therefore ROESY cross-peaks are observable even if $\omega_0\tau_c$ 1; in contrast, cross-peaks vanish in laboratory frame NOESY experiments if $\omega_0\tau_c$ 1. ROESY is very useful in studies of peptides in which laboratory frame NOEs are weak, but the experiment also has merits appropriate for the study of proteins. ROESY and NOESY experiments are very similar; consequently, comparisons to NOESY will be made throughout this discussion. A more detailed discussion of relaxation in the rotating frame is given in §4.3.

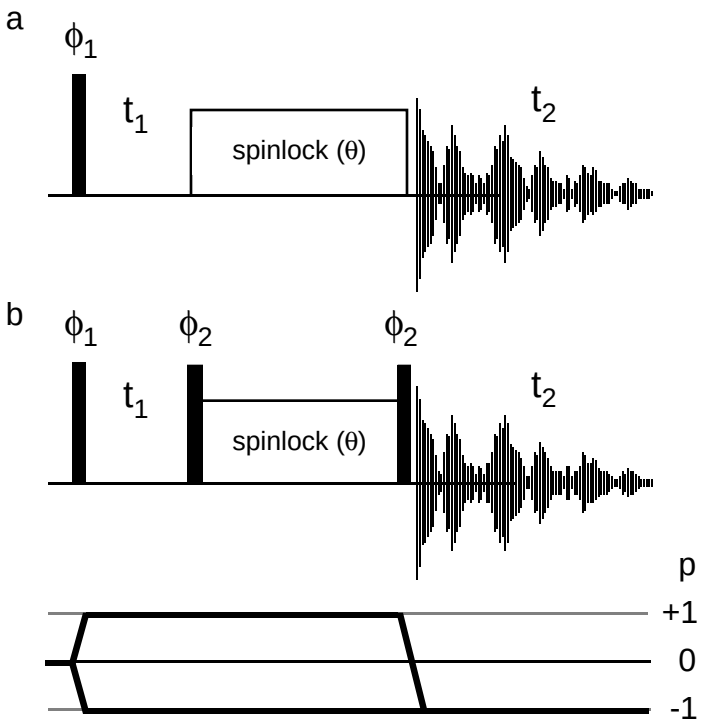

Figure 15. Pulse sequences and coherence level diagram for the ROESY experiments. In (a) the basic phase cycle is: $\phi_1 = x$, $-x$; and receiver = x, $-x$. The spin-lock phase $\theta = y$. In (b) the basic phase cycle is: $\phi_1 = x$, $-x$; $\phi_2 = x$; and receiver = x, $-x$. The spin-lock phase $\theta = x$. The full phase cycle is completed by performing CYCLOPS on all pulses and the receiver.

The original version of the ROESY experiment simply consisted of a 90° - t_1 - τ_m - t_2, sequence in which the spin-locking field during τ_m was provided by continuous low power irradiation (2-4 kHz), as illustrated in Figure 15a. For a scalar coupled two spin system, the evolution up to the mixing period is given by:

$$I_{1z} \xrightarrow{(\pi/2)_x - t_1} -I_{1y}\cos(\Omega_1 t_1)\cos(\pi J_{12} t_1) + 2I_{1x}I_{2z}\cos(\Omega_1 t_1)\sin(\pi J_{12} t_1) + I_{1x}\sin(\Omega_1 t_1)\cos(\pi J_{12} t_1) + 2I_{1y}I_{2z}\sin(\Omega_1 t_1)\sin(\pi J_{12} t_1) \quad [188]$$

During the subsequent spin locking period, any operators orthogonal to the rf field in a tilted rotating frame are dephased by rf inhomogeneity. The x-axes of the rotating and tilted reference frames are coincident; thus, all terms containing x-operators are dephased. The transformation of z- and y-operators into the tilted frame is performed using [82]:

$$
\begin{aligned}
I_{1y} &\Rightarrow I'_{1z}\sin\theta_1 + I'_{1y}\cos\theta_1 \\
2\,I_{1y}I_{2z} &\Rightarrow 2\Big(I'_{1z}\sin\theta_1 + I'_{1y}\cos\theta_1\Big)\Big(I'_{2z}\cos\theta_2 - I'_{2y}\sin\theta_2\Big) \\
&= 2\,I'_{1z}I'_{2z}\sin\theta_1\cos\theta_2 - 2\,I'_{1z}I'_{2y}\sin\theta_1\sin\theta_2 \\
&\quad +2\,I'_{1y}I'_{2z}\cos\theta_1\cos\theta_2 - 2\,I'_{1y}I'_{2y}\cos\theta_1\sin\theta_2
\end{aligned}
\qquad [189]
$$

in which θ_1 and θ_2 are the tilt angles for spins I_1 and I_2. The only terms that commute with the spin lock Hamiltonian are proportional to I'_{1z} and $2I'_{1z}I'_{2z}$. If K-1 spins (I_k for k = 2, ... K) are close in space to spin I_1, the resulting evolution of the longitudinal magnetization is:

$$
\begin{aligned}
&-I'_{1z}\sin\theta_1\cos(\Omega_1 t_1)\cos(\pi J_{12}t_1) \xrightarrow{\tau_m} \\
&\qquad -\sum_{k=1}^{K} I'_{kz}a_{1k}(\tau_m)\sin\theta_1\cos(\Omega_1 t_1)\cos(\pi J_{12}t_1)
\end{aligned}
\qquad [190]
$$

in which $a_{1k}(\tau_m) = [\exp(-\mathbf{R}\,\tau_m)]_{1k}$ is the (1, k)th element of the matrix exponential and **R** is the matrix of rotating frame relaxation rate constants $R_{kk}(\theta_i)$ and $\sigma_{jk}(\theta_i, \theta_j)$ (§4.3). Transforming back from the tilted frame to the rotating frame yields the observable operators:

$$
\sum_{k=1}^{K} I_{ky}a_{1k}(\tau_m)\sin\theta_1\sin\theta_k\cos(\Omega_1 t_1)\cos(\pi J_{12}t_1) \qquad [191]
$$

The I_{1y} term represents a diagonal peak and the remaining K-1 terms represent cross-peaks. Diagonal peaks and cross-peaks have in-phase absorptive lineshapes in F_1 and F_2. In the usual methods of acquisition, the cross-peaks are of opposite phase to the diagonal because ρ_j and σ_{jk} are both positive (*27*).

The two spin term $2I'_{1z}I'_{2z}$ does not cross-relax with other I_1 or I_2 spin operators during τ_m; however the amplitude of the operator is

reduced by relaxation (with relaxation rate constant designated R_{zz}). Transformation back into the rotating frame yields the observable operators:

$$\begin{aligned}&\left(2\,I_{1y}I_{2z}\sin\theta_1\cos\theta_2+2\,I_{1z}I_{2y}\cos\theta_1\sin\theta_2\right)\\&\qquad\times\sin\theta_1\cos\theta_2\sin\left(\Omega_1 t_1\right)\sin\left(\pi J_{12}t_1\right)\exp\left(-R_{zz}\tau_m\right)\end{aligned}\qquad[192]$$

The limitations of the simple ROESY experiment are now evident: (*i*) amplitude of cross peaks are reduced by a factor of $\sin\theta_1\sin\theta_k$, and (*ii*) two-spin order generates cross-peaks with anti-phase lineshapes in both dimensions that distort the in-phase multiplet patterns expected for ROESY cross-peaks.

Griesinger and Ernst developed a simple and clever modification to the ROESY pulse sequence that overcomes these limitations. In this sequence (Figure 15b) evolution through the 90°_x-t_1-90°_x block proceeds as described in [182]. The *y*-operators are dephased by the *x*-phase spin lock rf field. Transformation of the *z*- and *x*-operators into the tilted frame yields:

$$\begin{aligned}&-I_{1z}\cos\left(\Omega_1 t_1\right)\cos\left(\pi J_{12}t_1\right)+I_{1x}\sin\left(\Omega_1 t_1\right)\cos\left(\pi J_{12}t_1\right)\Rightarrow\\&\qquad-\left(-I'_{1x}\sin\theta_1+I'_{1z}\cos\theta_1\right)\cos\left(\Omega_1 t_1\right)\cos\left(\pi J_{12}t_1\right)\\&\qquad\quad+\left(I'_{1x}\cos\theta_1+I'_{1z}\sin\theta_1\right)\sin\left(\Omega_1 t_1\right)\cos\left(\pi J_{12}t_1\right)\end{aligned}\qquad[193]$$

The only term that commutes with the spin lock Hamiltonian is

$$\begin{aligned}&-I'_{1z}\left(\cos\theta_1\cos\left(\Omega_1 t_1\right)-\sin\theta_1\sin\left(\Omega_1 t_1\right)\right)\cos\left(\pi J_{12}t_1\right)=\\&\qquad-I'_{1z}\cos\left(\Omega_1 t_1+\theta_1\right)\cos\left(\pi J_{12}t_1\right)\end{aligned}\qquad[194]$$

Cross-relaxation during τ_m yields

$$-I'_{1z}\cos(\Omega_1 t_1+\theta_1)\cos(\pi J_{12}t_1)\xrightarrow{\tau_m} -\sum_{k=1}^{K} I'_{kz}a_{1k}(\tau_m)\cos(\Omega_1 t_1+\theta_1)\cos(\pi J_{12}t_1) \quad [195]$$

Transforming back from the tilted frame to the rotating frame and applying the last 90° pulse yields the observable operators:

$$\sum_{k=1}^{K}\left(I_{ky}\cos\theta_k - I_{kx}\sin\theta_k\right)a_{1k}(\tau_m)\cos(\Omega_1 t_1+\theta_1)\cos(\pi J_{12}t_1) \quad [196]$$

The offset dependence of the ROESY cross-peaks appears in [196] as a phase error of θ_1 in t_1 and θ_k in t_2. Because θ_k is approximately linear for $0 \le \Omega_k \le \gamma B_1$, the resonance offset effects are compensated by phase correction during processing. No two spin operators that commute with the spin lock Hamiltonian are created; therefore, the cross-peak multiplet structure is undistorted (minor contributions from evolution of zero-quantum coherences in the tilted frame have been ignored).

Although the Griesinger and Ernst approach eliminates the offset dependence that arises from the projection of the spin operators between tilted and untilted frames, the magnitudes of cross-relaxation rate constants in a ROESY experiment also depend upon resonance offset as shown by [133]. As a result, relaxation for off-resonance spins will contain a laboratory frame component (i.e. an NOE) as well as a rotating frame component. Interestingly (and somewhat counter intuitively) for large biomolecules, the apparent offset-dependent cross-relaxation rate between two spins is actually most efficient for cross-peaks along the anti-diagonal and least efficient for cross-peaks close to the diagonal away from the

center of the spectrum (*48*). Any quantitative analysis of ROESY cross-peak intensities must consider the offset dependence of the rate constants.

A practical problem encountered in the ROESY experiment is that the spin-lock pulse is capable of inducing isotropic mixing (*49*). The TOCSY (or *J* cross-peaks) are of the same sign as the diagonal; consequently, TOCSY transfer within a scalar coupled system tends to cancel the cross-relaxation components and render quantitation of the ROE (and hence the inter-proton separation) difficult. More insidiously, cross-peaks that arise through consecutive TOCSY and ROE magnetization transfers have the same sign as the actual ROE peaks (*50*) and can be misinterpreted. Fortunately, a long, weak pulse is not efficient at achieving a Hartman-Hahn match between two protons unless they are close in chemical shift or symmetrically disposed about the carrier position. Unambiguous ROE cross peaks can be identified by recording two ROESY spectra with very different rf carrier offsets (*50*). Development of pulse sequences that eliminate TOCSY transfer and generate pure ROE cross peaks is an area of active research (*51*).

The ROESY experiment has several redeeming qualities for studies of proteins. Foremost, as discussed above, the ROE is always positive and cross-peaks can be observed in ROESY spectra even if the peaks cannot be observed in NOESY spectra because $\omega_0 \tau_c \quad 1$.

A further advantage of ROESY over NOESY is that spin-diffusion (or three-spin effects) produces contributions to cross-peaks that are of opposite sign to the direct ROE peaks. Conceptually, the rotating frame cross-relaxation rate constant is positive, and magnetization transfer

between two spins occurs with inversion of sign. Thus, a diagonal peak and a cross-peak arising by a direct ROE between two spins have opposite signs. Transfer of the cross-peak magnetization to a third spin involves another change of sign. As a result, cross-peaks dominated by spin-diffusion will be of the same sign as the diagonal. If a small three-spin interaction contributes to a ROESY cross-peak, the measured intensity is reduced and may be interpreted as a longer inter-proton separation. Consequently the upper bound restraint applied in structure calculations will not be overly restrictive. The influence of spin-diffusion in NOESY spectra is particularly pronounced for NOEs involving geminal methylene groups. Efficient spin-diffusion between the $^{1}H^{\beta"}$ and $^{1}H^{\beta'}$ tends to equalize the intensity of NOEs to other protons even if the distances to $^{1}H^{\beta"}$ and $^{1}H^{\beta'}$ are not equal. Stereospecific assignment β-methylene protons plays an important role in defining side-chain conformation, and depends heavily on estimating the relative sizes of intra-residue and sequential distances to $^{1}H^{\beta"}$ and $^{1}H^{\beta'}$ (*52, 53*). The use of ROESY spectra for this process significantly reduces the chance of incorrectly making such assignments.

Another important facet of the ROESY experiment is that chemical exchange peaks are of the same sign as the diagonal, i.e. opposite in sign to peaks arising from direct cross-relaxation. Thus, rotating frame experiments are invaluable in the study of dynamic processes involving slow exchange between two or more states. Protein-protein or peptide-protein interactions are one area where discrimination of cross-relaxation and chemical exchange is not possible from NOESY, but is apparent from ROESY data. As with chemical exchange in TOCSY spectra (*54*), complex

situations can arise where peaks result from both cross-relaxation and exchange.

8 Investigations of protein dynamics by NMR spin relaxation

Dipolar nuclear magnetic spin relaxation of protonated heteronuclei, such as ^{13}C and ^{15}N, is mediated by overall rotational tumbling of the molecule and by internal motions of the X-H bond vector (*55, 56*); consequently, measurement of ^{13}C and ^{15}N spin relaxation parameters, primarily the spin-lattice and spin-spin relaxation rate constants and the steady state $\{^1H\}$-^{15}N nuclear Overhauser effect (NOE), is powerful technique for experimental investigation of dynamics in biological macromolecules (*21, 22*).

Methods for the determination of relaxation parameters for ^{15}N and ^{13}C spins in IS spin systems by proton-detected heteronuclear correlation inversion-recovery, Carr-Purcell-Meiboom-Gill (CPMG), and steady-state $\{^1H\}$-X NOE experiments have been described (*57-59*), as have techniques for measuring relaxation rate constants for antiphase coherence and two spin order (*60*). Techniques have been developed that minimize systematic contributions from cross-correlation between dipolar and chemical shift anisotropy (CSA) relaxation mechanisms (*61-63*) and from evolution of scalar coupling interactions during measurements of spin-spin relaxation rate constants (*62, 63*). Additional complexities that arise in ^{13}C AX_2 and AX_3 spins systems have been discussed elsewhere (*25, 64-67*).

The pulse schemes used to measure R_1, R_2, and the $\{^1H\}$-^{15}N NOE, are shown in Figure 16 (*68*). The R_1 and R_2 sensitivity enhanced pulse sequences consist of an initial refocussed INEPT transfer, the relaxation

period T, the t_1 evolution period, and reverse polarization transfer scheme. Proton-decoupling is performed using a composite pulse decoupling sequence during the relaxation delay of the inversion recovery experiments (Figure 16a) to suppress the time-dependent effects of dipolar ^{15}N-^{1}H cross-relaxation and of cross correlation between dipolar and CSA relaxation mechanisms. In order to suppress the time-dependent effects of cross-correlation between dipolar and CSA relaxation mechanisms in the CPMG experiments (Figure 16b), proton-decoupling is performed using synchronous proton 180° hard pulses during the relaxation delay T. The spin-echo delay in CPMG experiments must be short to minimize effects from evolution under the heteronuclear scalar coupling Hamiltonian; δ = 0.5 ms is sufficient for this purpose. Inversion recovery and CPMG decay curves are obtained by recording a series of 2D heteronuclear correlation spectra in which the relaxation period T is varied parametrically. The steady state NOE pulse sequence consists of the t_1 evolution period and the extended reverse polarization transfer scheme. The NOE enhancements are measured by recording pairs of spectra with and without saturation of protons during the recycle time between transients (Figure 16c). Saturation of protons during the recovery delay is performed using a composite pulse decoupling sequence. In all sequences, the H_2O resonance is suppressed by short spin lock purge pulses during the INEPT transfer steps to minimize the effects of saturation transfer from the solvent protons. These pulse sequences can be modified easily to utilize pulsed field gradients and “water flip back” techniques (*69*).

For the inversion recovery and CPMG experiments:

$$I(t) = I - [I - I_0]\exp[-T/R_1] \qquad [197]$$

$$I(t) = I_0 \exp[-T/R_2] + I \quad [198]$$

respectively. In [197] and [198], I_0 is the peak intensity for $T = 0$ and I is the limiting peak intensity as $T \rightarrow$. Peak intensities may decay to a non-zero limiting value in CPMG experiments as a consequence of pulse imperfections. For the NOE experiments, the NOE is calculated is given by:

$$\text{NOE} = 1 + \eta = I_{sat}/I_{unsat} \quad [199]$$

in which I_{sat} and I_{unsat} are the peak intensities in spectra recorded with and without saturation of protons during the recycle delay.

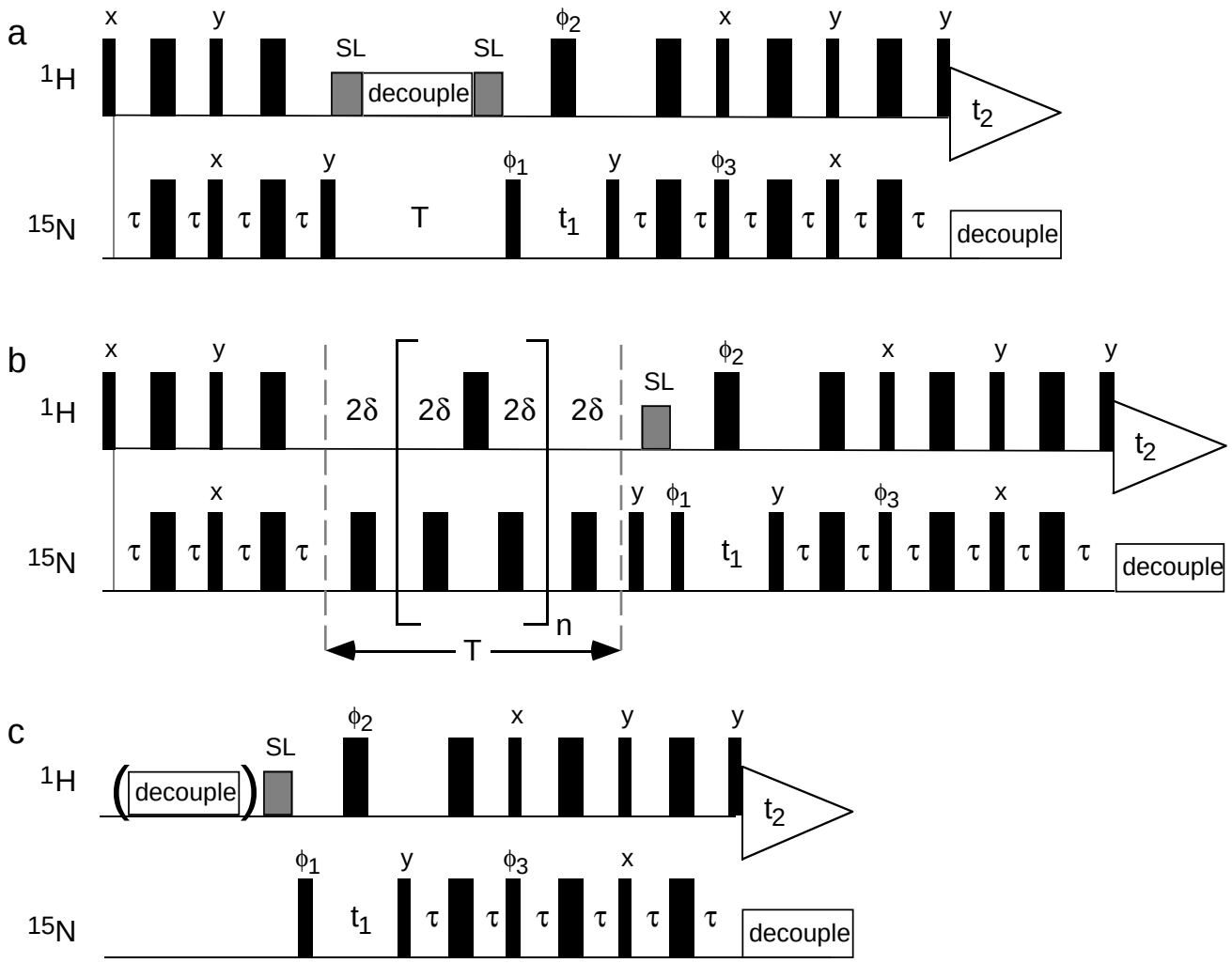

Figure 16. Pulse schemes used to measure (a) ^{15}N R_1, (b) ^{15}N R_2 and (c) {^{1}H}-^{15}N NOE. Similar sequence can be used to measure relaxation rates for the S spin of heteronuclear IS spin systems. The phase cycling used for R_1 and R_2 experiments is as follows: ϕ_1 = (x, -x, x, -x); ϕ_2 = 4(y), 4(-y); ϕ_3 = (y, y, -y, -y) and receiver (x, -x, -x, x). In the case of the {^{1}H}-^{15}N NOE experiments, the following phase cycles were employed: ϕ_1 = 2(x, -x x -x -x x -x x); ϕ_2 =16(y) 16(-y); ϕ_3 = 2(y, y, -y, -y), 2(-y, -y, y, y) and receiver = (x, -x, -x, x, -x, x,x, -x, -x, x, x, -x, x, -x, -x, x). In all cases, each t_1 experiment is recorded twice with the phase of the ^{15}N 90° pulse immediately after t_1 differing by 180°. Linear combinations of these two experiments are used to obtain the sensitivity enhancement (*34*). The 180° pulses without phase designations are applied along the *y*-axis. The value of τ is set to $1/(4J_{NH})$. For (a), and (b),the delay T is parametrically varied in a series of 2D experiments; for (c), pairs of spectra are acquired with and without proton saturation.

Three parameters, I_0, I_∞, and R_1, must be optimized when fitting [197] to experimental data. As has been discussed elsewhere, if the phase

of the radiofrequency pulse applied to the ^{15}N spins immediately prior to the relaxation period, T, in Fig. 1a and the phase of the receiver are inverted simultaneously on alternate acquisitions (extending the phase cycle by a factor of two) the contribution of the steady-state ^{15}N magnetization to the observed signal is canceled. In principle, this modification results in a single exponential time dependence of the observed signal with only two optimizable parameters, I_0 and R_1. In practice, a three parameter fit using an equation of the form of [198] may still be required to account for offsets and distortions of the baseline, and extension of the phase cycle may be undesirable. Nonetheless, satisfactory results can be obtained with either version of the inversion recovery experiment.

Relaxation of an amide ^{15}N nucleus spin at high field is dominated by the dipolar interaction with the directly attached proton spin and by the CSA mechanism. In addition, CPMG experiments are systematically affected by chemical exchange during the spin-echo delay. The phenomenological rates are thus

$$R_1 = R_2^{\mathrm{DD}} + R_2^{\mathrm{CSA}} \qquad [200]$$

$$R_2 = R_2^{\mathrm{DD}} + R_2^{\mathrm{CSA}} + R_{ex} \qquad [201]$$

$$NOE = 1 + (\sigma/R_1)\,(\gamma_H/\gamma_X) \qquad [202]$$

in which the dipolar and CSA relaxation rates are given in Tables 5 and 8. R_{ex} has been included in Eq. [201] to accommodate chemical exchange and other pseudo-first-order processes that contribute to the decay of transverse magnetization (*70*). For chemical exchange between two equally

populated sites, R_{ex} depends on the first order rate constant for the exchange process, k_{ex}; the chemical shift difference between the sites, ω_{ex}; and the spin echo period, δ. For $k_{ex} > \omega_{ex}$,

$$R_{ex} = k_{ex} - \sinh^{-1}\left[\delta k_{ex} \sinh(2u)/u\right]/(2\delta) \qquad [203]$$

in which $u^2 = \delta^2\left(k_{ex}^2 - \omega_{ex}^2\right)$. The chemical exchange contribution to R_2 is independent of δ if $\delta k_{ex} >> 1$ and is negligible if $\delta k_{ex} << 1$. Furthermore, conformational exchange is undetectable by NMR spectroscopy if the resonance frequency difference between conformers approaches zero.

Most commonly, the amplitudes and time scales of the intramolecular motions of the protein are determined from the relaxation data by using the model-free formalism pioneered by Lipari & Szabo (*19, 20*) and extended by Clore and coworkers (*71*). Protocols for determination of model free parameters from experimental data have been described elsewhere (*59, 67, 72*). Alternatively, values of the spectral density function can be determined directly via "spectral density mapping" if additional relaxation parameters for longitudinal two-spin order and antiphase coherence are measured (*60, 73*).

9 References

1. J. McConnell, "The Theory of Nuclear Magnetic Relaxation in Liquids," pp. 1-196, Cambridge University Press, New York, 1987.
2. A. Abragam, "Principles of Nuclear Magnetism," pp. 1-599, Clarendon Press, Oxford, 1961.
3. M. Goldman, "Quantum description of high-resolution NMR in liquids," pp. 1-268, Clarendon Press, New York, 1988.
4. F. Bloch, *Phys. Rev.* **70**, 460-474 (1946).
5. N. Bloembergen, E.M. Purcell, and R.V. Pound, *Phys. Rev.* **73**, 679-712 (1948).

6. I. Solomon, *Phys. Rev.* **99**, 559-565 (1955).
7. R.K. Wangsness and F. Bloch, *Phys. Rev.* **89**, 728-739 (1953).
8. A.G. Redfield, *Adv. Magn. Reson.* **1**, 1-32 (1965).
9. N.C. Pyper, *Mol. Phys.* **22**, 433-458 (1971).
10. R. Brüschweiler and D.A. Case, *Prog. NMR Spectrosc.* **26**, 27-58 (1994).
11. M. Goldman, *J. Magn. Reson.* **60**, 437-452 (1984).
12. L.G. Werbelow and D.M. Grant, *Advan. Magn. Reson.* **9**, 189-299 (1977).
13. N. Müller, G. Bodenhausen, K. Wüthrich, and R.R. Ernst, *J. Magn. Reson.* **65**, 531-534 (1985).
14. N.C. Pyper, *Mol. Phys.* **21**, 1-33 (1971).
15. M.H. Levitt, G. Bodenhausen, and R.R. Ernst, *J. Magn. Reson.* **53**, 443-461 (1983).
16. C. Griesinger and R.R. Ernst, *Chem. Phys. Lett.* **152**, 239-247 (1988).
17. P.S. Hubbard, *Phys. Rev.* **180**, 319-326 (1969).
18. D.M. Brink and G.R. Satchler, "Angular Momentum," pp. 1-170, Clarendon Press, Oxford, 1993.
19. G. Lipari and A. Szabo, *J. Am. Chem. Soc.* **104**, 4546-4559 (1982).
20. G. Lipari and A. Szabo, *J. Am. Chem. Soc.* **104**, 4559-4570 (1982).
21. A.G. Palmer, *Curr. Opin. Biotechnol.* **4**, 385-391 (1993).
22. G. Wagner, *Curr. Opin. Struc. Biol.* **3**, 748-753 (1993).
23. T.M.G. Koning, R. Boelens, and R. Kaptein, *J. Magn. Res.* **90**, 111-123 (1990).
24. H. Liu, P.D. Thomas, and T.L. James, *J. Mag. Reson.* **98**, 163-175 (1992).
25. L.E. Kay and D.A. Torchia, *J. Magn. Reson.* **95**, 536-547 (1991).
26. G.S. Harbison, *J. Am. Chem. Soc.* **115**, 3026-3027 (1993).
27. A.A. Bothner-By, R.L. Stephens, and J. Lee, *J. Am. Chem. Soc.* **106**, 811-813 (1984).
28. R.E. London, *J. Magn. Reson.* 410-415 (1990).
29. H. Wennerström, *Mol. Phys.* **24**, 69-80 (1972).
30. H.M. McConnell, *J. Chem. Phys.* **28**, 430-431 (1958).
31. R.R. Ernst, G. Bodenhausen, and A. Wokaun, "Principles of nuclear magnetic resonance in one and two dimensions," pp. 1-610, Clarendon Press, Oxford, 1987.

32. R.C. Cantor and P.R. Schimmel, “Biophysical Chemistry,” pp. 1-1371, W. H. Freeman, San Francisco, 1980.
33. R.M. Venable and R.W. Pastor, *Biopolymers* **27**, 1001-1014 (1988).
34. A.G. Palmer, J. Cavanagh, P.E. Wright, and M. Rance, *J. Magn. Reson.* **93**, 151-170 (1991).
35. A. Bax, M. Ikura, L.E. Kay, D.A. Torchia, and R. Tschudin, *J. Magn. Reson*. **86**, 304-318 (1990).
36. T.J. Norwood, J. Boyd, J.E. Heritage, N. Soffe, and I.D. Campbell, *J. Magn. Reson*. **87**, 488-501 (1990).
37. J.H. Noggle and R.E. Shirmer, “The Nuclear Overhauser Effect: Chemical Applications,” pp. 1-259, Academic Press, New York, 1971.
38. D. Neuhaus and M. Williamson, “The Nuclear Overhauser Effect in Structural and Conformational Analysis,” pp. 1-522, VCH Publishers, New York, 1989.
39. K. Wüthrich, “NMR of Proteins and Nucleic Acids,” pp. 1-292, Wiley, New York, 1986.
40. C. Griesinger, G. Otting, K. Wüthrich, and R.R. Ernst, *J. Am. Chem. Soc.* **110**, 7870-7872 (1988).
41. J. Cavanagh and M. Rance, *J. Magn. Reson.* **96**, 670-678 (1992).
42. G. Bodenhausen, H. Kogler, and R.R. Ernst, *J. Magn. Reson.* **58**, 370-388 (1984).
43. W. Denk, R. Baumann, and G. Wagner, *J. Magn. Res.* **67**, 386-390 (1986).
44. V. Stoven, A. Mikou, D. Piveteau, E. Guittet, and J.-Y. Lallemand, *J. Magn. Reson*. **82**, 163-168 (1989).
45. J. Fejzo, Z. Zolnai, S. Macura, and J.L. Markley, *J. Magn. Reson.* **88**, 93-110 (1990).
46. G.H. Weiss, J.E. Kiefer, and J.A. Ferretti, *J. Magn. Reson.* **97**, 227-234 (1992).
47. A. Bax and D.G. Davis, *J. Magn. Reson.* **63**, 207-213 (1985).
48. C. Griesinger and R.R. Ernst, *J. Magn. Reson.* **75**, 261-271 (1987).
49. L. Braunschweiler and R.R. Ernst, *J. Magn. Reson.* **53**, 521-528 (1983).
50. D. Neuhaus and J. keeler, *J. Magn. Reson.* **68**, 568-574 (1986).
51. T.-L. Hwang, M. Kadkhodaei, A. Mohebbi, and A.J. Shaka, *Magn. Reson. Chem*. **30**, S24-S34 (1992).

52. N. Müller, R.R. Ernst, and K. Wüthrich, *J. Am. Chem. Soc.* **108**, 6482-6496 (1986).
53. D. Marion and B. Bax, *J. Magn. Reson.* **80**, 528-533 (1988).
54. P. Plateau and M. Guéron, *J. Am. Chem. Soc.* **104**, 7310-7311 (1982).
55. R.E. London, *in* "Magnetic Resonance in Biology" (J.S. Cohen eds.), Vol. 1, pp. 1-69, Wiley, New York, 1980.
56. F. Heatley, *in* "Annual Reports on NMR Spectroscopy" (G.A. Webb eds.), Vol. 17, pp. 179-230, 1986.
57. L.E. Kay, D.A. Torchia, and A. Bax, *Biochemistry* **28**, 8972-8979 (1989).
58. G.M. Clore, P.C. Driscoll, P.T. Wingfield, and A.M. Gronenborn, *Biochemistry* **29**, 7387-7401 (1990).
59. A.G. Palmer, M. Rance, and P.E. Wright, *J. Am. Chem. Soc.* **113**, 4371-4380 (1991).
60. J.W. Peng and G. Wagner, *J. Magn. Reson.* **98**, 308-332 (1992).
61. J. Boyd, U. Hommel, and I.D. Campbell, *Chem. Phys. Lett.* **175**, 477-482 (1990).
62. L.E. Kay, L.K. Nicholson, F. Delagio, A. Bax, and D.A. Torchia, *J. Magn. Reson.* **97**, 359-375 (1992).
63. A.G. Palmer, N.J. Skelton, W.J. Chazin, P.E. Wright, and M. Rance, *Molec. Phys.* **75**, 699-711 (1992).
64. A.G. Palmer, P.E. Wright, and M. Rance, *Chem. Phys. Lett.* **185**, 41-46 (1991).
65. L.K. Nicholson, L.E. Kay, D.M. Baldisseri, J. Arango, P.E. Young, and D.A. Torchia, *Biochemistry* **31**, 5253-5263 (1992).
66. L.E. Kay, T.E. Bull, L.K. Nicholson, C. Griesinger, H. Schwalbe, A. Bax, and D.A. Torchia, *J. Magn. Reson.* **100**, 538-558 (1993).
67. A.G. Palmer, R. Hochstrasser, D.P. Millar, M. Rance, and P.E. Wright, *J. Am. Chem. Soc.* **115**, 6333-6345 (1993).
68. N.J. Skelton, M. Akke, J. Kördel, A.G.P. Palmer, M. Rance, and W.J. Chazin, *J. Magn. Reson., Ser. B* **102**, 253-264 (1993).
69. S. Grzesiek and A. Bax, *J. Am. Chem. Soc.* **115**, 12593-12594 (1993).
70. M. Bloom, L.W. Reeves, and E.J. Wells, *J. Chem. Phys.* **42**, 1615-1624 (1965).
71. G.M. Clore, A. Szabo, A. Bax, L.E. Kay, P.C. Driscoll, and A.M. Gronenborn, *J. Am. Chem. Soc.* **112**, 4989-4991 (1990).

72. A.M. Mandel, M. Akke, and A.G. Palmer, *J. Mol. Biol.* **246**, 144-163 (1995).
73. J.W. Peng and G. Wagner, *Biochemistry* **31**, 8571-8586 (1992).